

**NOVEL DEVELOPMENTS FOR INCREASED EFFICACY AND LONGEVITY OF
EXISTING CLINICALLY APPROVED ANTIBIOTICS**

Nurhasimah Awang Md Daud

MSc.

University of York

Department of Chemistry

December 2012

Abstract

Ciprofloxacin is a fluoroquinolone, broad spectrum antibacterial agent where it fights against both Gram positive and Gram negative bacteria. It usually enters the bacteria via porins such as OmpF in *E. coli* and binds with the DNA proteins called DNA gyrase or DNA topoisomerase IV and a bacterial DNA to form a ternary complex in the cytoplasm. Mutation in the regulatory gene of bacterial DNA affects the biological synthesis of porins where it reduces the porins, and this usually associates with overproduction of efflux pumps, which lead to low concentration of ciprofloxacin in the bacteria. Therefore, it does not reach to the fatal level and the bacteria are still able to survive even though they are exposed to antibiotics. This condition is called antibiotic resistance. 'Trojan Horse' strategy is one of the strategies to solve this phenomenon, where the antibiotic is smuggled into the cytoplasm of the bacteria by a vector called siderophore, which in nature, it is secreted by the bacteria to solubilise the ferric iron and enter the bacteria through the active pump for their survival. Our research group has synthesised many new siderophore-drug conjugates that based on the fluoroquinolone as the drug and δ -hydroxycarboxylate-type of siderophore as a vector. In this project, different polarities of 1,5-citrate ciprofloxacin conjugates were successfully synthesised and screened with a panel of clinically relevant bacteria and found that the using 1,5-citrate as a siderophore and hydrophilicity of siderophore-drug conjugates can improve marginally the efficacy of the drug conjugates.

Table of Contents

Abstract.....	a
Table of Contents.....	b
Abbreviation and Chemical Formulae.....	j
List of Figures.....	iv
List of Tables.....	v
List of Schemes.....	vi
List of Spectra.....	vii
Acknowledgement.....	viii
Author's Declaration.....	ix
1 Introduction.....	1
1.1 Antibiotics.....	1
1.2 Antibiotic Resistance.....	2
1.3 Development of Fluoroquinolone Antibiotics.....	5
1.3.1 Mode of Action.....	7
1.3.2 Resistance Mechanisms Displayed By Fluoroquinolone Antibiotics.....	10
1.4 Siderophores.....	12
1.4.1 Siderophore Classes.....	13
1.4.2 Fe (III)-Siderophore Complex Transport Mechanism.....	17
1.5 'Trojan Horse' System.....	20
1.5.1 Natural Siderophore-Drug Conjugates.....	20
1.5.2 Synthetic Siderophore-Drug Conjugates.....	21
1.6 Objectives.....	26
2 Results and Discussions.....	27
2.1 1, 5-Citrate-ciprofloxacin conjugate using Glycine as the linker.....	27
2.2 1,5-Citrate-ciprofloxacin conjugate using L-serine as the linker.....	38
2.3 Biological Screening.....	56
3 Conclusions and Future Work.....	59
3.1 Conclusions.....	59
3.2 Future work.....	60
4 Experimental.....	61

4.1	General.....	61
4.2	2-Hydroxy-4-methoxy-2-(2-methoxy-2-oxoethyl)-4-oxobutanoic acid (40).....	62
4.3	1,2,3-Trimethyl 2-hydroxypropane-1,2,3-tricarboxylate (41).....	64
4.4	Methyl 1-cyclopropyl-6-fluoro-4-oxo-7-(piperazin-1-yl)-1,4-dihydroquinoline-3-carboxylate (42).....	66
4.5	Methyl 7-[4-(2-[[<i>tert</i> -butoxy) carbonyl] amino] acetyl) piperazin-1-yl]-1-cyclopropyl-6-fluoro-4-oxo-1,4-dihydroquinoline-3-carboxylate (44).....	68
4.6	Methyl 7-[4-(2-[[<i>tert</i> -butoxy) carbonyl] amino] acetyl) piperazin-1-yl]-1-cyclopropyl-6-fluoro-4-oxo-1,4-dihydroquinoline-3-carboxylate (44) – modified synthesis.....	70
4.7	1,5-Dimethyl-3-[(2-{4-(1-cyclopropyl-6-fluoro-3-(methoxycarbonyl)-4-oxo-1,4-dihydroquinoline-7-yl] piperazin-1-yl)-2-oxoethyl} carbamoyl]-3-hydroxypentanedioate (45).....	71
4.8	3-({2-[4-(3-Carboxy-1-cyclopropyl-6-fluoro-4-oxo-1,4-dihydroquinoline-7-yl) piperazin-1-yl]-2-oxoethyl} carbamoyl)-3-hydroxypentanedioic acid (38).....	73
4.9	Methyl 7-[4-(2-[[<i>tert</i> -butoxy) carbonyl] amino]-3-hydroxypropanoyl) piperazin-1-yl]-1-cyclopropyl-6-fluoro-4-oxo-1,4-dihydroquinoline-3-carboxylate (48).....	75
4.10	Methyl 7-[4-[3-(acetyloxy)-2-[[<i>tert</i> -butoxy) carbonyl] amino] propanoyl]piperazin-1-yl]-1-cyclopropyl-6-fluoro-4-oxo-1,4-dihydroquinoline-3-carboxylate (50).....	77
4.11	2-(3-{4-[1-Cyclopropyl-6-fluoro-3-(methoxycarbonyl)-4-oxo-1,4-dihydroquinoline-7-yl]piperazin-1-yl}-2-[2-hydroxy-4-methoxy-2-(2-methoxy-2-oxoethyl)-4-oxobutanamido]-3-oxopropyl) 1,3-dimethyl 2-hydroxypropane-1,2,3-tricarboxylate (52).....	79
4.12	3-({1-[4-(3-Carboxy-1-cyclopropyl-6-fluoro-4-oxo-1,4-dihydroquinoline-7-yl)piperazin-1-yl]-3-hydroxy-1-oxopropan-2-yl} carbamoyl)-3-hydroxypentanedioic acid (39).....	81
5	Appendices.....	83
6	References.....	88

Abbreviations and Chemical Formulae

ABC	ATP-Binding Cassette
ATP	adenosine triphosphate
β	beta
Boc	<i>tert</i> -butyloxycarbonyl
Calc. <i>m/z</i>	calculated <i>m/z</i>
CDCl_3	deuterated chloroform
CID spectrum	Collision-induced dissociation
^{13}C NMR	Carbon-13 Nuclear Magnetic Resonance
cm^{-1}	reciprocal centimetre
COSY	Correlation spectroscopy
δ	delta
Da	Dalton
DFOB	desferrioxamine B
DHB	dihydroxybenzoate
DIPEA	diisopropylethylamine
DMF	dimethyl formamide
DMAP	dimethylamino pyridine
DMSO-d_6	deuterated dimethyl sulfoxide
DNA	deoxyribonucleic acid
EDDA	ethylenediamine <i>bis</i> (<i>o</i> -hydroxyphenyl) acetic acid
EDC.HCl	1-ethyl-3-(3'-dimethylamino) carbodiimide HCl salt
EMRSA	epidemic methicillin- resistant <i>Staphylococcus aureus</i>
ESI	electrospray ionisation

Fec	ferric citrate transport protein
Fep	ferric enterobaction binding protein
Fhu	ferric hydroxamate binding protein
FT-IR	Fourier transform infrared spectroscopy
Glu	glutamic acid
Gly	glycine
GyrA	gyrase A
HBTU	O-Benzotriazole- <i>N,N,N',N'</i> -tetramethyl-uronium-hexafluorophosphate
HOBt.H ₂ O	1-hydroxybenzotriazole hydrate
HCl	Hydrochloric acid
¹ H NMR	Proton Nuclear Magnetic Resonance
H ₂ SO ₄	sulfuric acid
Hz	hertz
IR	Infrared
<i>J</i>	<i>J</i> -coupling
K _{sp}	solubility product constant
L-ser	L-serine
M	Molar
Me	methyl
Meas. <i>m/z</i>	measured <i>m/z</i>
MeOH	Methanol
MeOH-d ₄	deuterated methanol
MHz	megahertz
MIC	minimum inhibition concentration
MRSA	Methicillin-resistant <i>Staphylococcus aureus</i>
<i>m/z</i>	<i>mass is to charge ratio</i>

Omp	outer membrane protein
ppm	parts per million
PTR	phase transfer reaction
QRDR	quinolone-resistance determining region
RNA	ribonucleic acid
rt	room temperature
Ser	serine
SOCl_2	thionyl chloride
TBAH	<i>tert</i> -butylammonium hydroxide
TEA	triethyl amine
ToF	time of flight
UV light	ultraviolet light

List of Figures

Figure 1: Structures of Penicillin **1**, tigecyclin **2**, clarithromycin **3** and ciprofloxacin **4**

Figure 2: A schematic diagram showing resistance mechanisms

Figure 3: Structure of amoxicillin **5** and clavulanic acid **6**

Figure 4: Structure of rifampicin **7**

Figure 5: Modification of chloroquinolone **8** to nalidixic acid **9**

Figure 6: 4-Quinolone pharmacophores

Figure 7: Proposed stacking of ciprofloxacin

Figure 8: Proposed important domains for stabilising the drug-DNA-enzyme complex

Figure 9: Iron-binding complex using hydroxamate siderophore

Figure 10: α -hydroxycarboxylate siderophores

Figure 11: Catecholate siderophores

Figure 12: Ferrioxamine siderophores

Figure 13: Mixed ligand siderophores

Figure 14: Natural siderophore-drug conjugates

Figure 15: Components in the 'Trojan Horse' System

Figure 16: Cyanuric- β -Lactam conjugate

Figure 17: Synthetic mixed ligands-drug conjugates

Figure 18: Synthetic citrate-based siderophore-drug conjugates

Figure 19: Synthetic citrate-ciprofloxacin conjugates

Figure 20: Structures of citric acid-ciprofloxacin conjugates

List of Tables

Table 1: Generations of 4-quinolone

Table 2: Hydrophobicity and molecular weight (Da) of fluoroquinolones

Table 3: Isolated yield of **44** using different solvents systems

Table 4: Yields of **45** with different solvent system

Table 5: The result for the investigation on pharmacophore of new siderophore-drug conjugates against clinically isolated bacteria

Table 6: The result for the investigation of polarity of new siderophore- drug conjugates against clinically isolated bacteria

List of Schemes

- Scheme 1: The proposed synthesis of **38**
- Scheme 2: Regioselective methyl protection of citric acid
- Scheme 3: Proposed cyclisation and fragmentation of 1, 5-dimethyl citric acid **40** in mass spectrometry, respectively
- Scheme 4: Synthesis of ciprofloxacin methanoate **42** from ciprofloxacin **4**
- Scheme 5: Amide coupling reaction of **44**
- Scheme 6: Multistep syntheses towards the synthesis of **45**
- Scheme 7: Synthesis of siderophore-drug conjugate **38**
- Scheme 8: Possible fragmented molecules from CID mass spectra
- Scheme 9: The proposed synthesis of **39**
- Scheme 10: Conjugation of ciprofloxacin methanoate **42** and *N*-(*tert*-butoxycarbonyl)-L-Ser- OH **47** gave two linker-drug conjugates **48** and **49**
- Scheme 11: Synthesis of **48** using HBTU as amide-coupling reagent
- Scheme 12: Acetylation reaction
- Scheme 13: Amide coupling reaction between the protected citric acid **40** and the drug conjugate **51**
- Scheme 14: New strategy towards the synthesis of **39**
- Scheme 15: New strategy forming **52**
- Scheme 16: Base hydrolysis of esters to form siderophore-drug conjugate **39**
- Scheme 17: *Cis-trans* isomerisation of amide bond
- Scheme 18: Possible fragmented molecule from CID spectrum

List of Spectra

Spectrum 1: Proton NMR spectrum of **38**

Spectrum 2: Partial ^1H NMR spectrum of the mixture of **48** and **49**

Spectrum 3: The spectrum of **39** at 400 MHz NMR at room temperature

Spectrum 4: Partial spectra of 400 MHz and 700 MHz ^1H NMR spectrum

Spectrum 5: COSY spectrum shows coupling between the pseudo triplet amide resonance and proton at position 20

Spectrum 6: Partial spectra of new siderophore-drug conjugate **39** with and without D_2O

Spectrum 7: Partially spectra of the second target molecule **39** at 400 MHz and 700 MHz at ambient temperature

Spectrum 8: Partial ^1H NMR of **39** at variable temperatures at 500 MHz NMR spectroscopy

Spectrum 9: Partial ^1H NMR spectra of the second target molecule **39** at 500 MHz at variable temperatures

Acknowledgement

I would like to thank to the Special Scholarship Fund of Human Resources, Department of Economic Planning and Development, Department of Prime Minister and Ministry of Education of Brunei for sponsoring my postgraduate one-year full time course in the University of York.

I also would like to thank to my lovely supervisors, Dr. Anne Routledge and Dr. Anne Duhme-Klair for supervising me for a year, giving the comments on my works as well as helping me on my research project.

Many thanks to Heather Fish for helping me a lot in my spectroscopy.

My special thanks to my parents (Hj. Awang Md Daud and Hjh Rokiah), my family (Hjh. Noranedah Fadilawati, Fairol Fadzleen, Amal Umi Khalsum, Farzalena, Fazidah, Mirady Floridzan, Hjh. Farihah, Dk. Aina, Hj. Mat Zain and Hjh. Husnah), my friends (Zyan, Antika, Azrina, Neesa, Raheemah, Zul, Abeda, Dan and Chris) and my hall mates especially Qiu and Huang for supporting, motivating and cheering me up throughout the year. Thank you!

Author's Declaration

I would like to declare that this thesis is original except where the reference has been made to other authors and co-workers. Biological data was taken by the collaborators from the University of Bradford, UK.

Nurhasimah Awang Md Daud

1 Introduction

1.1 Antibiotics

An antibiotic is a chemical agent used to delay or to stop the growth of bacteria and ultimately, kill the bacteria. An example of a naturally occurring antibiotic is the β -lactam antibiotic, Penicillin **1**, which is produced by fungal *Penicillium* strains^[1]. Extracting natural antibiotics from microorganisms gives only a limited quantity of potential drugs; therefore, scientists have designed and synthesised semi-synthetic and synthetic antibiotics which have a wide range of bacterial cell targets. Examples of semi-synthetic antibiotics are tigecycline **2**^[2] and clarithromycin **3**^[3]. An example of a synthetic antimicrobial agent is ciprofloxacin **4**, a member of the class of synthetic antimicrobials known as fluoroquinolones^[4, 5]. (Figure 1)

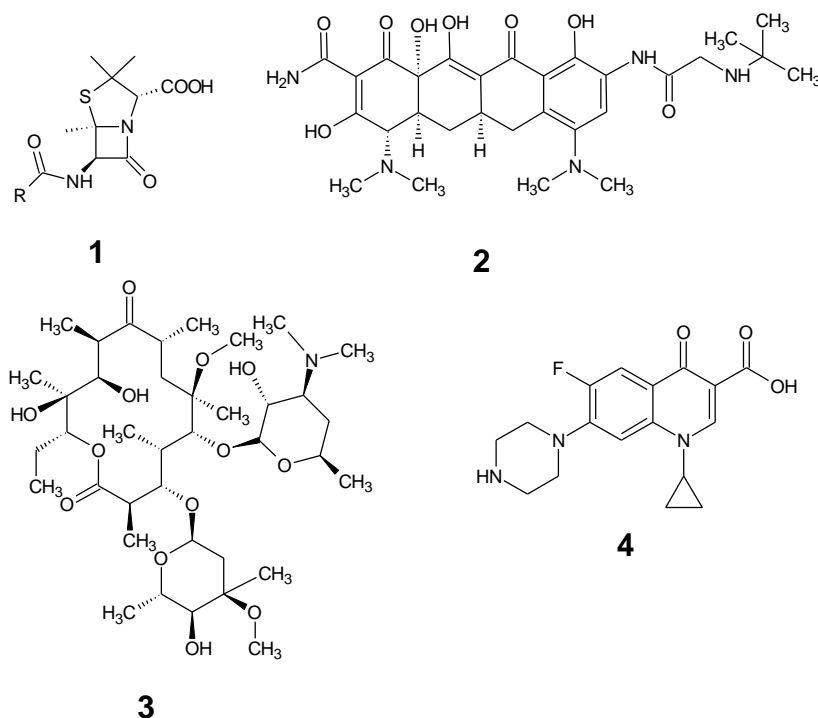


Figure 1: Structures of Penicillin **1**, tigecyclin **2**, clarithromycin **3** and ciprofloxacin **4**

1.2 Antibiotic Resistance

Antibiotic resistance is the phenomenon where the bacteria develop mechanisms to enable them to survive even though they are exposed to antibiotics^[5]. The overuse or misuse of antibiotics leads to mutations in the bacteria; they can develop these mutations during antibiotic therapy or after treatment. There are three common mechanisms of resistance (Figure 2); (1) production of enzymes that hydrolyse or chemically modify the antibacterial agent, (2) alteration of the target enzymes and (3) reduction of intracellular concentration of the antibiotic by either reduction of porins in the outer membrane of bacteria or up regulation of efflux pumps.

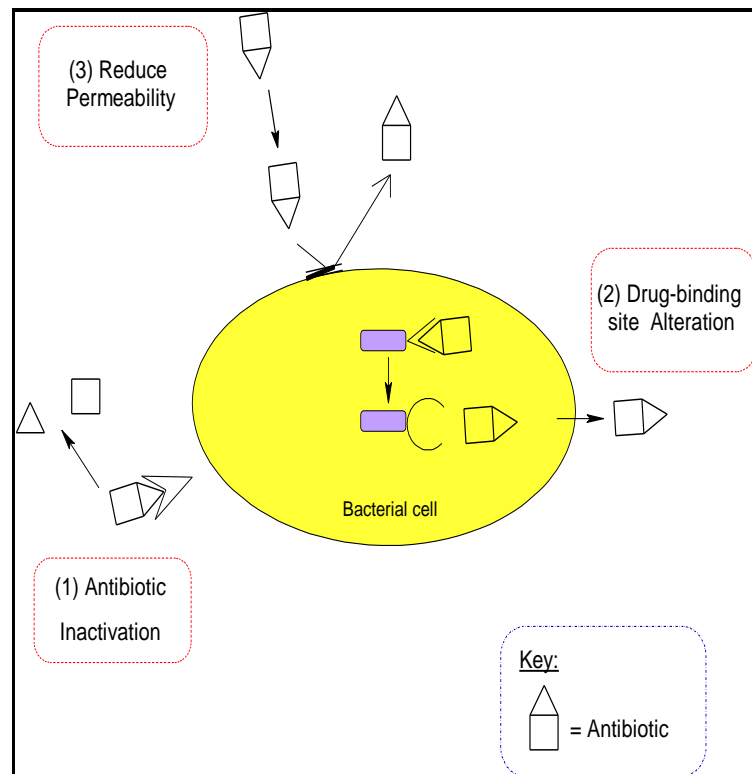


Figure 2: A schematic diagram showing resistance mechanisms

Escherichia coli shows examples of these resistance mechanisms. Frequent exposure to β -lactam antibiotics such as penicillin **1** and

cephalosporins^[6] lead to the β -lactamase gene in *E. coli* over expressing lactamase^[7]. In some cases, the overproduction is due to the mutation in an up-promoter gene^[8] or changes in transcriptional regulation^[9]. β -Lactamase is the enzyme produced by Gram negative and Gram positive bacteria in order to bind^[10, 11] or hydrolyse^[11] β -lactam antibiotics which ultimately prevent them from killing the bacteria. Since β -lactamase contains an active site that is structure specific for the β -lactam ring^[12], an irreversible inhibitor has been designed to combat the action of this enzyme. One treatment regime is the combination of amoxicillin **5** (the antibacterial agent) and clavulanic acid **6** (the β -lactamase inhibitor) (Figure 3). Unfortunately, the idea of combining the drug and the inhibitor still has some limitations, some strains of *E. coli* can produce β -lactamases that are not only capable of hydrolysing the antibiotic, but they also synthesise plasmid-encoded β -lactamase TEM-1 which is capable of combating the inhibitor^[6].

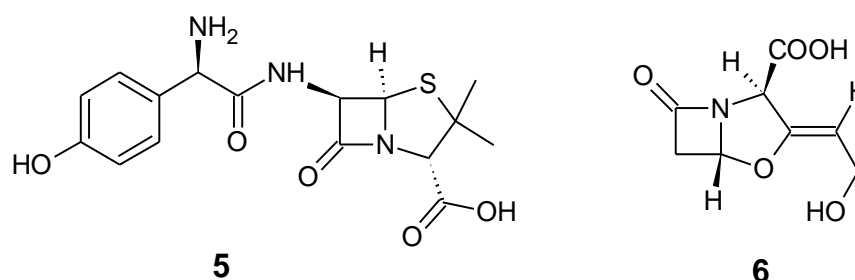
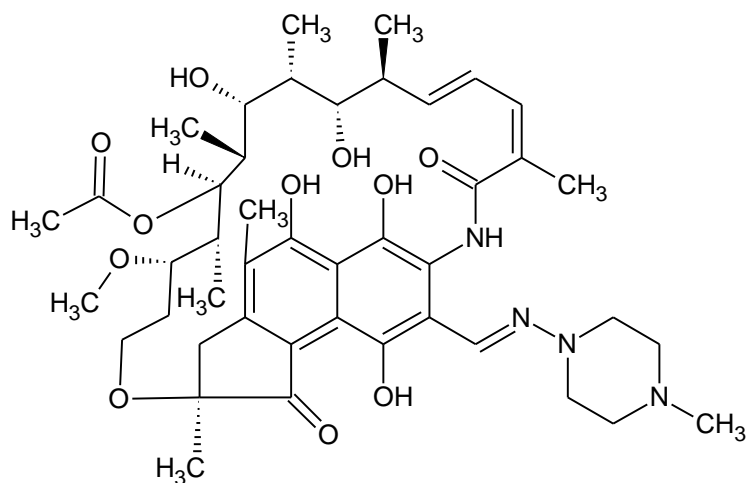


Figure 3: Structure of amoxicillin **5** and clavulanic acid **6**

A key resistance mechanism displayed by many bacteria is alteration of the antibiotic binding sites of the intracellular target^[13]. This type of antibiotic resistance is due to the numerous single amino acids substitutions which reduce the binding affinity of the antibiotic to a target enzyme^[13]. For example, rifampicin **7** (Figure 4) is an antibiotic that interacts with the β -sub unit of bacterial RNA polymerase^[14]. Changing of the structure of the active site for rifampicin **7** in RNA polymerase was due to amino acid substitutions, or small deletions and insertions within highly conserved regions of the RNA polymerase β -sub unit, resulting in antibiotic resistance^[15].



7

Figure 4: Structure of rifampicin **7**

Before an antibacterial agent can interact with an intracellular target protein or enzyme, it must pass through the bacterial cell membrane. Porins and passive diffusion through the cell membrane allow antibacterial agents to enter the bacterial cell. In some mutant Gram negative bacteria, the permeation of hydrophilic molecules through porins is reduced^[16] due to mutations in regulatory genes^[17]. For example resistance to fluoroquinolone antibiotics can be due to a decreased number of OmpF porins.

A number of strategies have been developed in order to combat resistance mechanisms especially those that lower the intracellular drug concentration.

1.3 Development of Fluoroquinolone Antibiotics

Nalidixic acid **9** was found during the synthesis of chloroquine **8**, an antimalarial agent^[18]. Nalidixic acid **9** had a modest bacteriostatic activity towards Gram negative bacteria. It was only used for the treatment of kidney infections^[5] and some enteric infections caused by members of the Enterobacteriaceae^[5]. Structurally nalidixic acid **9** contains *naphthyridone nucleus* (two rings containing nitrogen atoms at position 1 and 8)^[19] (Figure 5).

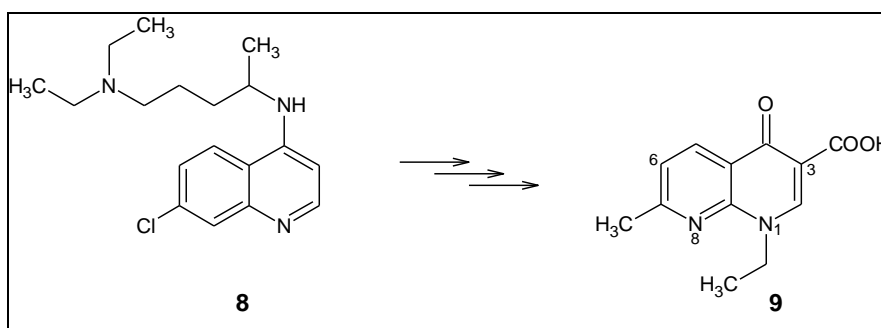


Figure 5: Modification of chloroquinolone **8** to nalidixic acid **9**

Soon after its introduction, pathogenic organisms showed resistance towards nalidixic acid **9**^[19]. Therefore, chemical modifications were explored in order to increase its potency and spectrum to bypass resistance.

Any chemical modification needs to retain the pharmacophore unit and structure, such as the carboxylic acid and the quinolone nucleus.

The first modification gave rosoxacin **10**^[19] (see Figure 6). Rosoxacin **10** showed the improvement in terms of activity over nalidixic acid **9**^[19].

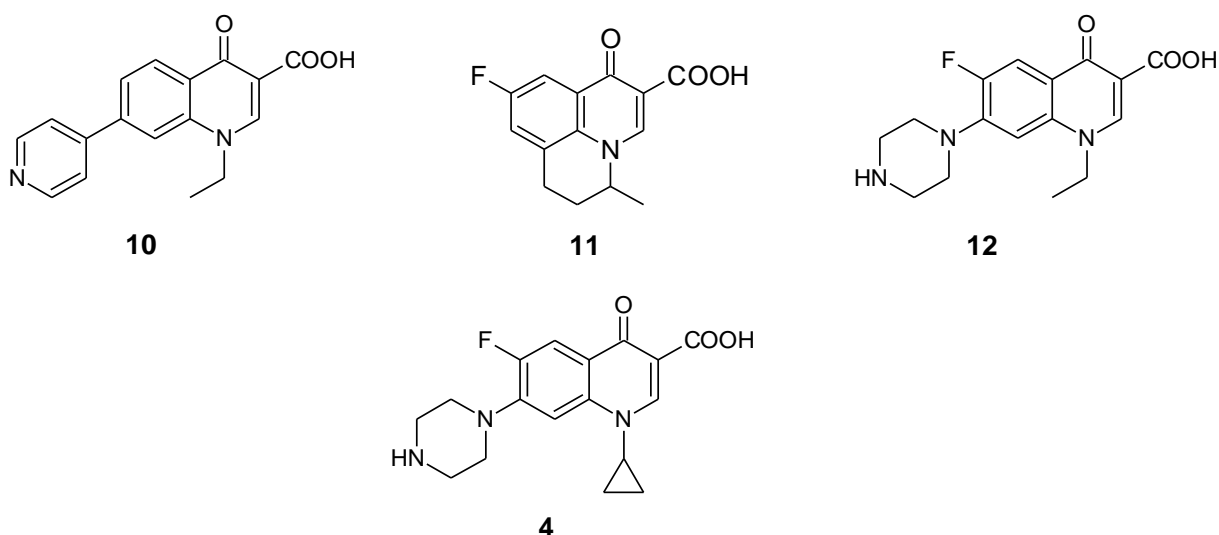


Figure 6: 4-Quinolone pharmacophores

Flumequine **11** (patented in 1973) was the first fluoroquinolone that substituted the hydrogen atom at position 6 with a fluorine atom which showed increased activity towards Gram positive bacteria because of greater DNA-gyrase inhibition activity and increase in cell penetration^[19].

Two decades after the introduction of nalidixic acid **9**^[19], norfloxacin **12** (patented in 1978) was synthesised. It contained the combination of a fluorine atom at position 6 and a piperazinyl ring at position 7. The addition of the piperazinyl ring at position 7 increased the spectrum of its activity as it could kill most Gram negative bacteria and had greater efficacy on Gram positive bacteria by improving the penetration of the drug through the bacteria cell wall^[19-21]. Unfortunately, norfloxacin **12** showed poor bioavailability^[5]. Therefore, it was not used in systemic infections^[19].

Ciprofloxacin **4** (patented in 1981) has the addition of cyclopropyl ring at nitrogen-1 position which broadened the spectrum and enhanced the activity. It can be used in systemic infections^[19].

There are newer developments in fluoroquinolone antibiotics. For example, sparfloxacin and levofloxacin have good activity against Gram positive bacteria in respiratory infections^[17]. Other newer fluoroquinolones are trovafloxacin and clinafloxacin which are used against anaerobic bacteria^[17].

Fluoroquinolone antibiotics are classified into four generations. (Table 1)

Generation	4- Quinolones	Activity strength
First	Nalidixic acid Cinoxacin	Moderate Gram negative
Second	Lemofloxacin Norfloxacin Enoxacin Ofloxacin <i>Ciprofloxacin</i>	Broad spectrum to Gram negative and atypical bacteria, but limited to Gram positive
Third	Levofloxacin Sparfloxacin Gatifloxacin Moxifloxacin	Broad to Gram negative and atypical bacteria. Also improve Gram positive
Fourth	Trovafloxacin Clinafloxacin	Broad Gram negative, improve Gram positive and kill some of anaerobic pathogens

Table 1: Generations of 4-quinolone

1.3.1 Mode of Action

1.3.1.1 Cell Penetration

Before inhibiting the target intracellular enzymes, fluoroquinolone must firstly penetrate through the bacterial cell wall and the inner cell membrane. In

Gram negative bacteria, there are three different ways for fluoroquinolones to enter the bacteria^[5]. They are hydrophilic pathways involving porins, hydrophobic pathways involving lipid bilayers and self-promoted pathways for cationic molecules^[5].

Cell uptake via porins is based on hydrophobicity and molecular weight^[5]. In order to enter a bacterial cell through these proteins, molecules must have a hydrophilic characteristic^[22] and molecular weight of 600 Daltons and less^[16]. Even though porins accept molecules with low molecular weight, they do not accept hydrophobic molecules. It has been reported by Caulcott *et al.* that ciprofloxacin shows enhanced uptake via OmpF when compared to Ofloxacin, this is proposed to be due to its three dimensional shape and hydrophilicity^[5, 23] (Table 2).

Polarity	4-Quinolone	Molecular weight (Da)
Hydrophilicity (Log <i>P</i> < 0.1)	Ciprofloxacin	331.4
	Norfloxacin	319.3
	Enoxacin	320.3
Intermediate polarity (Log <i>P</i> 0.1-2.0)	Miloxacin	263.2
	Ofloxacin	360.4
	Pefloxacin	333.4
Hydrophobicity (Log <i>P</i> > 2.0)	Nalidixic acid	232.2
	Oxolinic acid	261.2
	Difloxacin	399.4

Table 2: Hydrophobicity and molecular weight (Da) of fluoroquinolones

1.3.1.2 Intracellular target

After passing into the bacterial cytoplasm, fluoroquinolones inhibit cell division by interrupting the key DNA supercoiling enzymes, gyrase and topoisomerase IV.

Ciprofloxacin **4** inhibits DNA synthesis by targeting cytoplasmic gyrase (topoisomerase II) in Gram negative bacteria^[24, 25], or cytoplasmic topoisomerase IV in Gram positive bacteria^[24].

In Gram negative bacteria, cytoplasmic gyrase is responsible for changing relaxed DNA into super-coiled DNA^[17]. The gyrase protein is a tetramer containing A and B subunits. The A is responsible for DNA cleavage and re-sealing, and the B subunit responsible for the transfer of energy from ATP hydrolysis^[17]. Ciprofloxacin **4** disturbs gyrase during the re-sealing of double-stranded DNA by forming a quinolone-topoisomerase II-DNA ternary complex at its binding site in GyrA^[17, 24]. The formation of this ternary complex prevents the release of DNA which eventually leads to cell death^[20].

In Gram positive bacteria, the role of DNA topoisomerase IV is similar to cytoplasmic gyrase and is the primary target for ciprofloxacin^[24] in these strains. Fluoroquinolone also forms a ternary complex with DNA^[26] and topoisomerase IV during bacterial cell division, this then prevents the DNA replication, ultimately, causing cell apoptosis^[20].

Linus L Shen *et al.*^[27] hypothesised that in order for the cell to apoptose successfully, four molecules of ciprofloxacin **4** are required, and stack in the binding pocket^[27] (Figure 7). Intermolecular interactions such as hydrogen bonding and hydrophobic interactions are essential for stabilising the complex between drug, bacterial DNA and enzymes^[27]. Therefore, the functional groups in ciprofloxacin **4** play a role in stabilisation (Figure 8).

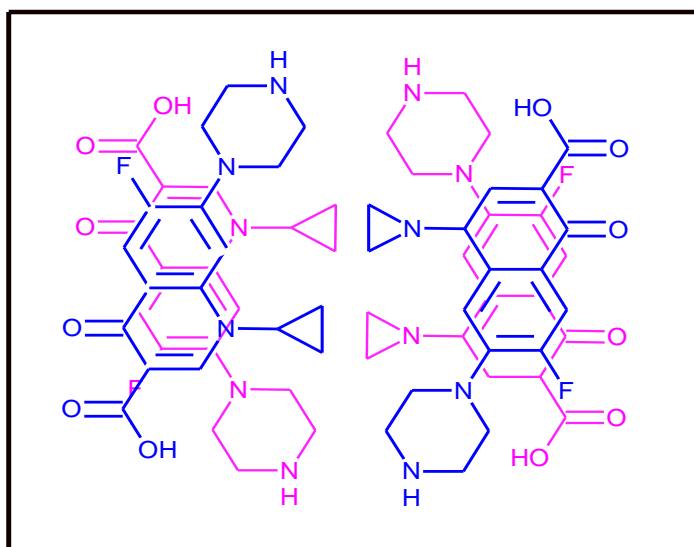


Figure 7: Proposed stacking of ciprofloxacin 4^[27]

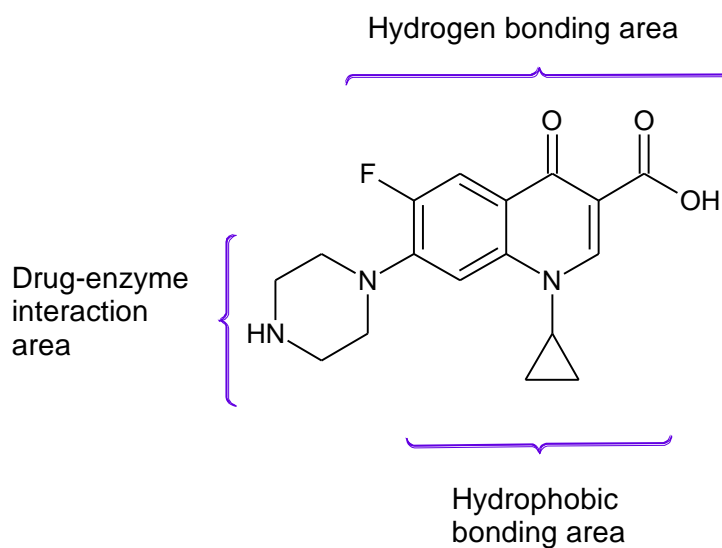


Figure 8: Proposed important domains for stabilising the drug-DNA-enzyme complex^[27]

1.3.2 Resistance Mechanisms Displayed By Fluoroquinolone Antibiotics

The primary resistance mechanism is the mutation of the target enzymes, DNA gyrase in Gram negative bacteria and DNA topoisomerase IV in Gram positive bacteria. Alteration is due to substitutions of amino acids^[28] within the quinolone-resistance determining region (QRDR) in the A subunit of gyrase or in the *parC* subunit in topoisomerase IV. In *E. coli*, QRDR is a narrow region between amino acid residues of 51 to 106 in DNA gyrase^[29]. The amino acid substitutions result in the fluoroquinolone no longer forming a complex with gyrase-bacterial DNA so bacterial cell division occurs even in the presence of intracellular fluoroquinolones.

The secondary resistance mechanism to fluoroquinolone is a decrease in cell membrane permeability^[30]. This is due to mutations in the regulatory genes^[17] which lead to a reduction in the expression of the outer membrane porins such as OmpF^a in *E. coli*^[31] and D2^a in *P. aeruginosa*^[32]. Decreased expression of cell membrane porins leads to a sub lethal intracellular concentration of fluoroquinolones.

Another factor that lowers the intracellular concentration of fluoroquinolones is overproduction of efflux proteins. Efflux proteins are proteins that expel the drug from the cell. For example *E. coli* has the AcrAB-TolC efflux system^[33] that pumps out toxic chemicals including fluoroquinolones. Overproduction of AcrA proteins will expel ciprofloxacin from the bacterial cell^[20] reducing the intracellular ciprofloxacin concentration allowing it to survive exposure to ciprofloxacin **4**.

Another more recently discovered mode of resistance is gyrase-protecting proteins. These proteins are designed to temporarily protect gyrase enzymes^[34] from attack by fluoroquinolones. For example, Qnr proteins protect DNA gyrase from interaction with ciprofloxacin **4**^[35] resulting in failure to form the DNA-gyrase-ciprofloxacin.

^a OmpF and D2 are responsible porins for the uptake of hydrophilic fluoroquinolones.

1.4 Siderophores

Iron is the fourth most abundant element in the Earth's crust^[36, 37]. It is one of the most important transition metals in biological proteins and is found in key enzymes such as haemoglobin. Under aerobic conditions, iron is present as ferric iron, which has a very low solubility in water at neutral pH (K_{sp} of $\text{Fe}(\text{OH})_3$ approx. 10^{-39} M)^[36, 38, 39].

Due to the limited availability of soluble iron in the environment, bacteria synthesise and secrete low molecular weight, high affinity ferric iron-chelating agents called *siderophores*^[37] in order to survive. The main function of siderophores is to capture, solubilise and transport the iron in the form of a Fe^{3+} -siderophore complex^[38].

All siderophores contain iron-binding sites^[36]. In order for the siderophore to successfully bind iron it has an arrangement of atoms which can chelate ferric iron^[36] forming an iron-siderophore complex. Since the bound ferric ion possesses a d^5 high-spin electronic configuration^[40] and the siderophore acts as a ligand, an octahedral complex is formed^[41] which generally contains three bidentate chelation units per ferric iron^[42] (Figure 9). Due to the chelate effect, the thermodynamic stability of these complex is increased^[42].

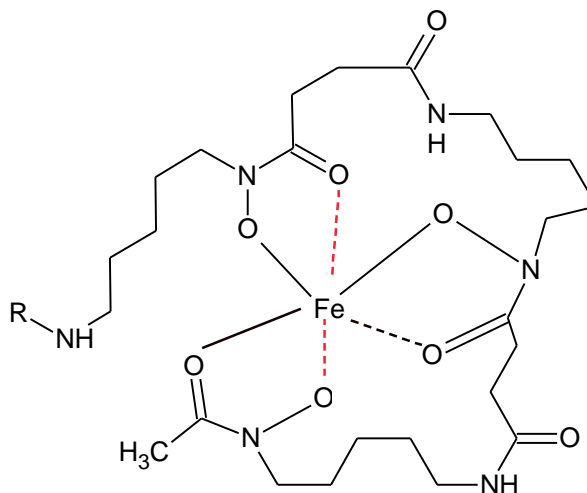


Figure 9: Iron (III) complex of a hydroxamate siderophore

1.4.1 Siderophore Classes

Siderophores can be divided into four different classes based on the nature of iron binding moieties: α -hydroxycarboxylate, catecholate/ phenolate, hydroxamate and mixed ligand siderophores.

1.4.1.1 α -Hydroxycarboxylate Siderophores

Siderophores that contain both hydroxyl and carboxylate ligands are classed as α -hydroxycarboxylate siderophores. The ligands are linked to a suitable backbone to form the siderophore. The simplest siderophore in this class is citric acid **14**^[38, 43] which is thought to carry the ferric iron as the *bis* ferric-citrato complex, (Fe-citrate)₂ which is recognised by the outer membrane protein, FecA^[38] in *E. coli*. A more structurally complex example of α -hydroxycarboxylate siderophore is achromobactin **13** which contains three α -hydroxycarboxylate groups: two α -hydroxycarboxylates from α -ketoglutarate and one from citric acid **14**^[38]. Other siderophores in this class, Staphyloferrin A **15**, secreted by *Staphylococcus hyicus*^[44] and Rhizoferrin **16** isolated from *Rhizopus* and members of *Zygomycetes*^[45], both have two citric acids units linked by ornithine and diaminobutane backbones^[38], respectively. Another example of this class of siderophore is vibrioferrin **17**, a *bis* α -hydroxycarboxylate siderophore, where the α -hydroxycarboxylate ligands are derived from citric acid and α -ketoglutarate^[38]. (Figure 10)

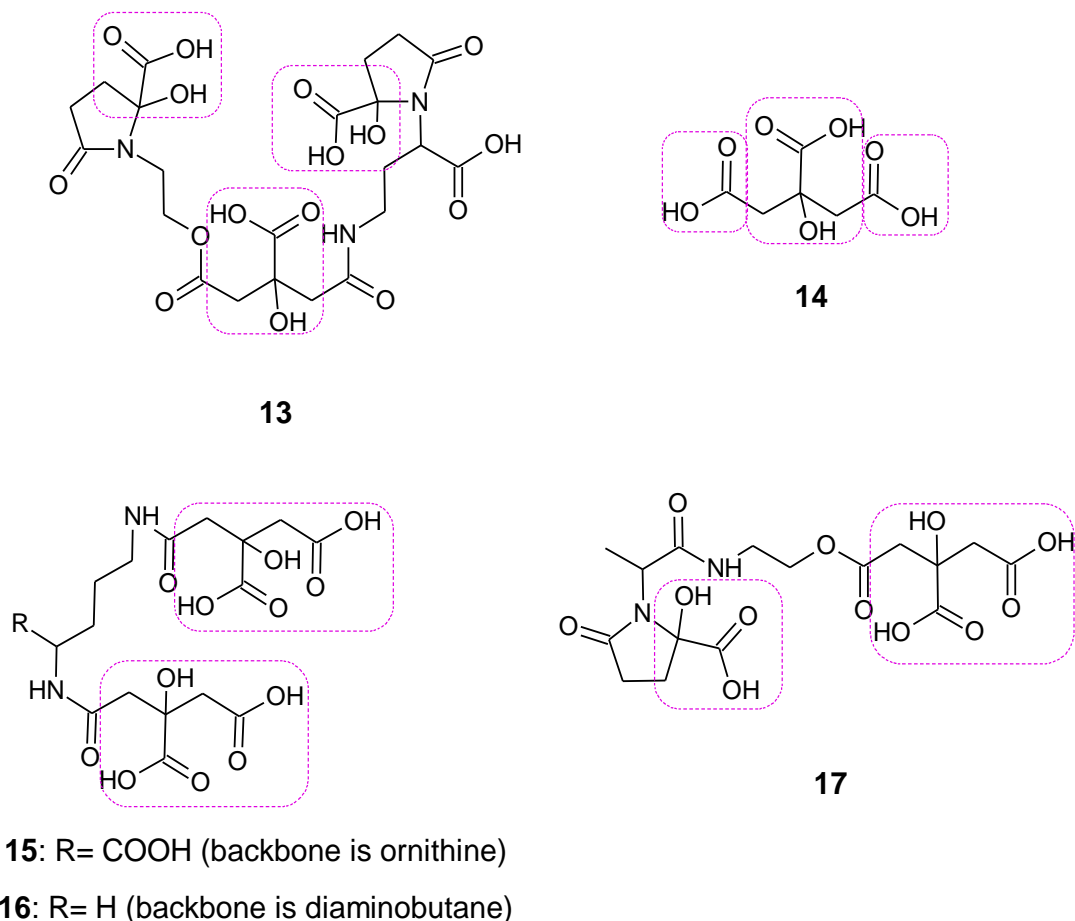


Figure 10: α -hydroxycarboxylate siderophores

1.4.1.2 Catecholate/ Phenolate Siderophores

Siderophores that utilise phenolate or 2, 3-dihydroxybenzoate (DHB) to chelate Fe^{3+} are classified as *catecholate/ phenolate* siderophores. The first tricatecholate siderophore isolated in 1970 was Enterobactin **18** which was isolated from culture fluids of *Aerobacter aerogenes*, *E. coli* and *Salmonella typhimurium*^[46]. Enterobactin **18** is cyclic *tris*-(2,3-dihydroxybenzoyl-L-serine)^[38] where L-serine forms a cyclic triester scaffold which holds the three catecholate ligands. Bacillibactin **19**, extracted from *Bacillus subtilis*^[47] is another cyclic *tris* catecholate siderophore which is structurally similar to Enterobactin. In Bacilibactin, L-threonine is used as a cyclic triester scaffold with glycine spacers elongating the chelating arms^[47]. Salmochelin **20**, isolated from *S. enteric* and uropathogenic *E. coli*^[38, 48] is a glucosylated

Enterobactin derivative, where the two catechols contain a glucose moiety^{38, 49]. (Figure 11)}

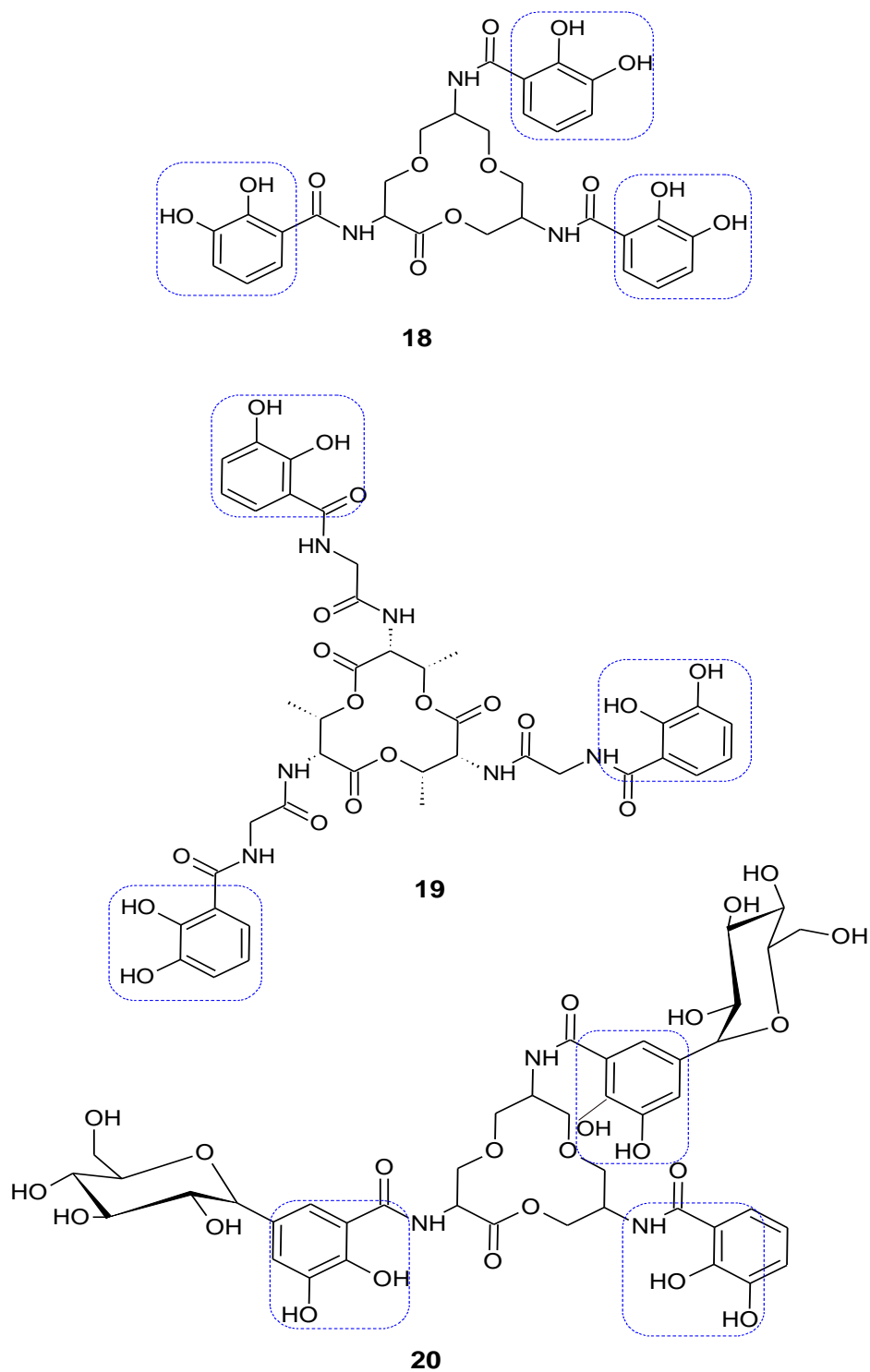


Figure 11: Catecholate siderophores

1.4.1.3 Hydroxamate Siderophores

Hydroxamate siderophores contain hydroxamate groups as their iron binding ligands. Microorganisms synthesise this type of siderophores by direct oxidation of amines followed by acylation^[50, 51]. Examples of *tris* hydroxamate siderophores are Ferrioxamines, which are comprised of alternate units of succinic acid and a monohydroxylated diamine^[38]. Desferrioxamine B (DFOB) **21** is used clinically for treating iron overload^[38, 52]. Other ferrioxamines are Desferrioxamine E **22** which is a cyclic siderophore and Desferrioxamine G **23** which is linear^[53]. (Figure 12)

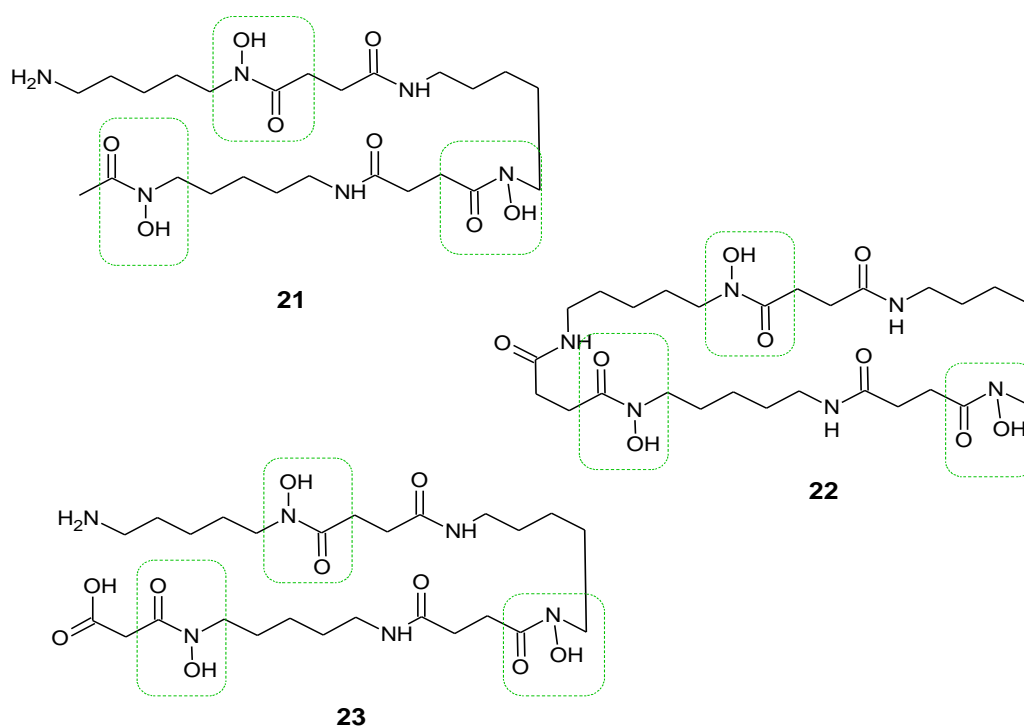


Figure 12: Ferrioxamine siderophores

1.4.1.4 Mixed Ligand Siderophores

Mixed ligand siderophores contain more than one type of ligand. An example is aerobactin **24** which contains α -hydroxycarboxylate and hydroxamate ligand moieties from citric acid and 6-[acetyl (hydroxy) amino]-2-aminohexanoic acid, respectively. Petrobactin **25**^[54], isolated from *Bacillus species*, is another example of a mixed ligand siderophore. This siderophore combines a α -hydroxycarboxylate with two 3,4-dihydroxybenzoyl ligand moieties. Ornibactin **26**^[55] isolated from strains of *Pseudomonas* is composed of linear hydroxamate and hydroxycarboxylate ligands. (Figure 13)

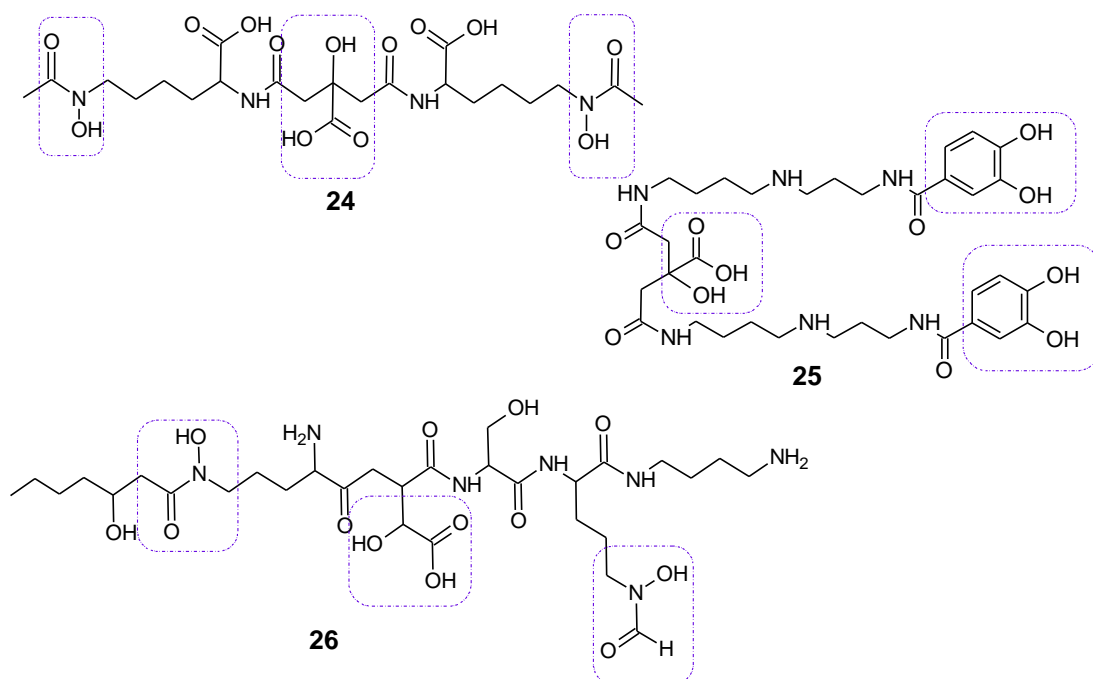


Figure 13: Mixed ligand siderophores

1.4.2 Fe (III)-Siderophore Complex Transport Mechanism

The ferric iron may be released from the siderophore complex by reduction to ferrous iron at the extracellular surface of the bacteria and the iron is taken up^[40]. Alternatively, the whole siderophore complex is internalised by the bacteria and the iron released inside the cell^[40].

Gram negative bacteria contain an outer membrane, periplasmic space and a cytoplasmic membrane; whereas in Gram positive bacteria have one thick peptidoglycan cell wall and cytoplasmic membrane. In Gram negative bacteria, the transportation of the ferric iron-siderophore complex is more complex than in Gram positive bacteria.

In bacteria, especially Gram negative bacteria, an energy dependent system is required in order for the whole complex^[56] to pass from the extracellular space to the intracellular cytoplasmic space. Firstly, the complexes need to be recognised by the outer membrane binding protein which carries the complex into the periplasm. The complex is taken by the cytoplasmic membrane transport proteins to the cytoplasm of the bacteria^[38]. In Gram positive bacteria, the Fe³⁺- siderophore complexes are recognised by specific membrane receptor proteins and directly transported into the cytoplasm by ABC-transport proteins^[38, 57].

1.4.2.1 Outer Membrane Recognition

The outer membrane of Gram negative bacteria contains receptors used to recognise Fe(III)-siderophore complexes. This outer membrane receptor-Fe (III) ion-siderophore interaction is highly specific^[58]. The specificity depends on the ligands used to form the iron siderophore complex. There are many receptors that have been discovered through the crystallisation method, X-ray and genetic analyses^[38]. FhuA is used to transport the hydroxamate type of siderophore^[59], FepA, the catecholate-type of siderophore^[60] and FecA receptor for δ -hydroxycarboxylate-type of siderophores^[61] in *E. coli*.

All of these membrane proteins have similar core structures and domains. All of them consist of a 22 antiparallel β -strand barrel and a 'cork'^[62]. The difference between these protein receptors is the protein-iron-siderophore complex binding site where it is 'unique' to the particular metal-siderophore complexes^[38].

The outer membrane receptor interacts with tonB-ExbB-ExbD complex that is anchored in the inner membrane^[38, 63]. This complex is responsible for the transduction of the proton motive force energy to the receptor protein so that the Fe³⁺-siderophore complex can enter the periplasmic space^[38, 63].

1.4.2.2 Periplasmic-Binding Protein

Once it has entered the periplasmic space, the complex is bound and delivered into the cytoplasmic membrane by periplasmic binding proteins such as FhuD (hydroxamate siderophores)^[64], FepB (enterobactin)^[65], and FecB (ferric dicitrate)^[66].

1.4.2.3 Cytoplasmic ABC Transporters

After binding to the periplasmic-binding protein, the ferric iron-siderophore complex is then translocated across the cytoplasmic membrane by an ABC transporter (**A**T**P** **B**inding **C**assette)^[38]. This protein consists of two subunits: one which is used to span the membrane and the second is able to hydrolyse ATP to supply energy for translocation^[37]. Hydrolysis or/and binding of ATP causes a change the conformation of the protein so that the whole complex can enter the cytoplasmic space of the bacteria^[67].

1.4.2.4 Iron Release

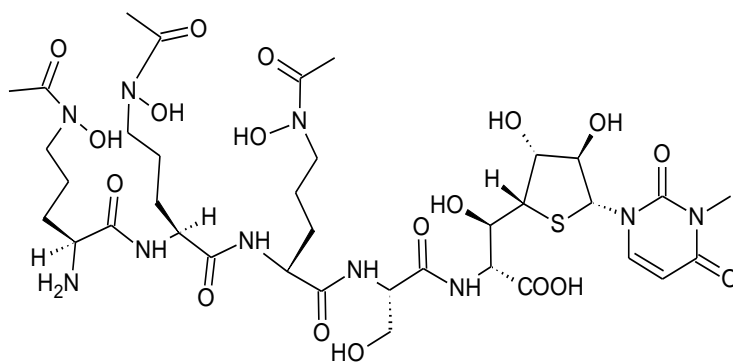
Once it has entered the cytoplasm, iron is released by mechanisms involving either degradation or chemical modification of the iron carrier and/or reduction of the iron(III) to iron(II)^[68, 69]. For example, pyoverdinin in *P. aeruginosa*, iron is released not through the mechanism of chemical modification, but it is released from the chelator by reduction of iron^[69, 70].

1.5 'Trojan Horse' System

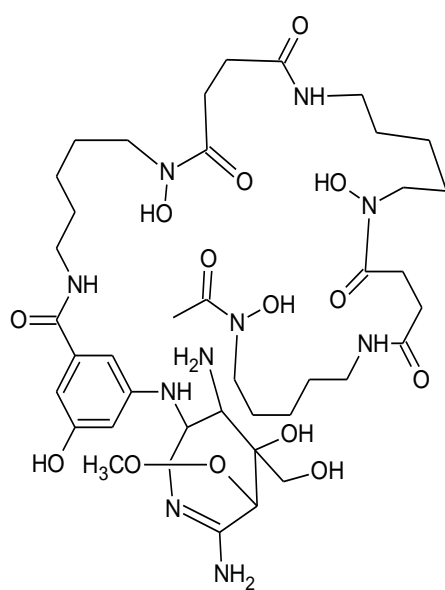
Hydrophilic molecules such as ciprofloxacin **4** usually enter the bacteria via porins, such as OmpF. The resistance mechanism that reduces the expression of these porins can lead to a sub-lethal concentration of antibiotic. In order to circumvent this problem, a 'Trojan horse' strategy has been devised, where a drug can be delivered by the ferric-siderophore transport system. This strategy is inspired by natural siderophore-drug conjugates^[40]. Examples of natural siderophore-drug conjugates are Albomycin **27**^[71], Ferrimycin **28**^[72] and Salmycin D **29**^[73] (Figure 14).

1.5.1 Natural Siderophore-Drug Conjugates

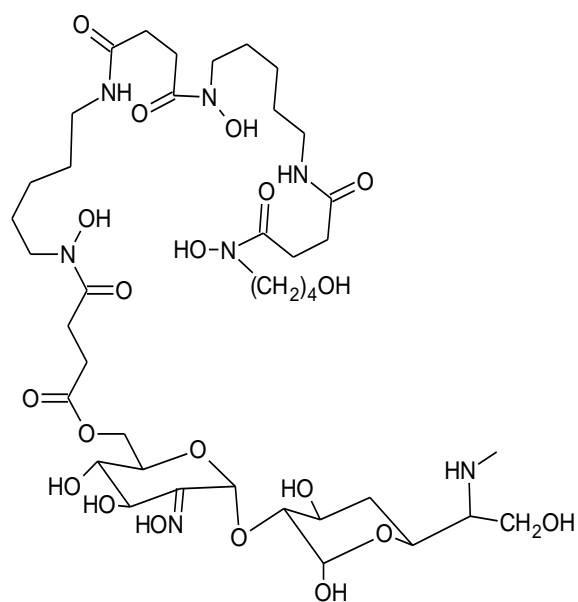
The 'Trojan Horse' strategy is inspired by the natural siderophore-drug conjugates. Albomycins **27**^[71], use δ -*N*-hydroxy- δ -*N*-acetyl-L-ornithine residues to chelate ferric iron, with the antibiotic attached via serine spacer^[36, 74]. Another example of natural siderophore-drug conjugates is Ferrimycins **28**^[72] which uses ferrioxamine B as the siderophore, conjugated to a toxin via an amide linker. Salmycins D **29**^[73] utilise a trihydroxamate siderophore conjugated to an aminoglycoside antibiotic through a dicarboxylic acid spacer^[74]. These three natural siderophore-drug conjugates are not being used clinically since they are not readily available and their antibiotic modes of action are complex^[36]. It has also been shown that organisms rapidly develop resistance to these natural siderophore-drug conjugates^[36, 75]. (Figure 14)



27



28



29

Figure 14: Natural siderophore-drug conjugates

1.5.2 Synthetic Siderophore-Drug Conjugates

The components of a synthetic 'Trojan Horse' strategy consist of a siderophore, a linker and a drug (Figure 15). The siderophore must retain the ability to bind iron to enable it to be taken up into the bacterial cell. The linker is used to chemically conjugate the drug to the siderophore. This linker will either remain attached the drug to the complex or released chemically or

enzymatically within the bacterial cell^[76]. The choices of the drug are depending on the bacterial target and its suitability towards chemical conjugation^[51].

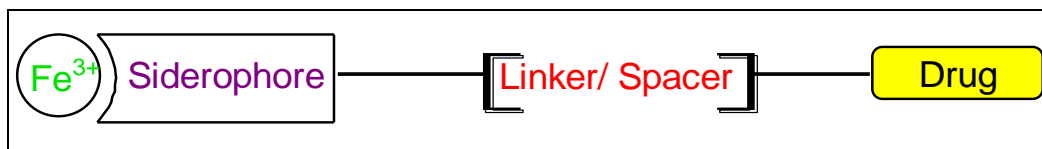


Figure 15: Components in the 'Trojan Horse' System

1.5.2.1 Cyanuric Acid- β -Lactam Conjugates

Manuka Ghosh and Marvin J. Miller have successfully synthesised cyanuric acid-based siderophore- β -lactam conjugates **30** (Figure 16) and evaluated their biological activities^[77]. Carbacephalosporin and its derivative-Lorabid, were used as the antibiotics and isocyanuric-based trihydroxamate as the siderophore component. They also have shown that these type of synthetic siderophore-drug conjugates were active against *E. coli* X580 in preliminary biological test^[77].

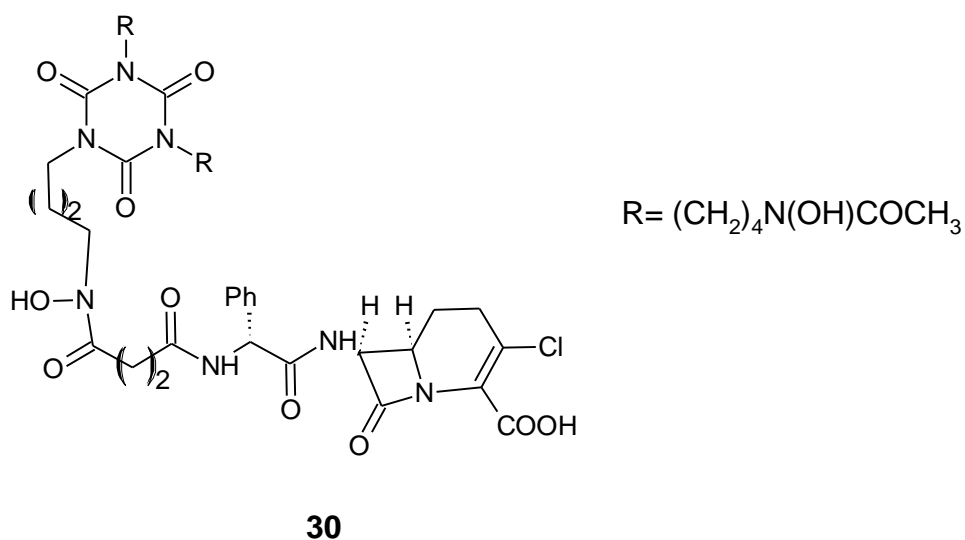
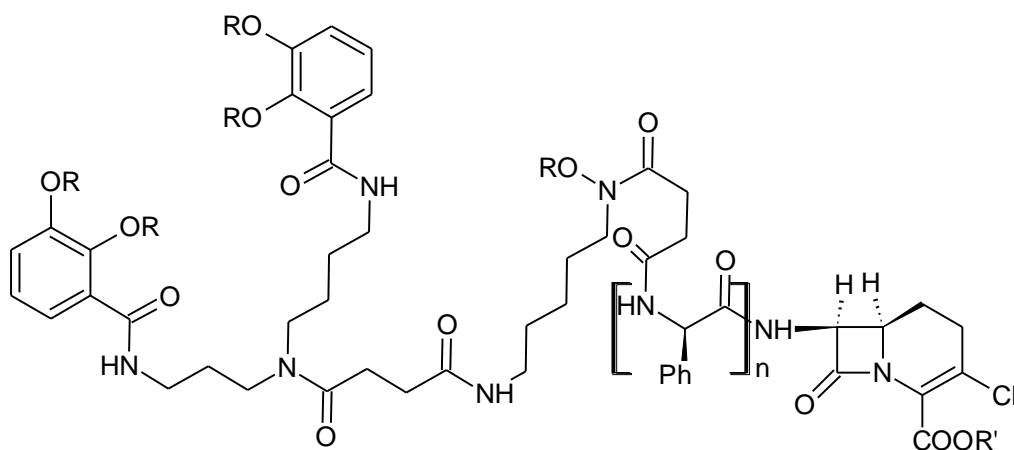


Figure 16: Cyanuric- β -Lactam conjugate

1.5.2.2 Mixed-Ligand Siderophore- β -Lactam Conjugates

Arun Ghosh *et al.*^[78] have successfully synthesised synthetic siderophore-drug conjugates which consist of two *bis* catecholates and one hydroxamate ligands conjugated to β -lactam antibiotics, carbacephem and Lorabid to form mixed ligand-carbacephem **31** and mixed ligand-Lorabid **32**^[78] (Figure 17). They also evaluated the biological activity of the synthetic conjugates and found that using mixed ligand siderophores gave active compounds. They proposed success in using mixed ligand siderophores was due to the presence of multiple siderophore transport pathways in the outer cell membrane of the bacteria^[78].



31: R=R'=H, n= 0

32: R=R= H, n= 1

Figure 17: Synthetic mixed ligand-drug conjugates

1.5.2.3 Citrate Based- β -Lactam Conjugates

Arun Ghosh and Marvin J. Miller^[79] have reported citrate based- β -lactam conjugates using citric acid as the siderophore and carbacephem and Lorabid as the antibacterial agents to form citrate-carbacephem conjugate **33** and citrate-Lorabid conjugate **34**^[79] (Figure 18). They also evaluated the efficacy of these conjugates against *E. coli* X580, and illustrated that both of the conjugates suppressed bacterial growth in iron-sufficient media, and completely inhibited the growth of the bacteria in iron-deficient conditions^[79]. It was concluded that a simple α -hydroxycarboxylate siderophore was accepted by the bacteria and delivered via the active-delivery system^[79].

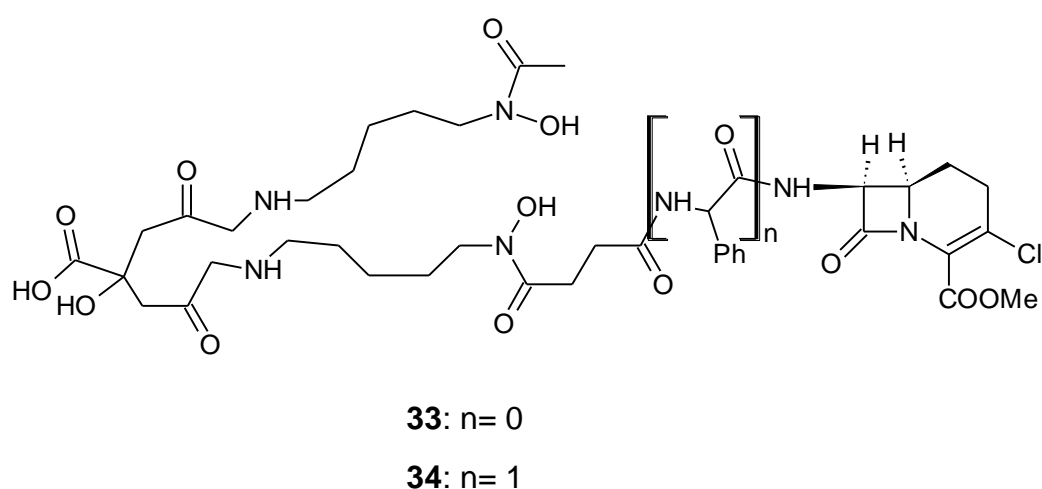


Figure 18: Synthetic citrate-based siderophore-drug conjugates

1.5.2.4 Citrate Based-Ciprofloxacin Conjugates

Recently, Md Saleh *et al.*^[80] successfully synthesised citrate based-ciprofloxacin conjugates, 1,3-citric acid-ciprofloxacin **35** and 1,5-citric acid-ciprofloxacin **36** (Figure 19). They also evaluated the drug conjugates efficacy against clinically relevant bacteria. It was proposed that both citrate based-ciprofloxacin conjugates were able to reach to the intracellular target, but there was no improvement on the activity of the drug conjugates when compared to the parent antibiotic, ciprofloxacin **4**^[80].

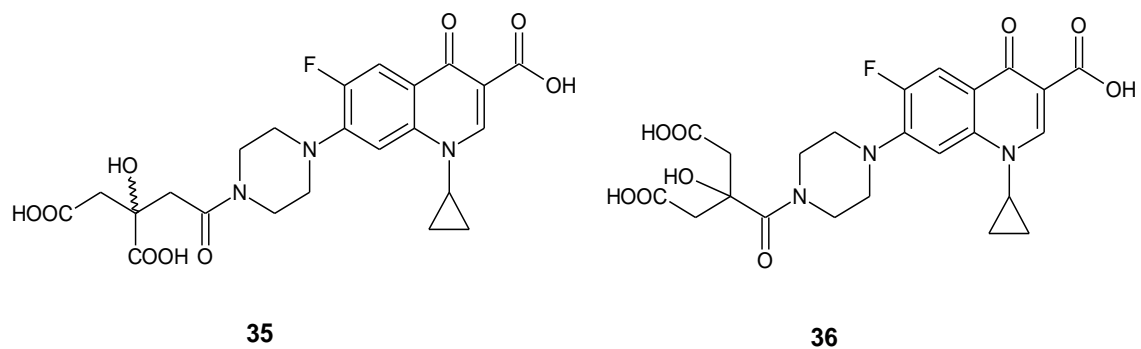


Figure 19: Synthetic citrate-ciprofloxacin conjugates

1.6 Objectives

The aim of this project is to synthesise new siderophore-drug conjugates with ciprofloxacin as the drug and a citric acid as the siderophore unit. Different amino acids will be used as linkers to provide a spacer between the siderophore and the drug. A citrate-ciprofloxacin conjugate with a glycine linker **37** has been synthesised previously and it showed antimicrobial activity albeit lower than the parent antibiotic. The citrate-ciprofloxacin conjugate **38** with glycine linker but with different regiochemistry at the citric acid moiety will be synthesised to allow a direct comparison with **37**. An alternative linker, L-serine will also be explored as this linker has hydrogen bonding potential, increasing the hydrophilicity of the siderophore-drug conjugate **39**. The conjugates will be screened in the Bradford Infection Group, University of Bradford.

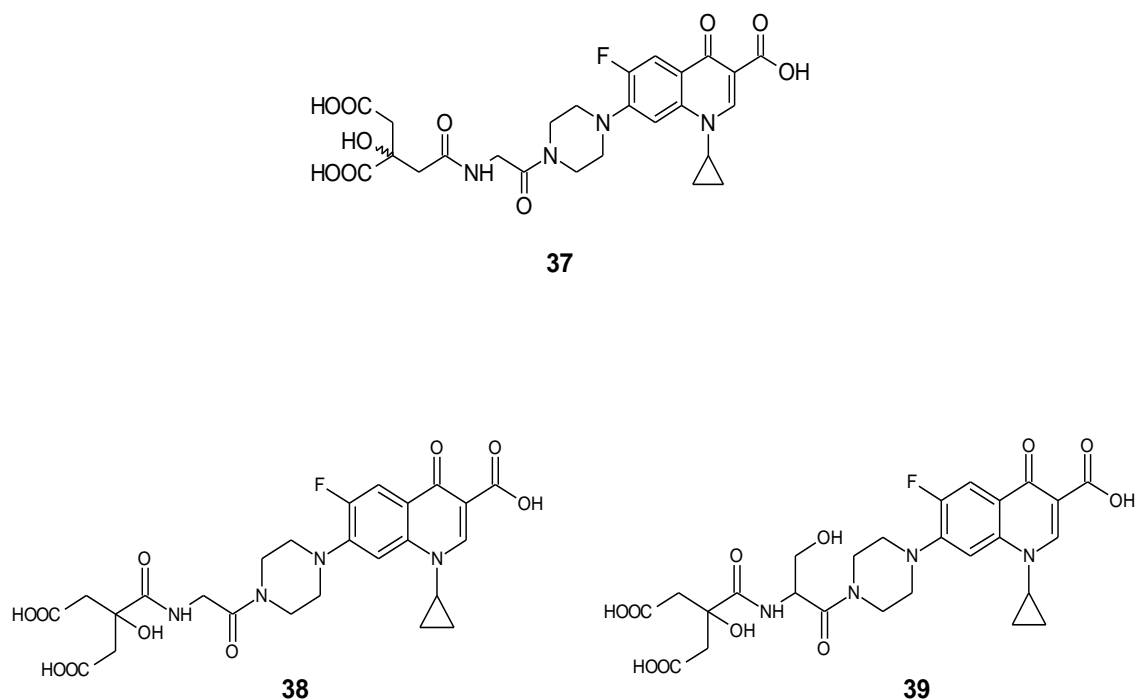
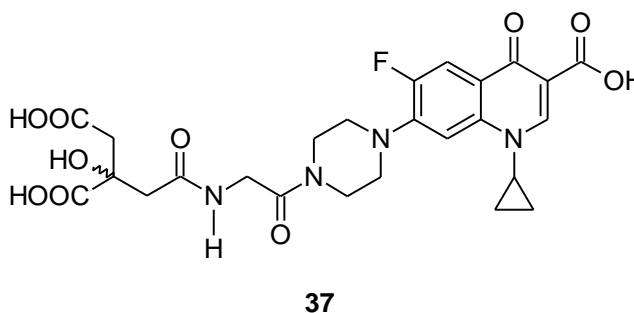


Figure 20: Structures of citric acid-ciprofloxacin conjugates

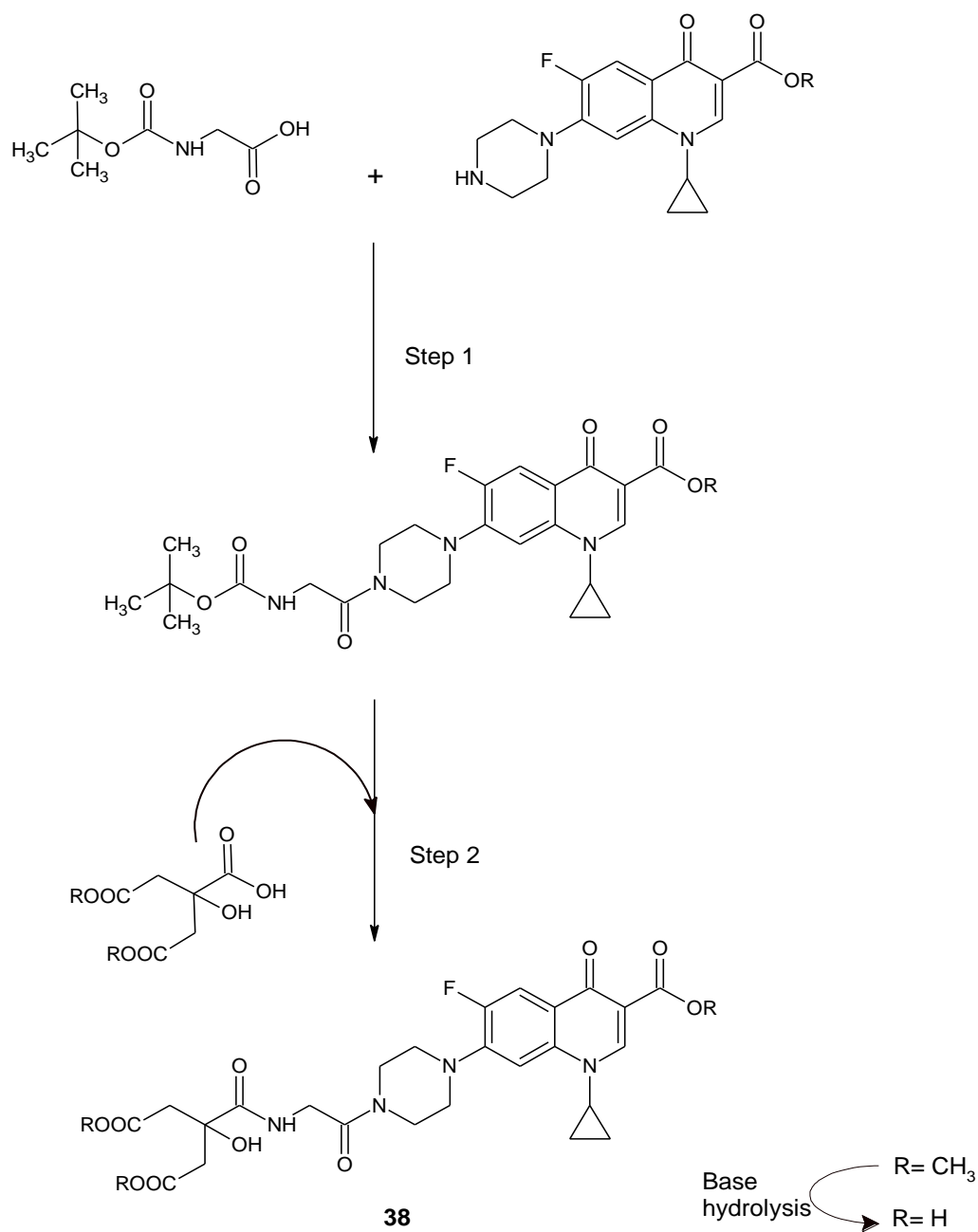
2 Results and Discussions

2.1 1, 5-Citrate-ciprofloxacin conjugate using Glycine as the linker

Citric acid **14** is one of the simplest siderophores^[37]. It is a δ -hydroxycarboxylate-type siderophore containing two potential iron-binding groups, hydroxyl and carboxylic acid. *E. coli*^[81] and *P. aeruginosa*^[82] use citric acid **14** to solubilise, capture and transport Fe^{3+} from the environment via the active pumps such as FecA, even though citric acid itself has low affinity for Fe (III)^[83]. The successful use of citric acid by bacteria, means that it has potential to be used as a shuttle for transporting an antibiotic across the bacterial membrane via the siderophore transport mechanism in the Trojan Horse strategy. The 1,3-citrate-glycine-ciprofloxacin conjugate **37** has been synthesised^[84], and screened against a panel of clinically relevant bacteria. Synthesis of the regioisomeric conjugate **38** would allow investigation into the influence of the citrate residue on the antimicrobial activity of the conjugate.

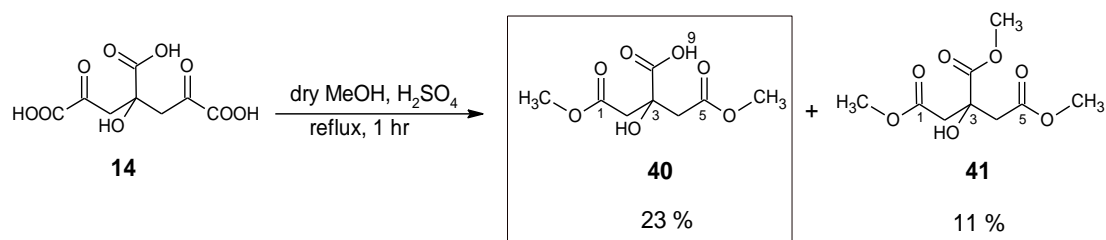


The proposed synthesis of the first target molecule; 1,5-citrate-Glyciprofloxacin conjugate **38** is shown in Scheme 1.



Scheme 1: The proposed synthesis of **38**

The first step toward the target molecule requires selective protection of the primary carboxylic acid groups. This was achieved by carefully controlled methylation^[85] (Scheme 2).

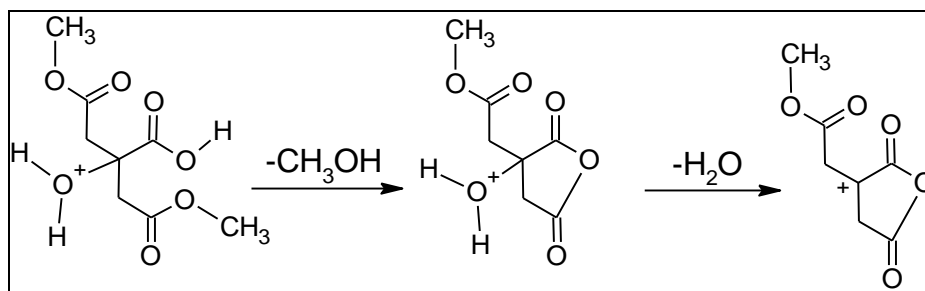


Scheme 2: Regioselective methyl protection of citric acid

1,5-dimethyl citrate **40** was successfully synthesised from commercially available citric acid **14** using sulfuric acid in anhydrous methanol. The reaction gave 23 % yield of 1,5-dimethyl citrate **40**. Reaction time is critical when synthesising **40** as prolonged reaction time gives an increased amount of 1,3,5-trimethyl citrate **41**. Any **41** formed in the reaction was separated from 1,5-dimethyl citrate **40** by extraction into chloroform, the minimum amount of 1,3,5-trimethyl citrate **41** formed in the reaction was limited to 11 %.

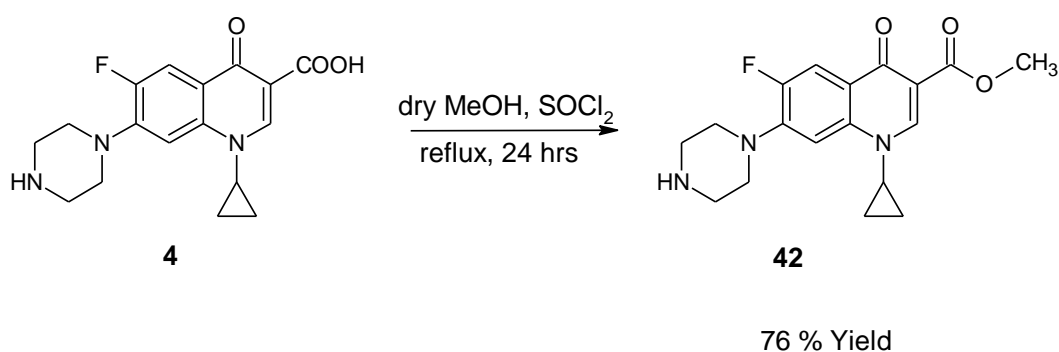
The successful synthesis of **40** was supported by ^1H NMR spectroscopy. Inspection of the spectrum showed a signal at 3.66 ppm with a relative integration of six, corresponding to two methyl groups at position 1 and 5. In the mass spectrum, m/z peak at 221.0658 $[\text{M}+\text{H}]^+$ was observed corresponding to the molecular formula of $\text{C}_8\text{H}_{13}\text{O}_7$.

Two other peaks were observed in the mass spectrum at m/z 189 and 171. The m/z peak 189 is proposed to arise from the parent ion m/z 221 through cyclisation. Further fragmentation results in m/z peak 171 (Scheme 3).



Scheme 3: Proposed cyclisation and fragmentation of 1,5-dimethyl citric acid **40** in mass spectrometry, respectively

Ciprofloxacin methanoate **42** was synthesised from free ciprofloxacin **4** using thionyl chloride-mediated methylation (Scheme 4).



Scheme 4: Synthesis of ciprofloxacin methanoate **42** from ciprofloxacin **4**

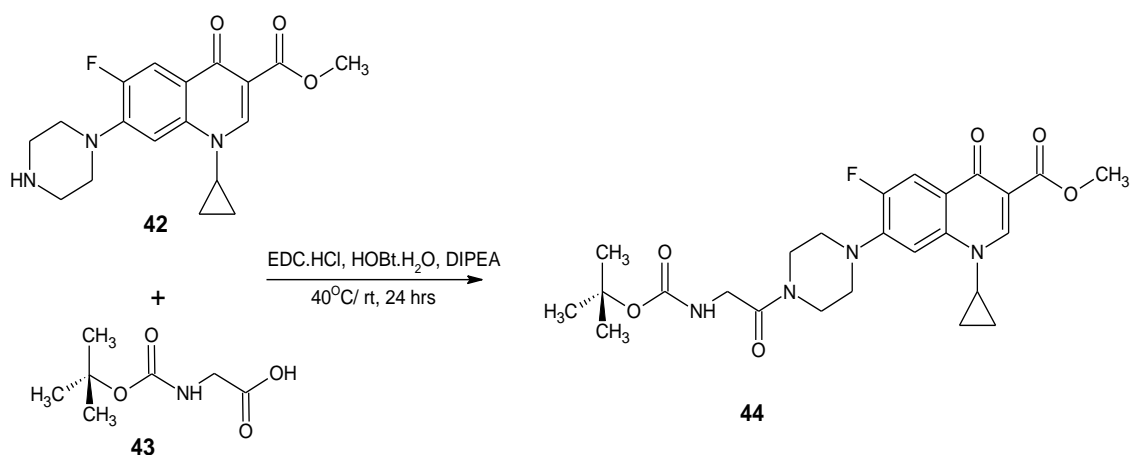
Commercially available ciprofloxacin **4** was esterified using anhydrous methanol under reflux in the presence of thionyl chloride. Ciprofloxacin methanoate **42** was isolated in 76 % crude yield.

The successful synthesis of **42** was supported by ¹H NMR spectroscopy, the spectrum showed a signal at 3.90 ppm with a relative integration of three due to the methyl group. The presence of the methyl group was also

supported by analysis of the carbon-13 spectra, where an extra peak at 51.7 ppm was observed.

The successful synthesis of ciprofloxacin methyl ester **42** was confirmed by mass spectrometry where the m/z peak at 346.1563 $[M+H]^+$ was observed corresponding to molecular weight of $C_{18}H_{21}FN_3O_3$.

Ciprofloxacin methanoate **42** was then conjugated with the amino acid linker, *N*-(*tert*-butoxycarbonyl)-Gly-OH **43** using EDC-mediated coupling reaction^[86]. Nakajima *et. al*^[87] states that the coupling reaction is best done under basic conditions, and therefore, a non-nucleophilic Hünig base, diisopropylethylamine (DIPEA) was used in the reaction (Scheme 5).



Scheme 5: Amide coupling reaction of **44**

The linker-drug conjugate **44** was initially synthesised using anhydrous DMF as a solvent, but it gave only 55 % crude yield contaminated by DMF impurities. Therefore, in order to avoid using DMF, different solvents such as anhydrous methanol and methanol-aqueous media were explored. Using methanol as a solvent is, in theory, problematic due to its ability to act as a nucleophile and the amide coupling reaction being a nucleophilic acyl

substitution reaction. Therefore, a polar-aprotic solvent was expected to be the best for this reaction. Using anhydrous methanol increased the reaction yield by 14 %. Methanol-aqueous media was also tried at higher temperature and was observed to double the yield compared to the reaction with anhydrous DMF (Table 3).

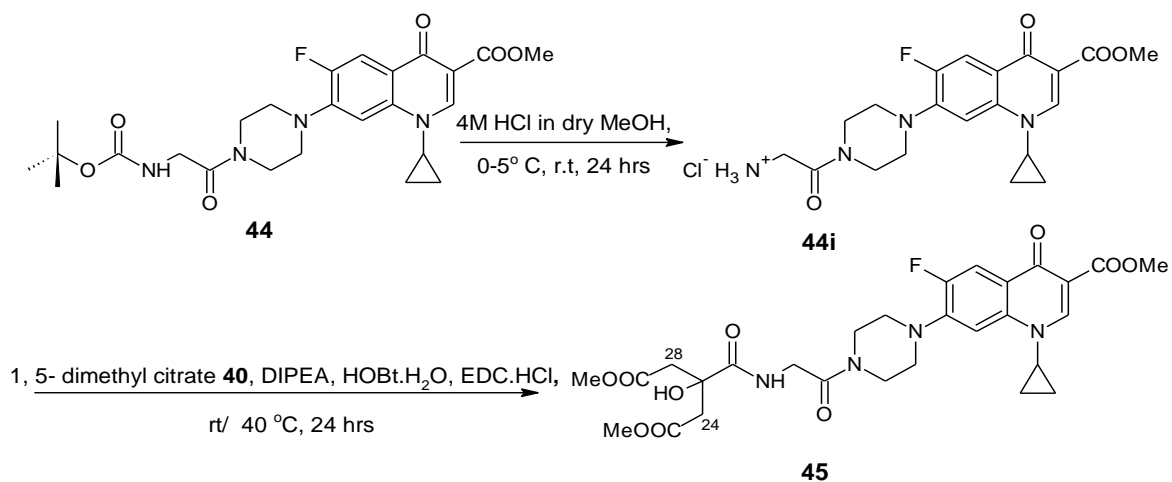
Reaction	Solvent	Percentage yield of isolated 44	Temperature °C
1	dry DMF	55	25
2	dry MeOH	69	25
3	MeOH-aqueous media	84	40

Table 3: Isolated yield of **44** using different solvents systems

The idea of using this polar-protic solvent with EDC.HCl as an activator was proposed by Yangwei *et al.*^[88].

The successful conjugation of ciprofloxacin methanoate **42** and *N*-(*tert*-butyloxycarbonyl)-Gly-OH **43** to form conjugate **44** was supported by ¹H NMR spectroscopy where the equivalent methyl protons of the *N*-(*tert*-butyloxycarbonyl) protecting group were found at 1.47 ppm in the spectrum. The singlet corresponding to the secondary piperazinyl amine proton of ciprofloxacin methanoate **42** at 2.17 ppm was absent, replaced by a triplet signal at 5.51 ppm. The triplet peak was due to the enantiotropic protons of the glycine group. This was confirmed by COSY where the amide proton at 5.51 ppm coupled with the enantiotropic protons at 4.04 ppm (Appendix 5). Therefore, this shows the presence of glycine in the linker-drug conjugate **44**. Mass spectrometry showed a *m/z* peak at 503.2320 [M+H]⁺ was observed corresponding to molecular weight of C₂₅H₃₂FN₄O₆.

After successfully synthesising both 1,5-dimethyl citrate **40** and *N*-(*tert*-butoxycarbonyl)-Gly-ciprofloxacin methanoate **44**, they were then coupled to form methyl protected siderophore-drug conjugate **46** (Scheme 6).



Scheme 6: Multistep syntheses towards the synthesis of **45**

Before coupling 1,5-dimethyl citrate **40** to the drug conjugate **44**, the *N*-(*tert*-butoxycarbonyl) protecting group of glycine was deprotected by acid hydrolysis using 4M HCl in anhydrous methanol^[89] to form an ammonium salt. The salt was not isolated, but coupled to 1,5-dimethyl citrate **40** using EDC.HCl and HOBt.H₂O under basic conditions.

Synthesis of **45** was initially carried out using anhydrous DMF, which gave only 33 % yield of **45**, contaminated by DMF impurity. Different solvents were explored. Anhydrous acetonitrile was used since its boiling point is low^b and, it can, therefore, easily be removed from the reaction. Unfortunately, it dissolved the ammonium salt slowly and only gave 21 % isolated yield of **45** (Table 4).

^b Boiling point of acetonitrile is 81.6 °C

Methanol-aqueous media was also explored as this solvent system improved the previous reaction but no significant improvement was observed here since it only gave 35 % overall yield of **45** (Table 4).

Therefore, it can be concluded that changing the solvent system does not improve the yield of **45** within experimental error.

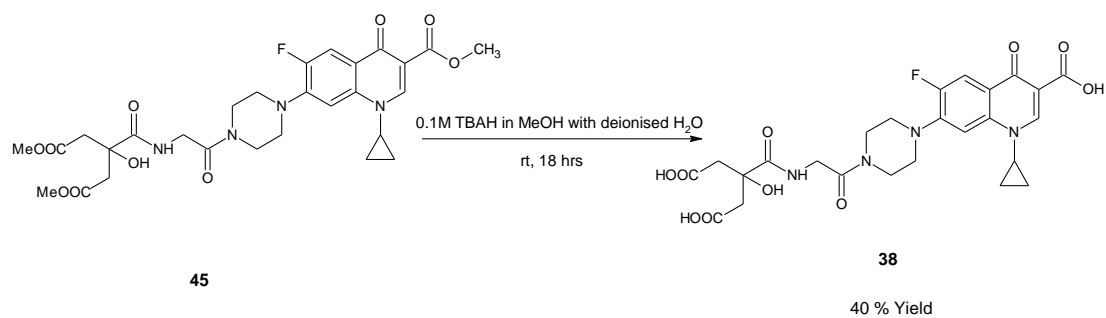
Reaction	Solvent	Percentage of yield of 45	Temperature °C
1	DMF	33	25
2	Acetonitrile	21	25
3	MeOH: aqueous media	35	25

Table 4: Yields of **45** with different solvent system

Another strategy was to maintain anhydrous DMF as the reaction solvent, as this dissolves the organic salt, but the temperature was increased to 40 °C. Work up of the reaction gave 40 % yield of **45**.

The successful synthesis of **45** in all reaction was supported in ESI-MS and ¹H NMR spectroscopy. This was supported by the ¹H NMR spectrum which showed the single peak for *tert*-butyl of *N*-(*tert*-butoxycarbonyl) protecting group at 1.45 ppm was missing, and a new peak had appeared at 3.55 ppm with a relative integration of six protons corresponding to the methyl esters of 1,5-dimethyl citrate apparent. From the mass spectrometry, the *m/z* peak at 605.2257 [M+H]⁺ was observed corresponding to the molecular formula of C₂₈H₃₄FN₄O₁₀.

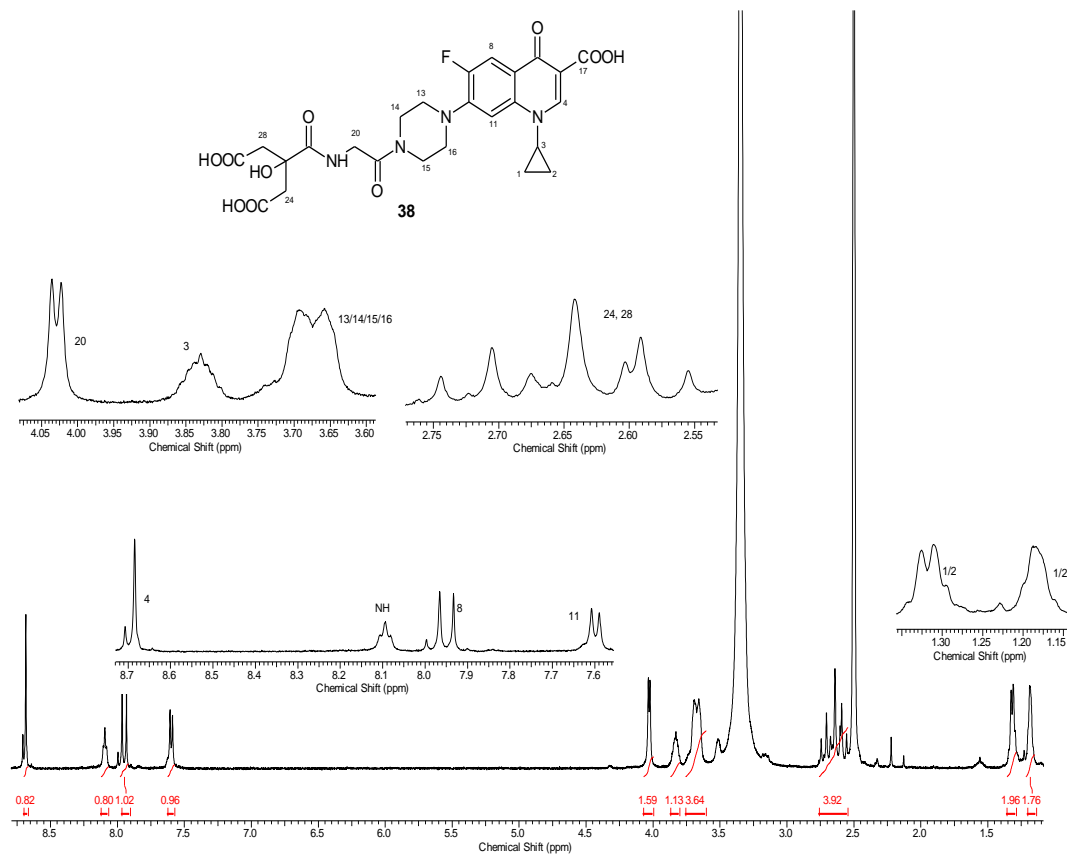
The methyl protected siderophore-drug conjugate **45** was then deprotected using base-mediated hydrolysis to give siderophore-drug conjugate **38** (Scheme 7).



Scheme 7: Synthesis of siderophore-drug conjugate **38**

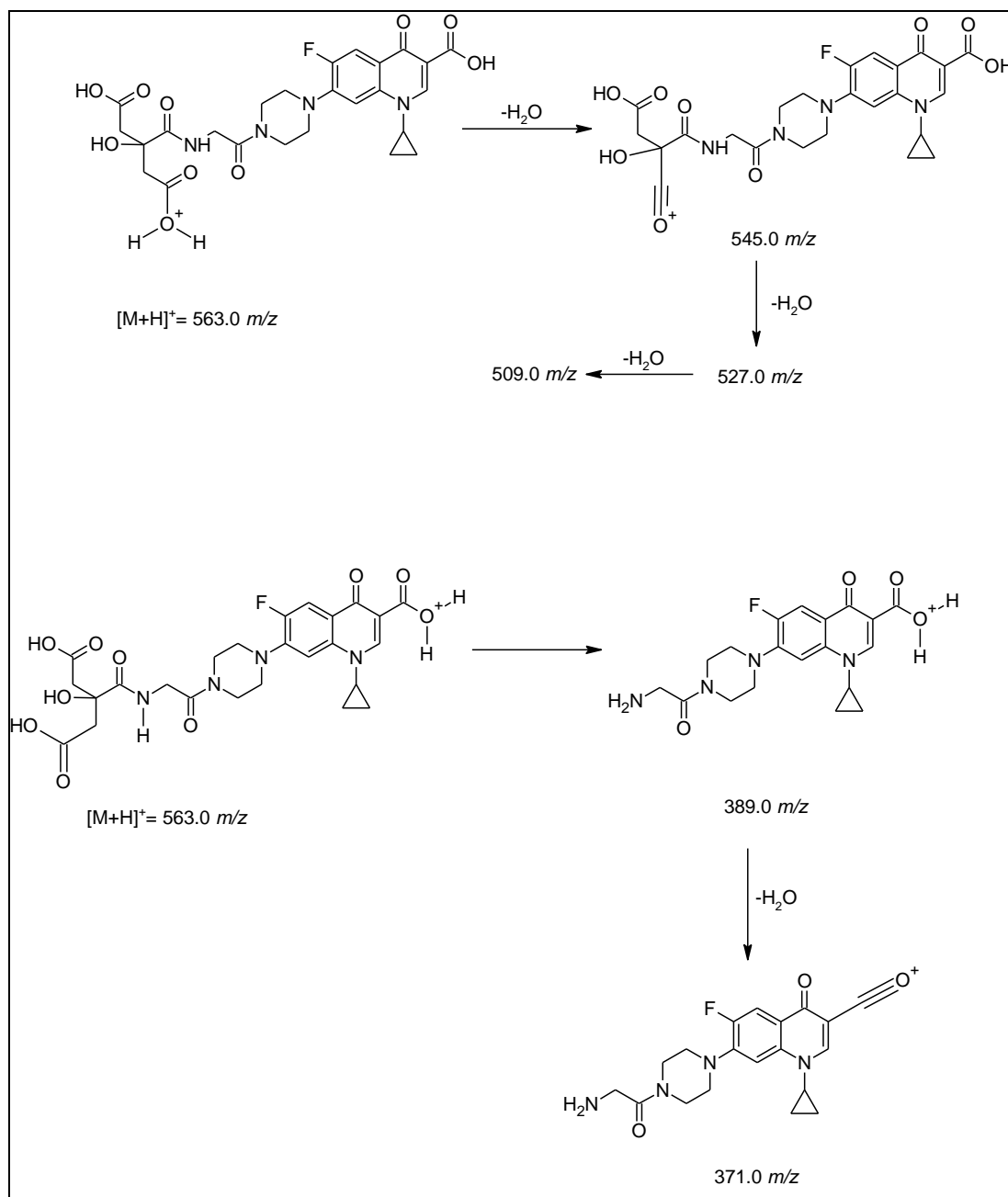
The new siderophore-drug conjugate **38** was synthesised by the global deprotection of methyl esters by base hydrolysis with 0.1M of tetrabutylammonium hydroxide (TBAH) in methanol, this gave **38** in 40 % isolated yield.

This successful synthesis of **38** was firstly inspected from ^1H NMR spectrum, where peaks at 3.55 ppm and 3.73 ppm for methyl esters in 1,5-citric acid and ciprofloxacin respectively were absent (Spectrum 1). Successful cleavage of the methyl ester protecting groups was also supported by ^{13}C NMR spectroscopy, where the carbon-13 peaks at 51.5 ppm and 55.1 ppm were absent (Spectrum not shown).



Spectrum 1: Proton NMR spectrum of **38**

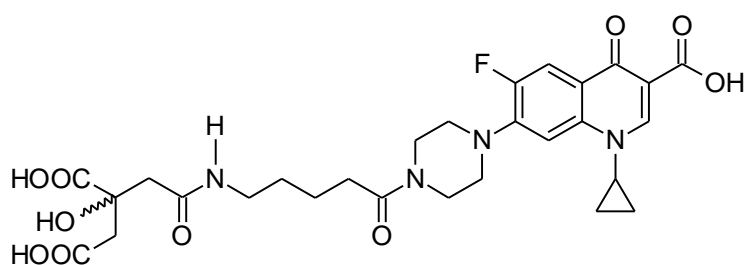
The successful synthesis of **38** was further investigated by mass spectrometry using ESI (+) and ESI (-). The protonated molecular ion was fragmented using collision induced dissociation (CID). From the CID experiment, six peaks were investigated: 563 $[M+H]^+$, 545, 527, 509, 389 and 371 (Scheme 8).



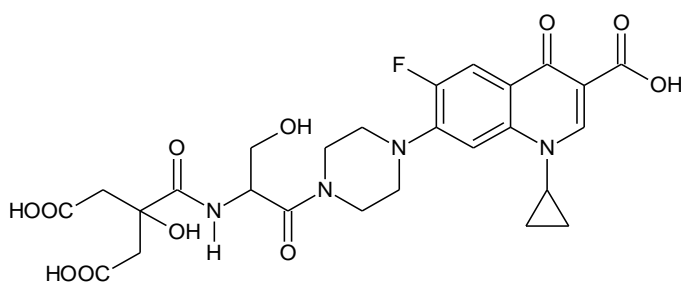
Scheme 8: Possible fragmented molecules from CID mass spectra

2.2 1,5-Citrate-ciprofloxacin conjugate using L-serine as the linker

The 1,3-citrate-ciprofloxacin conjugate **46** with a hydrophobic linker was previously synthesised by our research group^[84]. Its antimicrobial activity was determined on a panel of clinically relevant bacterial strains. From the biological investigation, the siderophore-drug conjugate **37** was consistently more active than **46**. It is suggested that the lower activity of **46** is probably due to the lower hydrophilicity. A new siderophore-drug conjugate **39** with increase hydrophilicity, when compared to **37** and **46** was designed and synthesised. L-serine was chosen as the linker, due to the presence of CH₂-OH, which can potentially increase the hydrogen bonding.

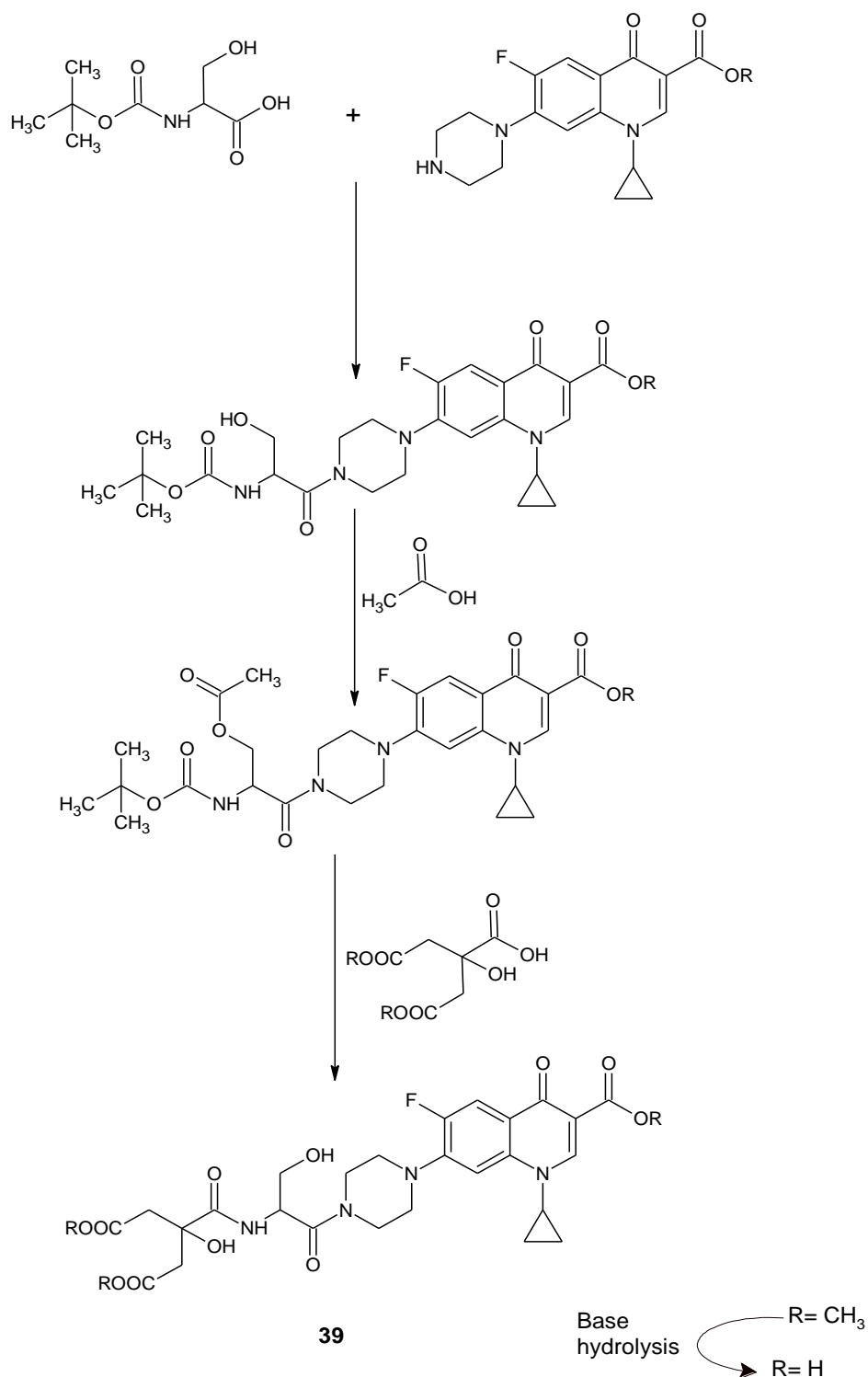


46



39

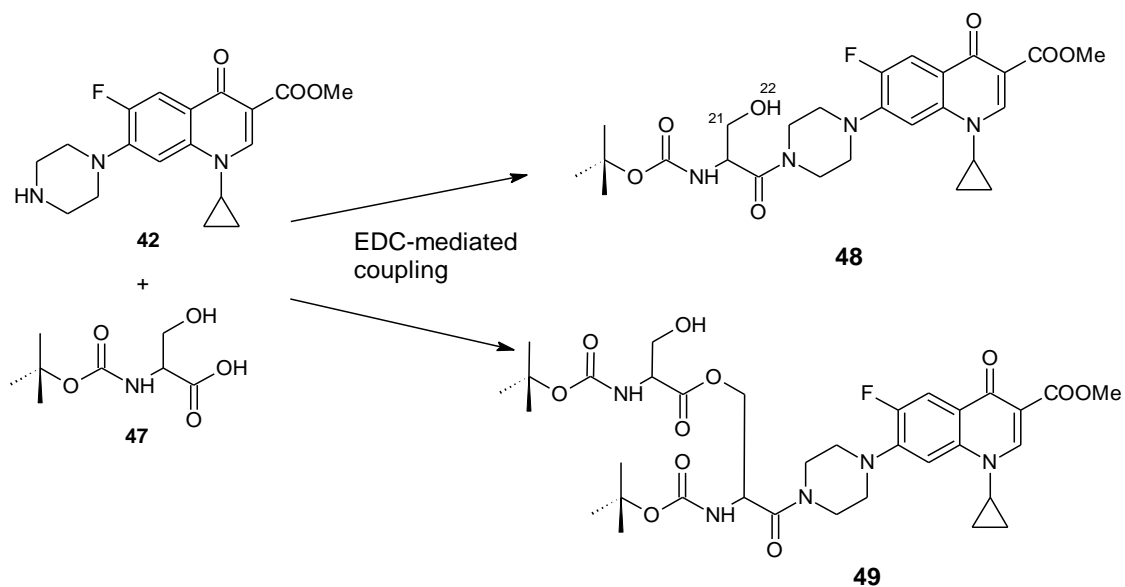
The proposed synthesis of the second target molecule **39** is shown in Scheme 9.



Scheme 9: The proposed synthesis of **39**

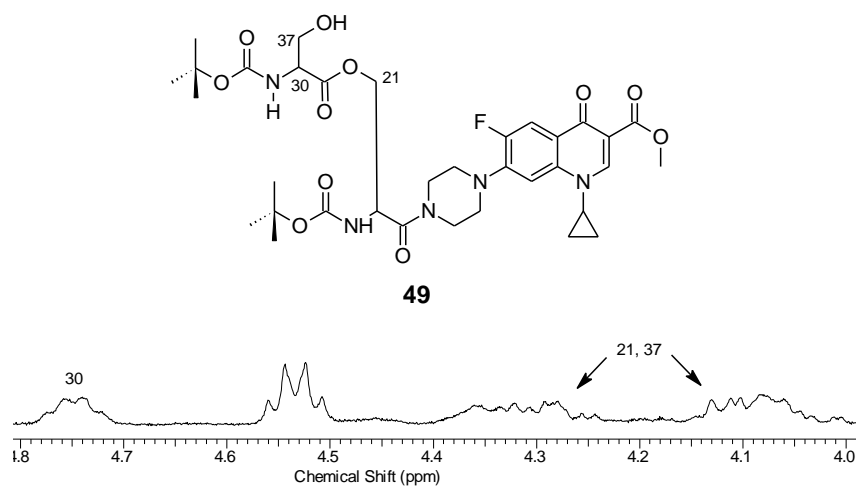
In order to successfully synthesise siderophore-drug conjugate **39**, ciprofloxacin methanoate **42** was firstly conjugated with *N*-(*tert*-butoxycarbonyl)-L-Ser-OH **47** by EDC-mediated coupling reaction (Scheme

10). *N*-(*tert*-butoxycarbonyl)-L-Ser-OH **47** was chosen, as Yangwei *et al.* reports that no protection is required for sensitive functional groups such as the hydroxyl group^[88] using an EDC-mediated coupling. In our hands, the hydroxyl group of L-serine was reactive, giving **49** as a by-product of the reaction.



Scheme 10: Conjugation of ciprofloxacin methanoate **42** and *N*-(*tert*-butoxycarbonyl)-L-Ser-OH **47** gave two linker-drug conjugates **48** and **49**

This was confirmed by ¹H NMR spectroscopy where the spectrum showed the resonances indicative of **49** (Spectrum 2). The formation of **49** was also supported by mass spectrometry where a signal *m/z* 720.3250 was observed corresponding to the molecular formula of C₃₄H₄₇FN₅O₁₁.



Spectrum 2: Partial ^1H NMR spectrum of the mixture of **48** and **49**

These two products were problematic to separate by chromatography so attention was turned to alternative coupling reagents.

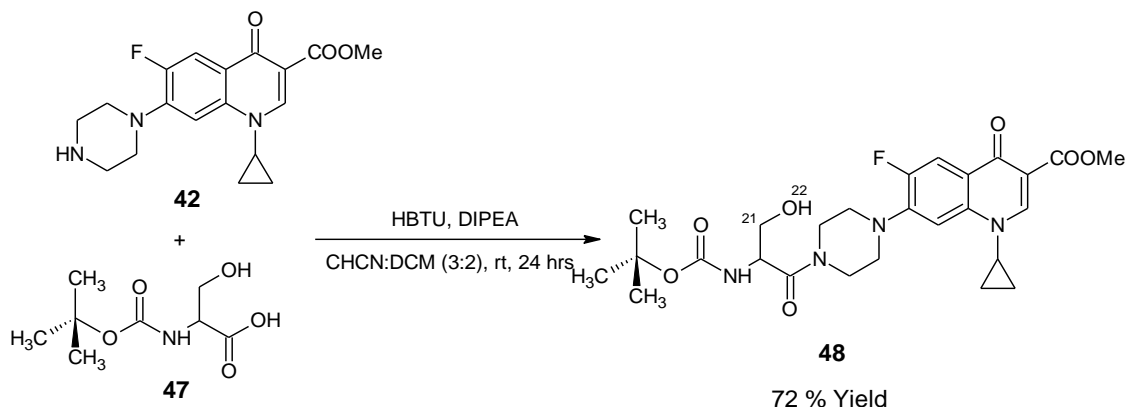
HBTU was tried and only one spot was detected by TLC analysis of the crude reaction mixture.

When using HBTU as a coupling reagent, tetramethyl urea is formed in the reaction. After work up, tetramethyl urea was detected in ^1H NMR analysis with a signal at 2.68 (NMR spectrum not shown). Alternative reaction work ups were explored in order to isolate pure **48**.

Julius T. Su *et al.*^[90] report that tetramethyl urea can be removed by trituration with hexane. The crude linker-drug conjugate **48** was trituated but tetramethyl urea was still present.

Luttringhaus and Dirksen^[91] report that tetramethyl urea is soluble in aromatic hydrocarbons^[91]. Therefore, trituration with toluene was tried, tetramethyl urea was successfully removed as the singlet peak for tetramethyl

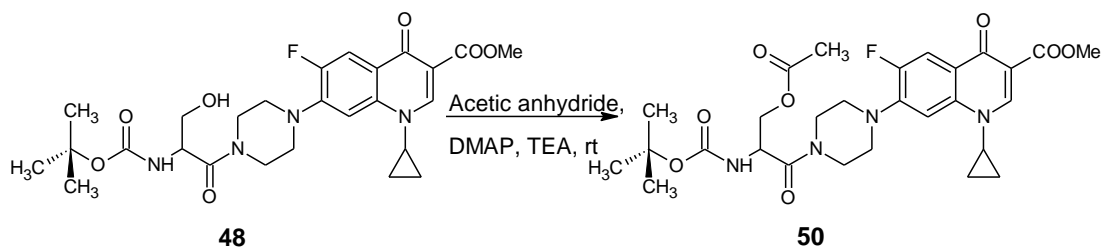
urea was absent in the proton NMR spectrum of 49. After modifying the work up, **48** was isolated in 72 % yield (Scheme 11).



Scheme 11: Synthesis of **48** using HBTU as amide-coupling reagent

The successful synthesis of the linker-drug conjugate **48** was supported by ^1H NMR spectroscopy where a singlet peak at 1.38 ppm with a relative integration of nine corresponding to the *tert* butyl of the *N*-(*tert*-butoxycarbonyl) protecting group was observed. The presence of two doublet-doublet peaks due to the protons at position 21 and a singlet, broad peak at 4.44 ppm due to the proton from the hydroxyl group were also present. In addition, the peak for the amine in ciprofloxacin methanoate **42** at 2.17 ppm was absent and replaced by a doublet for the amide bond at 6.89 ppm. The splitting for this signal is due to the coupling of the amide proton with only one enantiotopic proton from L-serine (COSY at Appendix 8). The successful synthesis of **48** was further supported by mass spectrometry where an m/z peak at 533.2407 $[\text{M}+\text{H}]^+$ was observed corresponding to the molecular formula of $\text{C}_{26}\text{H}_{34}\text{FN}_4\text{O}_7$.

Before removal of the *N*-(*tert*-butoxycarbonyl) protecting group, the hydroxyl group of L-Serine was firstly protected with acetyl group (Scheme 12).



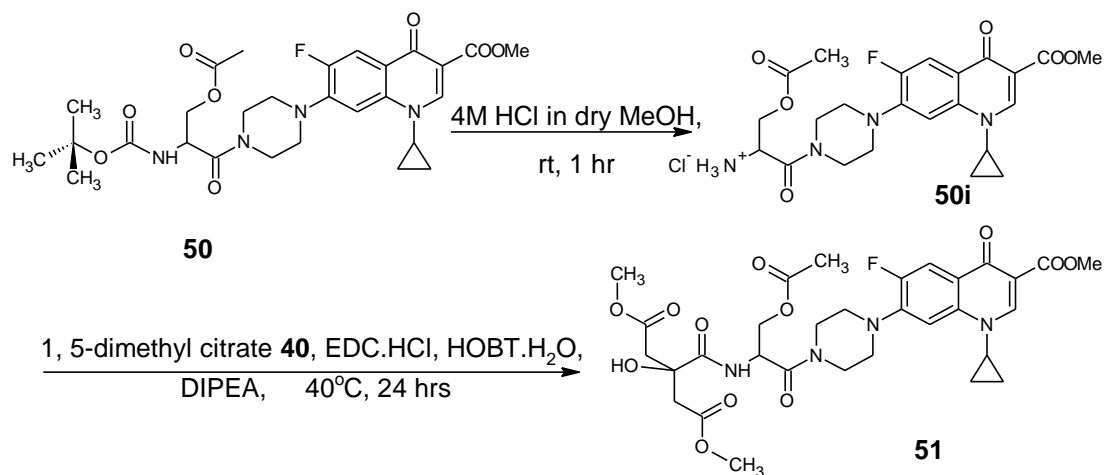
Scheme 12: Acetylation reaction

The linker-drug conjugate **50** was first isolated only by a simple aqueous washing. Unfortunately, this gave only 33 % crude yields of **50** contaminated by acetic acid. The low yield was due to the cleavage of the acetyl group during washing with 0.05M aqueous hydrochloric acid during work up.

Therefore, in order to improve the yield as well as purify the compound **50**, the work up was optimised by washing with saturated sodium hydrogen carbonate and brine, this followed by purification with column chromatography gave 79 % isolated yield of **50**.

The successful synthesis of **50** was confirmed by inspection of the proton NMR spectrum where a signal at 1.99 ppm with a relative integration of three was observed, due to the methyl protons of the acetyl protecting group. The successful synthesis of **50** was also supported by mass spectrometry where a m/z peak at 575.2527 $[M+H]^+$ was observed corresponding to the molecular formula of $C_{28}H_{36}FN_4O_8$.

After successfully synthesising the linker-drug conjugate **50**, it was then conjugated with 1,5-dimethyl citrate **40** using an EDC-mediated coupling reaction after removal of the *N*-(*tert*-butoxycarbonyl) protecting group (Scheme 13).

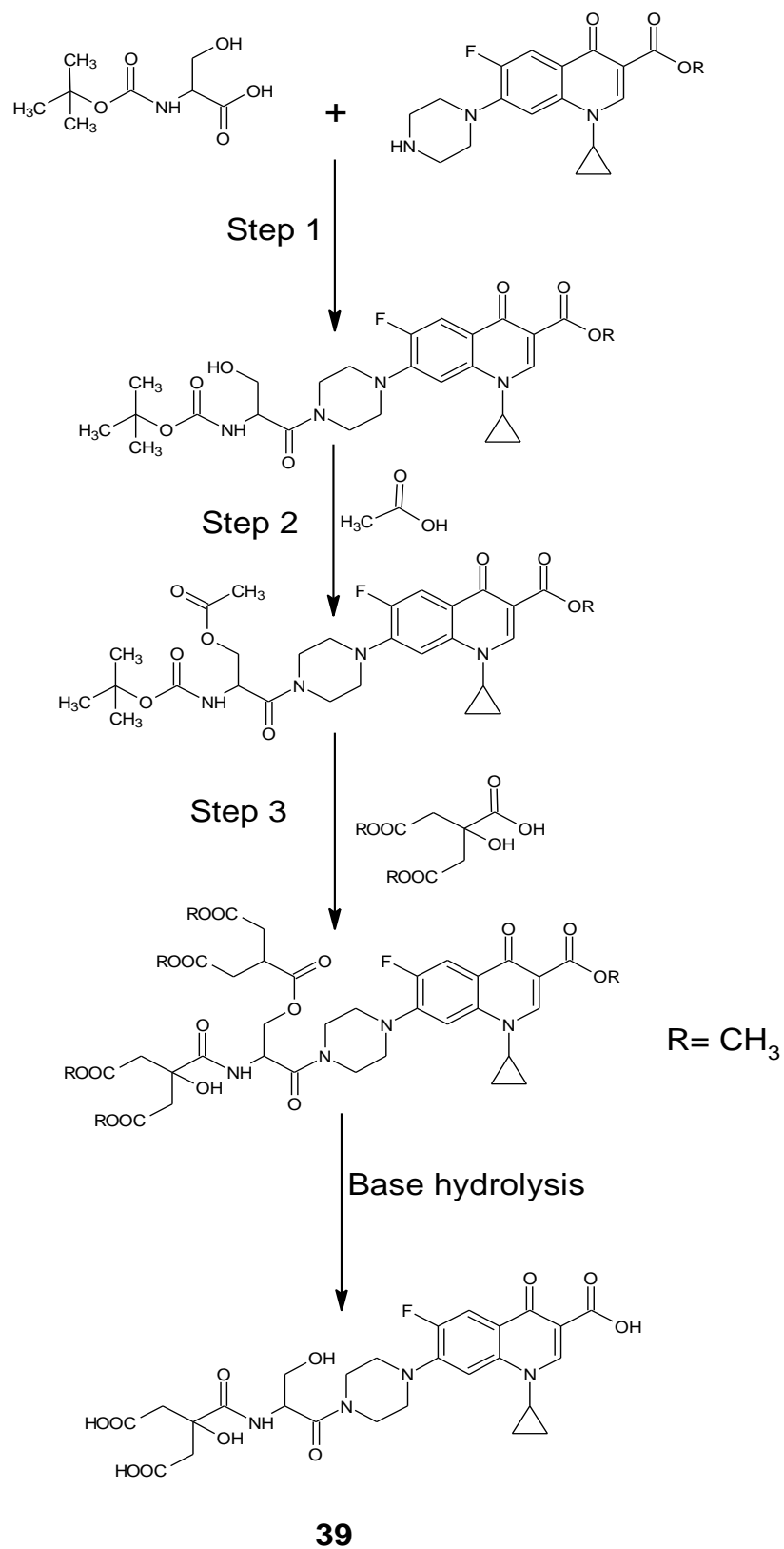


Scheme 13: Amide coupling reaction between the protected citric acid **40** and the drug conjugate **51**

Synthesis of the protected siderophore-drug conjugate **51** initially began with the deprotection of the *N*-(*tert*-butoxycarbonyl) protecting group by acid hydrolysis using 4M HCl in anhydrous MeOH^[89]. The reaction was then followed by conjugation with 1,5-dimethyl citrate **40** using similar technique used in the successful synthesis of **45**.

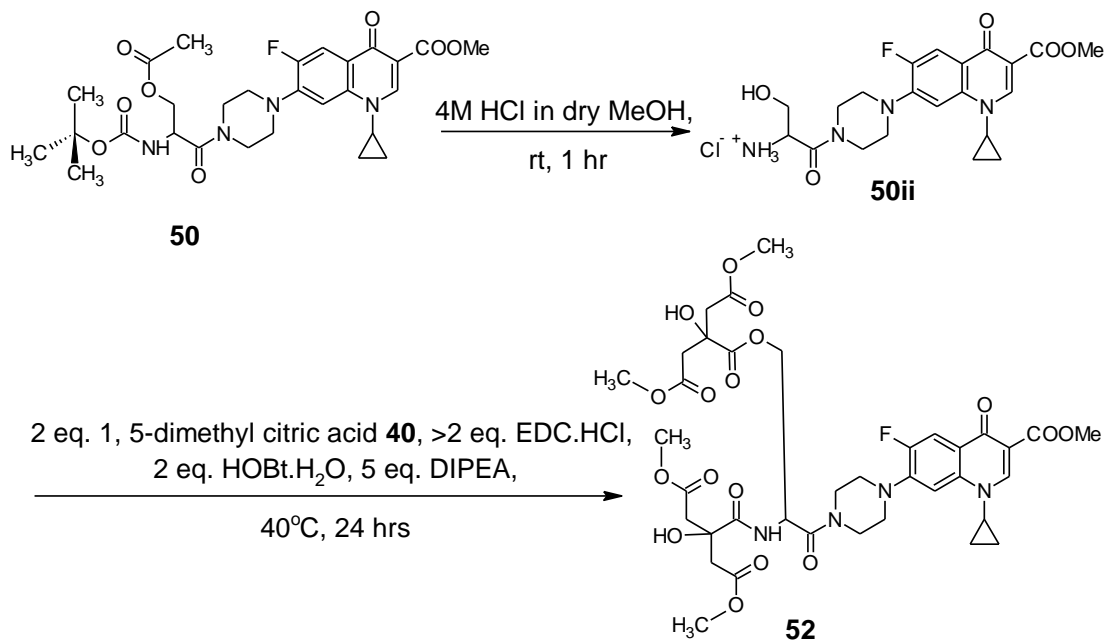
Unfortunately, **51** was not observed in neither the ¹H NMR spectrum nor the mass spectrum, it appeared that, not unsurprisingly, the acetyl protecting group was cleaved on treatment with 4M aqueous HCl. This unwanted deprotection was confirmed by proton NMR spectroscopy, where in the spectrum, the peak of methyl from the acetyl group at 1.99 ppm was absent. This was supported by mass spectrometry, a peak at *m/z* 433.1900 [M+H]⁺ was observed corresponding to the molecular weight of C₂₁H₂₆FN₄O₅, the *m/z* peak of ammonium salt **50ii** (Scheme 15).

The acid hydrolysis used for the deprotection of *N*-(*tert*-butoxycarbonyl) protecting group had hydrolysed the acetyl group. Hence, the strategy towards the synthesis of **39** was modified (Scheme 14).



Scheme 14: New strategy towards the synthesis of **39**

Instead of the acetyl protecting group being used to protect the hydroxyl group, 1,5-dimethyl citrate **40** was used. Therefore, two equivalents of 1, 5-dimethyl citrate **40** were used during the coupling reaction after removal of the *N*-(*tert*-butoxycarbonyl) and acetyl protecting groups (Scheme 15).



Scheme 15: New strategy forming **52**

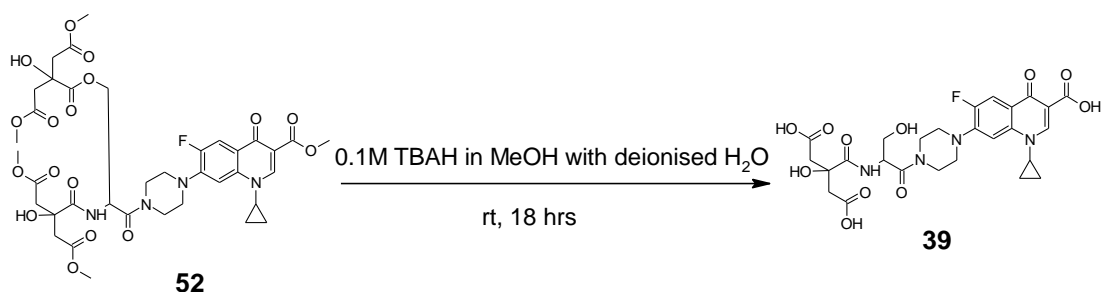
However, even though two equivalents of 1,5-dimethyl citrate **40** were added during the reaction, two spots were observed in the TLC analysis of the crude reaction mixture. Prolonged reaction time did not result in further reaction. One equivalent of EDC.HCl was added every three hours until only one spot was observed by TLC analysis. Purification by column chromatography afforded 56 % yield of **52**.

The successful synthesis of **52** was confirmed by the proton NMR spectrum where the singlet peak of *N*-(*tert*-butoxycarbonyl) protecting group at 1.39 ppm was absent. The presence of two molecules of 1,5-dimethyl citrate **40** in **52** was supported by the presence of signals at 2.74-3.01 ppm with a

relative integration of eight corresponding to eight protons from four diastereotopic protons of two 1,5-dimethyl citrate molecules in **52**.

From the mass spectrum, it showed a m/z peak at 837.2849 $[M+H]^+$ corresponding to the molecular formula of $C_{37}H_{46}FN_4O_{17}$.

Finally, the protected siderophore-drug conjugate **52** underwent the global methyl ester deprotection **39** (Scheme 16).

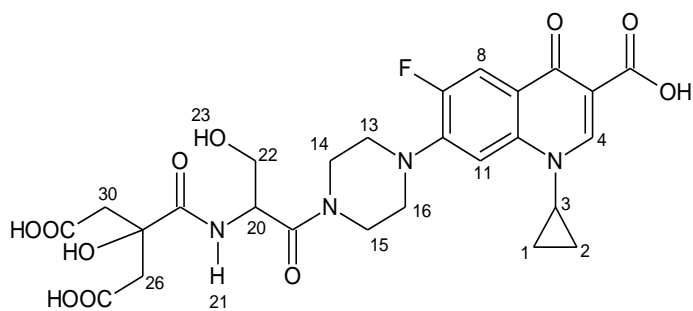


Scheme 16: Base hydrolysis of esters to form siderophore-drug conjugate **39**

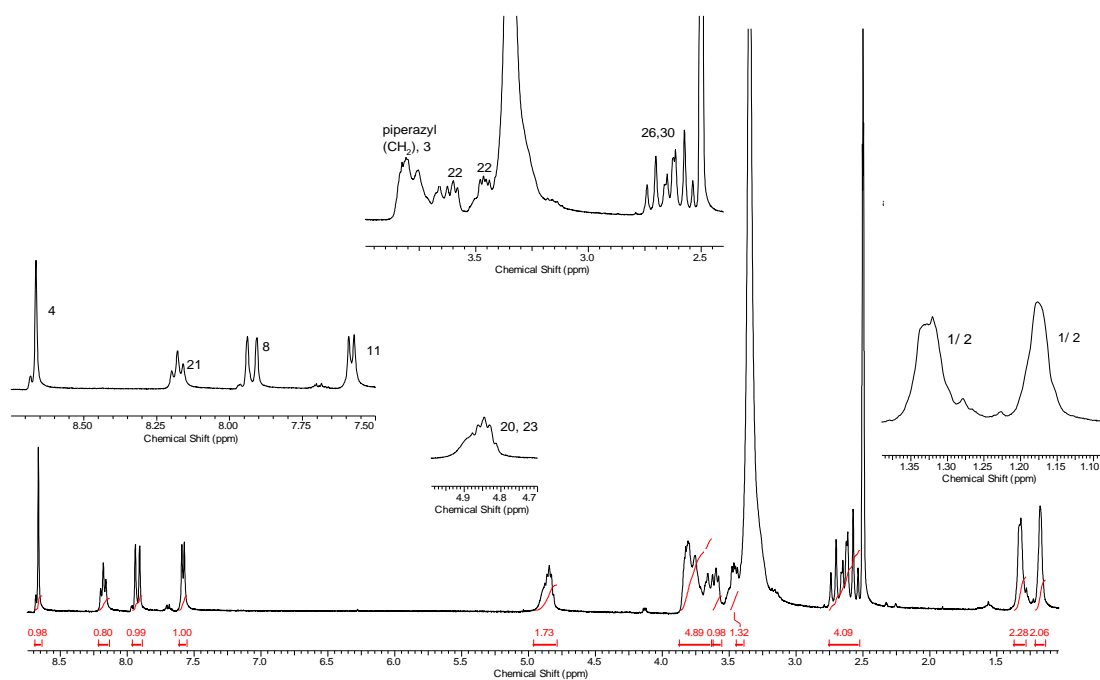
The protected siderophore-drug conjugate **52** was reacted with 0.1M TBAH in methanol. This base hydrolysis gave 29 % yield of **39**.

Successful synthesis of **39** was confirmed by ¹H NMR spectroscopy. The spectrum showed the methyl peak of ciprofloxacin and 1,5-citrate at 3.85 ppm and 3.64-3.71 ppm, respectively, were absent (Spectrum 3).

The removal of 1,5-citrate ester bond of L-serine was also confirmed by the proton NMR spectrum where the integration at 2.53-2.74 ppm was reduced from eight to four showing only two CH₂ from only one 1, 5-citric acid moiety (Spectrum 3).

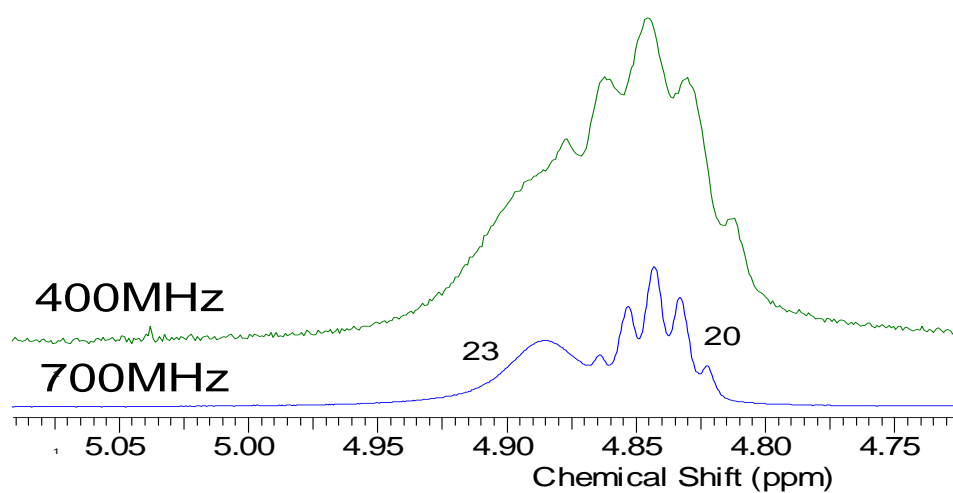


39



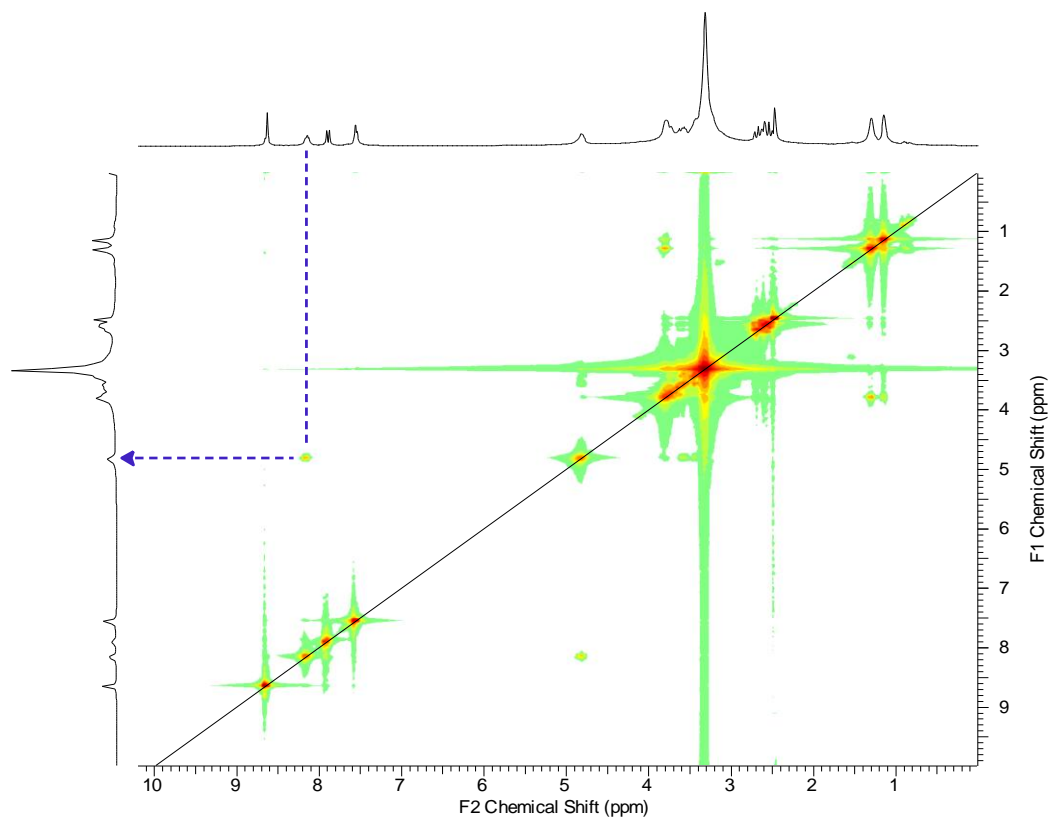
Spectrum 3: The spectrum of **39** at 400 MHz NMR at room temperature

The cleavage of 1, 5-citric acid in hydroxyl ester was also confirmed by the presence of the hydrogen from the free hydroxyl group in the L-serine linker. In the 400MHz NMR spectrum, the broad, singlet peak for hydroxyl resonance overlapped the proton resonance at 4.78-4.95 ppm. The signals were resolved in the 700 MHz NMR spectrum (Spectrum 4). The presence of hydroxyl group in L-serine was proven by a D₂O shake (B in Spectrum 6).



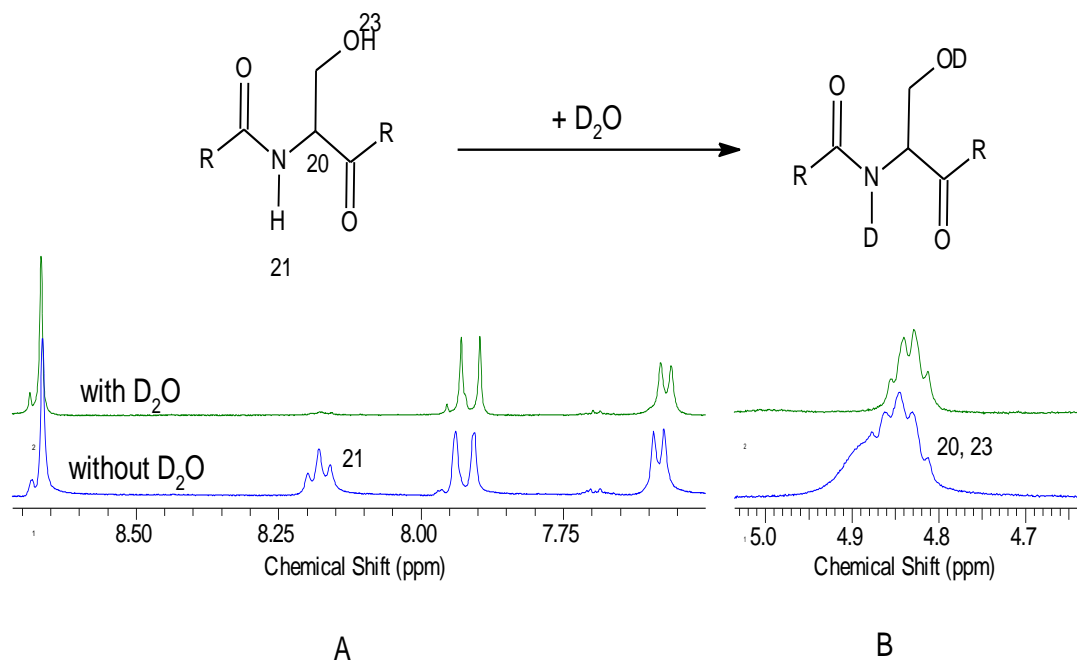
Spectrum 4: Partial spectra of 400 MHz and 700 MHz ¹H NMR spectrum

On close inspection of the ¹H NMR spectrum of **39**, the resonance for the amide proton appeared as a pseudo triplet at 8.18 ppm. COSY supported that this was indeed the amide proton as it was observed to couple with the proton at position 20 (Spectrum 5).



Spectrum 5: COSY spectrum shows coupling between the pseudo triplet amide resonance and proton at position 20

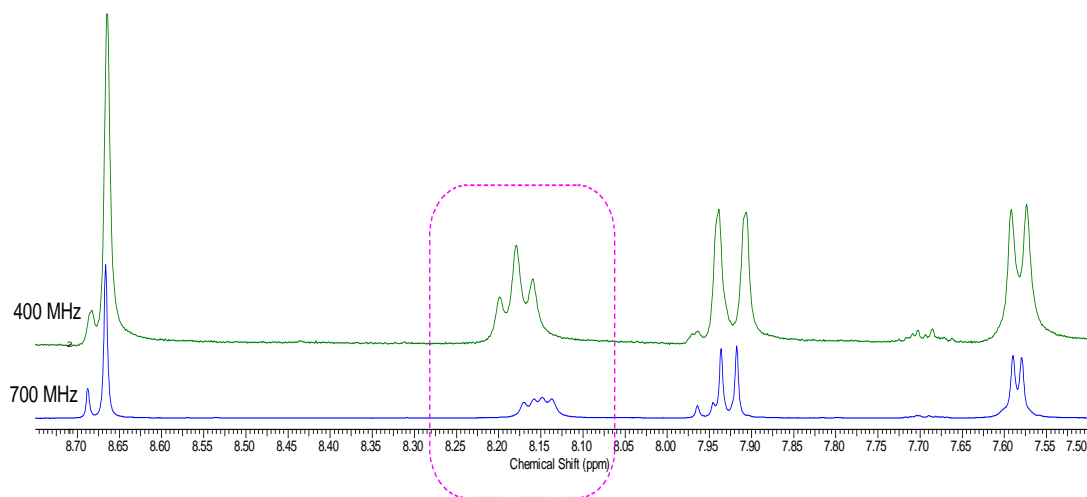
This was then confirmed by deuterium exchange^[92]. A D₂O shake resulted in the disappearance of the pseudo triplet peak. In addition, during the deuteration process, the resonance peak of the proton at position 20 changed from a sextet to quartet, showing that this proton only coupled to the diastereotopic protons of R-CH₂-OD (Spectrum 6).



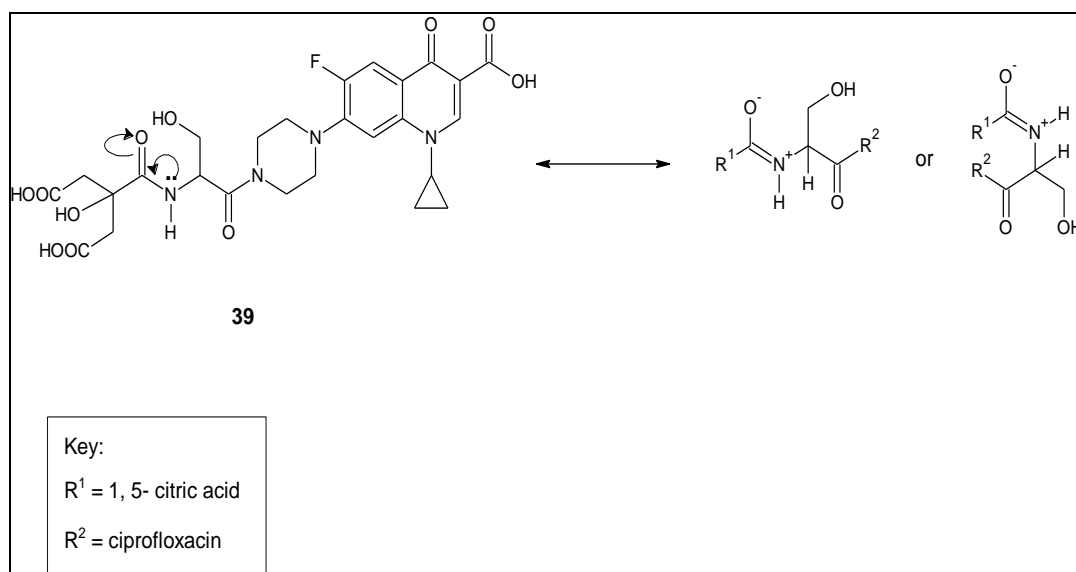
Spectrum 6: Partial spectra of new siderophore-drug conjugate **39** with and without D_2O

The pseudo triplet signal could be due to racemisation during ester hydrolysis with a base. During hydrolysis, the pH was approximately 11 at room temperature. Daft and Coghill^[93] suggest (without experimental evidence) that serine could be racemised at pH 9 at room temperature within one hour. However, Crawhall and Elliot^[94] found that serine was readily racemised at pH 11.4, but at temperatures above 100 °C. Therefore, it was highly unlikely that a mixture of D and L-serine isomers were present in **39**.

The pseudo triplet resonance was further investigated using 700 MHz NMR spectroscopy. From the inspection of the spectrum, the pseudo triplet was resolved to form a doublet-doublet signal (Spectrum 7). From this it appears that the doublet-doublet was the amide proton from two different rotamers (Scheme 17).



Spectrum 7: Partially spectra of the second target molecule **39** at 400 MHz and 700 MHz at ambient temperature

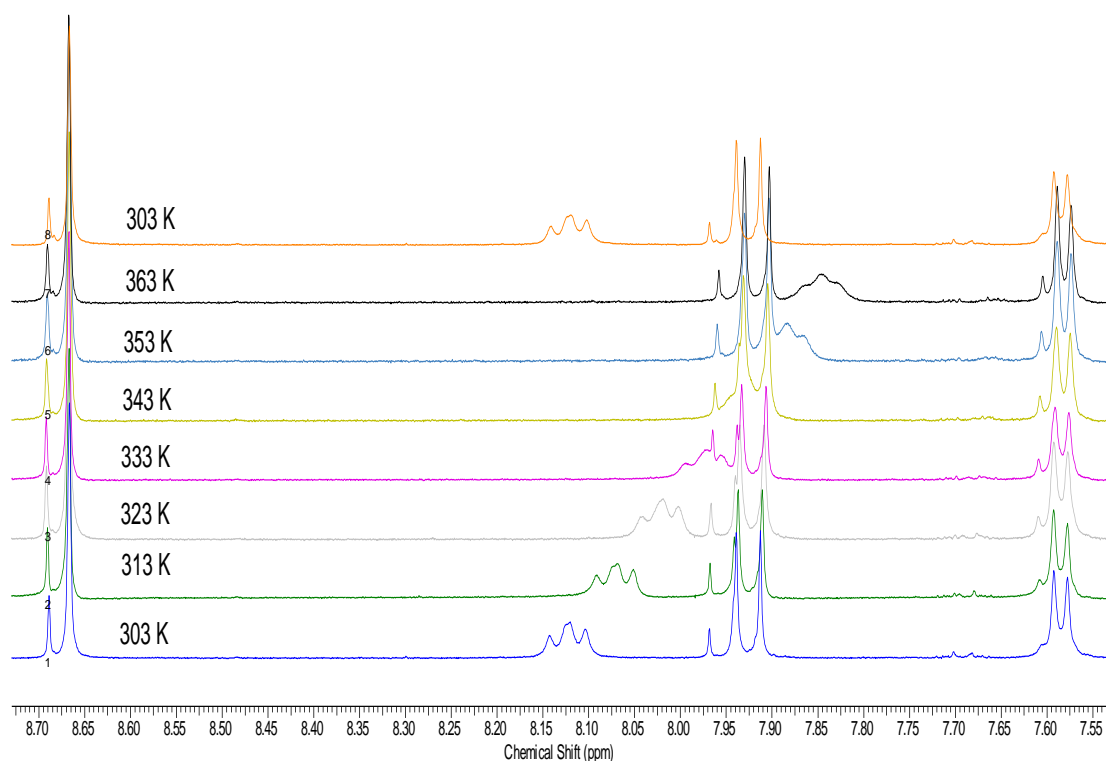


Scheme 17: *Cis-trans* isomerisation of amide bond

This process was further investigated by variable temperatures ¹H NMR spectroscopy.

From the analysis of 500 MHz NMR spectroscopy at variable temperatures, the chemical shift of the pseudo triplet was shifted to high field when the temperature was increased (Spectrum 11).

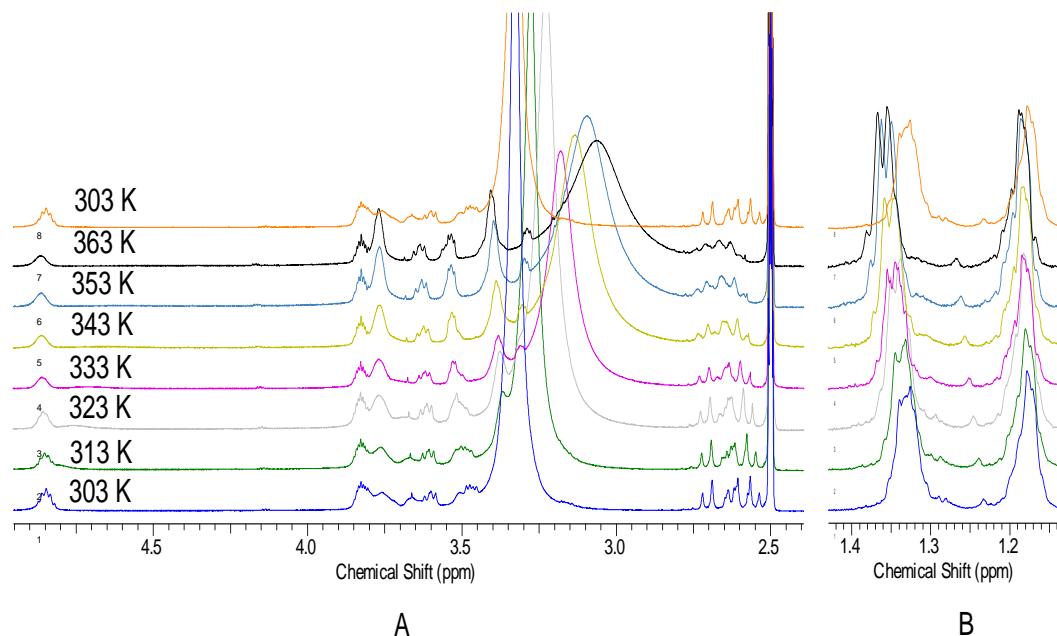
The pseudo-triplet was also observed to broaden slowly once the temperature was increased, and at 363 K the pseudo triplet resonance appeared to come close forming a coalescence peak, unfortunately, the probe temperature could not be increased further. Therefore, the free activation energy could not be calculated. Once the temperature was reset to the ambient temperature, the broad pseudo triplet resonance returned to its original chemical shift (Spectrum 8).



Spectrum 8: Partial ¹H NMR of **39** at variable temperatures at 500 MHz NMR spectroscopy

As the temperature of the probe was increased, the aliphatic portion of **39**, which includes the 1,5-citric acid and L-serine signals became broad (A in

the Spectrum 9). The aromatic signals of **39** (B of Spectrum 9) showed no difference at higher temperatures.

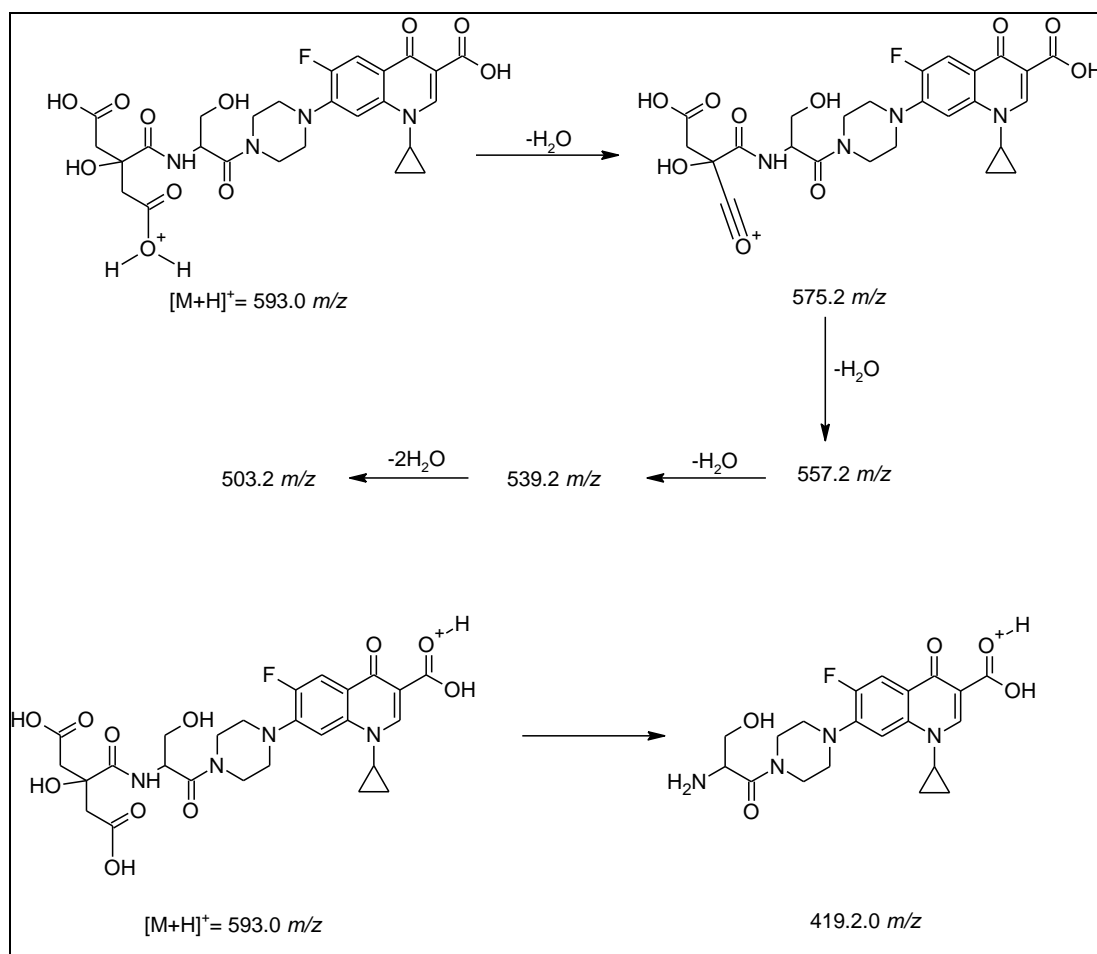


Spectrum 9: Partial ^1H NMR spectra of the second target molecule **39** at 500 MHz at variable temperatures

Thus, it can be concluded that the pseudo triplet of amide proton was due to the rotation barrier of *cis* and *trans* isomers around the amide bond.

Successful synthesis of the new siderophore-drug conjugate **39** was supported by mass spectrometry. The spectrum showed an m/z peak at 593.1912 $[\text{M}+\text{H}]^+$ corresponded to the molecular formula of $\text{C}_{26}\text{H}_{30}\text{FN}_4\text{O}_{11}$. ESI-MS in negative mode was also used, and a m/z peak at 591.1763 $[\text{M}-\text{H}]^-$ was observed corresponding to the molecular formula of $\text{C}_{26}\text{H}_{28}\text{FN}_4\text{O}_{11}$.

In CID, six signals were investigated: 593 $[\text{M}+\text{H}]^+$, 575.2, 557.2, 539.2, 503.2, 419.2 (Scheme18). The data obtained from CID was consistent with the proposed structure of **39**.



Scheme 18: Possible fragmented molecule from CID spectrum

2.3 Biological Screening

Two new siderophore-drug conjugates, **38** and **39** were successfully synthesised, and they were then screened against clinically relevant bacteria. The MIC ($\mu\text{g}/\text{mL}$) reported was converted into nmol/mL . Free ciprofloxacin **4** was used as a reference.

From table 5 it shows that conjugate **38** is more active than conjugate **37** against a wide variety of bacterial strains. Changing the regiochemistry of the citrate has marginally improved the efficacy of **38** towards Gram positive bacteria and no significant improvement in activity was observed with Gram negative bacteria.

Therefore, changing the regiochemistry of 1,3-citrate to 1,5-citrate siderophore improves the activity of the drug conjugates.

From table 6 it shows that **39** was more active than **38** against few bacterial strains. Changing the polarity of the linker from glycine to L-serine does not improve the activity of the drug towards Gram positive bacteria, but only slightly improve towards Gram negative bacteria.

Therefore, there is a marginal increase in the efficacy of the new siderophore-drug conjugates, **38** and **39** when the regiochemistry of the citrate was 1,5 and the lipophobicity was increased. These changes do not give activity comparable to free ciprofloxacin **4**.

Gram bacteria	Bacterial strains	Control		Siderophore-drug conjugates					
		Ciprofloxacin		38			37		
		MIC		MIC		Ratio	MIC		Ratio
		µg/ mL	nmol/ mL	µg/ mL	nmol/ mL		µg/ mL	nmol/ mL	
+	Staphylococcus aureus (Oxford) NCTC 6571	0.25	0.755	4	7.11	9.42	16	28.4	37.6
	Staphylococcus aureus (HG-1) ^{c d}								
	Staphylococcus aureus-15 NCTC 13142 ^e	0.5	1.51	4	7.11	4.71	16	28.4	18.8
	Staphylococcus aureus-16 NCTC 13143 ^{c e}								
	Staphylococcus aureus BIG 0052 ^{c d}	0.5	1.51	4	7.11	4.71	16	28.4	18.8
	Staphylococcus epidermidis NCTC 11047	0.125	0.377	2	3.56	9.44	16	28.4	75.3
	Staphylococcus epidermidis NCTC 2749	0.25	0.755	2	3.56	4.72	8	14.2	18.8
	Staphylococcus haemolyticus NCTC 11042	0.125	0.377	2	3.56	9.44	16	28.4	75.3
-	Escherichia coli NCTC 10418	0.06	0.181	0.125	0.222	1.23	0.125	0.222	1.23
	Escherichia coli BIG 0046 ^c								
	Coliform BIG 0051 ^c								
	Pseudomonas aeruginosa (Environmental) BIG 0039	0.25	0.755	2	3.56	4.72	2	3.56	4.72
	Pseudomonas aeruginosa (Clinical) BIG 0037	2	6.04	16	28.4	4.7	16	28.4	4.70
	Pseudomonas aeruginosa NCTC 10662	0.25	0.755	4	7.11	9.42	2	3.56	4.72
	Pseudomonas aeruginosa BIG 0063	0.25	0.755	2	3.56	4.72	8	14.2	18.8
	Serratia marcescens BIG 0011 = NCTC 1377	0.06	0.181	1	1.78	9.83	0.5	0.889	4.91
	Burkholderia cepacia BIG 0009 = NCTC 10744	0.5	1.51	8	14.2	9.4	8	14.2	9.40
	Burkholderia cepacia BIG 117	1	3.02	8	14.2	4.7	8	14.2	4.70
	Burkholderia cepacia BIG 118	0.25	0.755	2	3.56	4.72	8	14.2	18.8
	Burkholderia cepacia BIG 119	4	12.1						
	Burkholderia cepacia BIG 120	2	6.04	16	28.4	4.7			
	Burkholderia cepacia BIG 121	8	24.1						
	Stenotrophomonas maltophilia N1127 ^f	2	6.04	16	28.4	4.7			
	Stenotrophomonas maltophilia N1124 ^f	4	12.1						
	Stenotrophomonas maltophilia N1119 ^f	1	3.02	16	28.4	9.4			

Table 5: The result for the investigation on pharmacophore of new siderophore-drug conjugates against clinically isolated bacteria

^c Ciprofloxacin resistance

^d Methicillin-resistant staphylococcus aureus (MRSA)

^e Epidemic methicillin-resistant staphylococcus aureus (EMRSA)

^f Bacterial strain isolated from throat

key	Not active
-----	------------

Gram bacteria	Bacterial strains	Control		Siderophore-drug conjugates					
		Ciprofloxacin		38			39		
		MIC		MIC		Ratio	MIC		Ratio
		µg/ mL	nmol/ mL	µg/ mL	nmol/ mL		µg/ mL	nmol/ mL	
+	Staphylococcus aureus (Oxford) NCTC 6571	0.25	0.755	4	7.11	9.42	2	3.38	4.48
	Staphylococcus aureus (HG-1) ^{c,d}								
	Staphylococcus aureus-15 NCTC 13142 ^e	0.5	1.51	4	7.11	4.71	8	13.5	8.94
	Staphylococcus aureus-16 NCTC 13143 ^{c,e}								
	Staphylococcus aureus BIG 0052 ^{c,d}	0.5	1.51	4	7.11	4.71	4	6.75	4.47
	Staphylococcus epidermidis NCTC 11047	0.125	0.377	2	3.56	9.44	2	3.38	8.97
	Staphylococcus epidermidis NCTC 2749	0.25	0.755	2	3.56	4.72	2	3.38	4.48
	Staphylococcus haemolyticus NCTC 11042	0.125	0.377	2	3.56	9.44	2	3.38	8.97
-	Escherichia coli NCTC 10418	0.06	0.181	0.125	0.222	1.23	0.125	0.211	1.17
	Escherichia coli BIG 0046 ^c								
	Coliform BIG 0051 ^c								
	Pseudomonas aeruginosa (Environmental) BIG 0039	0.25	0.755	2	3.56	4.72	2	3.38	4.48
	Pseudomonas aeruginosa (Clinical) BIG 0037	2	6.04	16	28.4	4.7	16	27	4.47
	Pseudomonas aeruginosa NCTC 10662	0.25	0.755	4	7.11	9.42	2	3.38	4.48
	Pseudomonas aeruginosa BIG 0063	0.25	0.755	2	3.56	4.72	2	3.38	4.48
	Serratia marcescens BIG 0011 = NCTC 1377	0.06	0.181	1	1.78	9.83	0.5	0.844	4.66
	Burkholderia cepacia BIG 0009 = NCTC 10744	0.5	1.51	8	14.2	9.4	4	6.75	4.47
	Burkholderia cepacia BIG 117	1	3.02	8	14.2	4.7	8	13.5	4.47
	Burkholderia cepacia BIG 118	0.25	0.755	2	3.56	4.72	2	3.38	4.48
	Burkholderia cepacia BIG 119	4	12.1						
	Burkholderia cepacia BIG 120	2	6.04	16	28.4	4.7	16	27	4.47
	Burkholderia cepacia BIG 121	8	24.1						
	Stenotrophomonas maltophilia N1127 [†]	2	6.04	16	28.4	4.7	8	13,5	2.24
	Stenotrophomonas maltophilia N1124 [†]	4	12.1				16	27	2.23
	Stenotrophomonas maltophilia N1119 [†]	1	3.02	16	28.4	9.4	8	13.5	4.47

Table 6: The result for the investigation of polarity of new siderophore- drug conjugates against clinically isolated bacteria

3 Conclusions and Future Work

3.1 Conclusions

The Trojan horse strategy is a tool to target pathogenic bacteria where an antibacterial agent is conjugated to an essential nutrient such as a siderophore then taken into the bacterial cell by the nutrient transport pathway. The idea was inspired by natural siderophore-drug conjugates such as albomycins **27**^[71].

Two siderophore-fluoroquinolone conjugates were successfully synthesised in this research. The siderophore component, carboxylate and the fluoroquinolone component, ciprofloxacin were linked by amino acids of different hydrophilicity. Conjugate **38** was synthesised using a 1,5-citrate unit and a glycine link to ciprofloxacin. Conjugate **39** used a 1,5-citrate unit and a serine link to ciprofloxacin.

The two synthesised carboxylate-ciprofloxacin conjugates were screened against a panel of clinically relevant bacteria. From the screening data, the carboxylate ciprofloxacin conjugates were found to be less effective than the parent drug ciprofloxacin. Conjugate **39** was marginally more active than **38** against some bacterial strains. The differences in activity could not be considered significant and no structure activity relationship (SAR) information could be concluded from the limited number of compounds synthesised.

3.2 Future work

In order to prove whether the lowering of antimicrobial activity of **38** and **39** when compared to the parent antibiotic is due to the lack of active transport across the bacterial cell membrane, a wider selection of conjugates need to be synthesised. The carboxylate siderophores used in this research are weak iron binders so the use of the siderophore components that show stronger iron binding could be explored.

If the lowering of antimicrobial activity is due to reduced affinity towards the cytoplasmic target, DNA gyrase, the introduction of a bio-linker that allows the release of the antimicrobial inside the cytoplasm could also be explored.

4 Experimental

4.1 General

Solvents were purchased from Sigma Aldrich and stored over 4 Å molecular sieves.

Thin layer chromatography was carried out using commercially available Merck F₂₅₄ aluminium backed silica plates and the mobile phase indicated. Compounds were visualized using UV light (254 nm) or with indicators such as iodine, *p*-anisaldehyde and potassium permanganate.

Melting points were recorded using a Bibby Stuart melting point apparatus and are uncorrected.

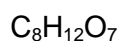
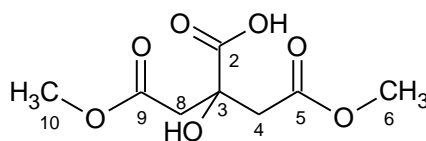
All non-aqueous reactions were carried out under nitrogen, using flame dried glassware. Petrol refers to the fraction of petroleum ether boiling in the range 40-60°C. Brine refers to a saturated aqueous solution of NaCl. Water is deionised water.

Flash column chromatography was carried out using Davisil Flash Silica, 35-60 micron.

Infra-red spectra were recorded on an ATI Mattson Genesis FT-IR spectrometer. All samples were dried under vacuum before analysis.

Proton and carbon NMR spectra were recorded on a Jeol ECX-400 (400 MHz) and (100 MHz) or a Bruker V-700 (700 MHz), with chemical shifts quoted in parts per million relative to CHCl₃ [δ_{H} 7.26 and δ_{C} 77.0], DMSO [δ_{H} 2.54 and δ_{C} 42.45], or CD₃OD [δ_{H} 3.35 and δ_{C} 4.78]. Carbon NMR spectra were assigned using DEPT experiments. Coupling constant (*J*) are quoted in Hertz. Positive and negative electrospray (ESI) mass spectra were acquired on a Finnigan LCQ mass spectrometer or a Bruker MicroToF mass spectrometer.

4.2 2-Hydroxy-4-methoxy-2-(2-methoxy-2-oxoethyl)-4-oxobutanoic acid (**40**)



220.08 g/mol

To a mixture of 2-hydroxypropane-1,2,3-tricarboxylic acid **14** (10.0 g, 52.1 mmol, 1 eq.) in anhydrous methanol (70 mL) was added concentrated sulphuric acid (0.2 mL, 3.8 mmol, 0.12 eq.). The reaction mixture was heated under reflux for 1 hour, and then allowed to cool to room temperature. The reaction mixture was diluted with deionised water (40 mL) and neutralised with the addition of solid calcium hydroxide. Excess calcium hydroxide was removed by filtration, and the filtrate was reduced *in vacuo* giving white solid.

The white solid was suspended in deionised water (20 mL), and sonicated for 15 mins. And undissolved solid was removed by filtration. The filtrate was acidified to pH 0 by addition of concentrated hydrochloric acid. A white precipitate formed which was isolated then dissolved in an aqueous solution of sodium hydrogen carbonate (25 mL, 0.08 g/mL). The aqueous solution was washed with chloroform (3 x 40 mL). The aqueous layer was acidified to pH 0 with concentrated hydrochloric acid (2 mL) and **40** precipitated as a white solid (2.60 g, 11.8 mmol, 23 %).

Rf= 0.4 (DCM: MeOH: Formic acid; 10:1:1);

$^1\text{H NMR}$ (400 MHz, MeOH- d_4) δ (ppm): 3.66 (s, 6H, CH_3), 2.94 (d, $^2J_{\text{H-H}}= 15.4$ Hz, 2H, CH_2), 2.82 (d, $^2J_{\text{H-H}}= 15.4$ Hz, 2H, CH_2);

$^{13}\text{C NMR}$ (100 MHz, MeOH- d_4) δ (ppm): 176.4 (s, **C-2**), 171.8 (s, **C-5**, **C-9**), 74.2 (s, **C-3**), 52.2 (s, **C-6**, **C-10**), 44.0 (s, **C-4**, **C-8**);

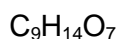
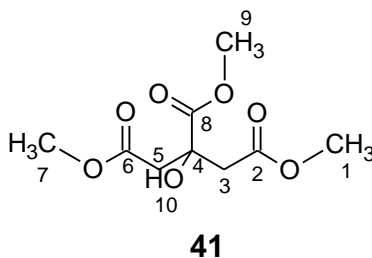
IR (KBr, cm^{-1}): 3428 (br, **OH**), 1742 (s, **C=O**), 1438 (m, **CH₂**), 1401 (w, **CH₃**), 1368 (w, **CH₃**), 1300 (s, **C-O**), 1214 (s, **C-O**), 1126 (s, **C-O**);

m.p. ($^{\circ}\text{C}$): 105.1-107.2 $^{\circ}\text{C}$;

***m/z* (ESI):** 221 ($[\text{M}+\text{H}]^{+}$, 100 %);

HRMS (ESI): Calc. for $\text{C}_8\text{H}_{13}\text{O}_7$ 221.0656 $[\text{M}+\text{H}]^{+}$, found 221.0658 (-1.0 ppm error).

4.3 1,2,3-Trimethyl 2-hydroxypropane-1,2,3-tricarboxylate (**41**)



234.2 g/mol

To a mixture of 2-hydroxypropane-1,2,3-tricarboxylic acid **14** (10.0 g, 52.1 mmol, 1 eq.) in anhydrous methanol (70 mL) was added concentrated sulphuric acid (0.2 mL, 3.8 mmol, 0.12 eq.). The reaction mixture was heated under reflux for 1 hour and then allowed to cool to room temperature. The reaction was diluted with deionised water (40 mL) and neutralised with the addition of solid calcium hydroxide. Excess calcium hydroxide was removed by filtration, and the filtrate was reduced *in vacuo* forming a white solid.

The solid was suspended in deionised water (20 mL) and sonicated for 15 mins. And undissolved solid was removed by filtration. The filtrate was acidified to pH 0 by addition of concentrated hydrochloric acid forming a white precipitate. The precipitate was isolated, and dissolved in an aqueous solution of sodium hydrogen carbonate (25 mL, 0.08 g/mL). The aqueous solution was extracted with chloroform (3 x 40 mL). The organic extract was dried over anhydrous MgSO_4 (s), filtered and concentrated *in vacuo* affording **41** as a white solid (1.33 g, 5.68 mmol, 11 %).

Rf= 0.79 (DCM: MeOH: Formic acid, 10:1:1);

$^1\text{H NMR}$ (400 MHz, CDCl_3) δ (ppm): 4.12 (s, 1H, **H-10, OH**), 3.83 (s, 3H, **H-9, CH₃**), 3.68 (s, 6H, **H-1, H-7, CH₃**), 2.92 (dd, $^2J_{\text{H,H}} = 15.6$ Hz, 2H, **H-3/ H-5, CH₂**), 2.81 (dd, $^2J_{\text{H,H}} = 15.6$ Hz, 2H, **H-3/ H-5, CH₂**);

¹³C NMR (100 MHz, CDCl₃) δ (ppm): 173.8 (s, 1C, **C-8**), 170.2 (s, 2C, **C-2, C-6**), 73.2 (s, 1C, **C-4**), 53.2 (s, 1C, **C-9**), 52.0 (s, 2C, **C-1, C-7**), 43.0 (2C, **C-3, C-5**);

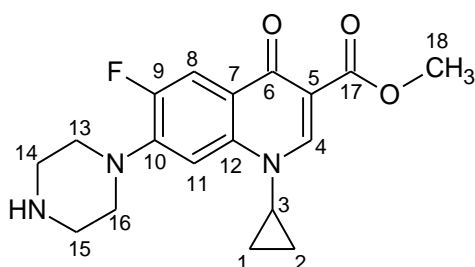
IR (KBr, cm⁻¹): 3476 (w, **OH**), 1756 (s, **C=O**), 1740 (s, **C=O**), 1437 (m, **CH₂**), 1405 (w, **CH₃**), 1372 (w, **CH₃**), 1343 (w, **CH₃**), 1229 (m, **C-O**), 1204 (m, **C-O**), 1127 (m, **C-O**), 1070 (m, **C-O**);

m.p. (°C): 97.7-99.4 °C;

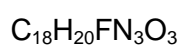
m/z (ESI): 235 ([M+H]⁺, 100 %);

HRMS (ESI): Calc. for C₉H₁₅O₇ 235.0812 [M+H]⁺, found 235.0817 (-2.3 ppm error).

4.4 Methyl 1-cyclopropyl-6-fluoro-4-oxo-7-(piperazin-1-yl)-1,4-dihydroquinoline-3-carboxylate (42)



42



345.37 g/mol

Thionyl chloride (13.1 mL, 181 mmol, 20 eq.) was added dropwise to a stirred solution of 1-cyclopropyl-6-fluoro-4-oxo-7-(piperazin-1-yl)-1,4-dihydroquinoline-3-carboxylic acid **4** (3.0 g, 9.1 mmol, 1 eq.) in anhydrous methanol (100 mL) at 0-5 °C. The reaction was heated under reflux for 24 hours. The reaction mixture was cooled to room temperature and concentrated *in vacuo* to give a yellow oil.

The residue was basified to pH 10 by addition of a 5 % w/v aqueous solution of potassium carbonate (100 mL). The aqueous solution was extracted with dichloromethane (5 x 50 mL). The organic layer was then washed with deionised water (2 x 40 mL), diluted with 5 % w/v aqueous solution of potassium carbonate (100 mL) and re-extracted with dichloromethane (5 x 50 mL). The organic layers were dried over anhydrous $\text{MgSO}_{4(s)}$ filtered and the solvent was removed *in vacuo* to give **42** (2.38 g, 6.89 mmol, 76 %).

Rf = 0.30 (CHCl_3 : MeOH; 3:1);

$^1\text{H NMR}$ (400 MHz, CDCl_3) δ (ppm): 8.53 (s, 1H, **H-4, CH**), 8.01 (d, $^3J_{\text{H-F}} = 13.2$ Hz, 1H, **H-8, CH**), 7.25 (d, $^4J_{\text{H-F}} = 7.0$ Hz, 1H, **H-11, CH**), 3.90 (s, 3H, **CH₃**), 3.40-3.45 (m, 1H, **cyclopropane, CH**), 3.23-3.26 (m, 4H, **piperazine, CH₂**), 3.09-3.12 (m, 4H, **piperazine, CH₂**), 2.17 (s, 1H, **NH**), 1.29-1.34 (m, 2H, **cyclopropane, CH₂**), 1.12-1.15 (m, 2H, **cyclopropane, CH₂**);

¹³C NMR (100 MHz, CDCl₃) δ (ppm): 173.3 (d, ⁴J_{C-F} = 3.1 Hz, **C-6**), 166.5 (s, **C-17**), 153.6 (d, ¹J_{C-F} = 247.8 Hz, **C-9**), 148.5 (s, **C-4**), 145.2 (d, ²J_{C-F} = 10.0 Hz, **C-10**), 138.2 (s, **C-12**), 122.9 (d, ³J_{C-F} = 7.3 Hz, **C-7**), 113.0 (d, ²J_{C-F} = 23.8 Hz, **C-8**), 109.8 (s, **C-5**), 104.8 (d, ⁴J_{C-F} = 2.3 Hz, **C-11**), 51.7 (s, **C-18**), 50.9 (s, **C-13/14/15/16**), 50.8 (s, **C-13/14/15/16**), 45.7 (s, **C-13/14/15/16**), 34.2 (s, **C-3**), 7.6 (s, **C-1, C-2**);

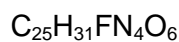
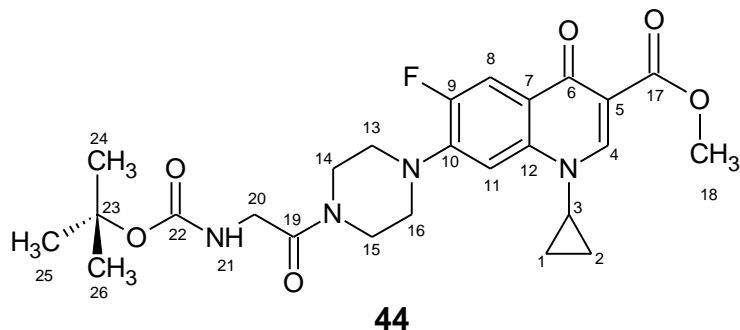
IR (KBr, cm⁻¹): 2949 (w, **CH**), 2913 (w, **CH**), 2827 (w, **CH**), 1719 (s, **C=O**), 1617 (s, **C=O**), 1486 (m, **CH₂**), 1474 (w, **CH₂**), 1343 (w, **CH₃**), 1311 (m, **C-O**), 1258 (s, **C-F**), 1160 (w, **C-O**), 1086 (m, **C-O**);

m.p. (°C): 227.2-227.5 °C;

m/z (ESI): 346 ([M+H]⁺, 100 %);

HRMS (ESI): Calc. for C₁₈H₂₁FN₃O₃ 346.1561 [M+H]⁺, found 346.1563 (-0.5 ppm error)

4.5 Methyl 7-[4-(2{[(*tert*-butoxy) carbonyl] amino} acetyl) piperazin-1-yl]-1-cyclopropyl-6-fluoro-4-oxo-1,4-dihydroquinoline-3-carboxylate (**44**)



502.54 g/mol

To a stirred suspension of methyl 1-cyclopropyl-6-fluoro-4-oxo-7-(piperazin-1-yl)-1,4-dihydroquinoline-3-carboxylate **42** (0.25 g, 0.724 mmol, 1 eq.), *N*-(*tert*-butoxycarbonyl)-Gly-OH **43** (0.13 g, 0.724 mmol) and HOBT. H₂O (0.10 g, 0.724 mmol) in anhydrous MeOH (20 mL) was added EDC.HCl (0.17 g, 0.87 mmol) and DIPEA (130 μ L, 0.01 mmol). The reaction mixture was stirred for 24 hours at room temperature.

The solvent was removed *in vacuo* affording a white residue which was diluted with deionised water (60 mL), and extracted with DCM (3x 80 mL). The organic extract was washed with deionised water (2x 50 mL), 0.05M aqueous HCl (2x 50 mL), 0.05M aqueous NaHCO₃ (2x 50 mL), brine (2x 50 mL) and deionised water (2x 50 mL). The organic extract was dried over anhydrous MgSO₄ (s), then concentrated *in vacuo* to give **44** as a white solid (0.25 g, 0.50 mmol, 69 %).

R_f = 0.8 (CHCl₃: MeOH, 3:1);

¹H NMR (400 MHz, CDCl₃) δ (ppm): 8.54 (s, 1H, H-4, CH), 8.09 (d, ³J_{H-F} = 13.2 Hz, 1H, H-8, CH), 7.26 (d, ⁴J_{H-F} = 7.0 Hz, 1H, H-11, CH), 5.51 (t, ³J₂₁₋₂₀ = 4.4 Hz, 4.4 Hz, 1H, NH), 4.03 (d, ³J₂₀₋₂₁ = 4.4 Hz, 2H, H-20, CH₂), 3.90 (s, 3H, CH₃), 3.86-3.88 (m, 2H, piperazine, CH₂), 3.62-3.66 (m, 2H, piperazine,

CH₂), 3.40-3.45 (m, 1H, **cyclopropane, CH**), 3.22-3.25 (m, 4H, **piperazine, CH₂**), 1.45 (s, 9H, **H-24, H-25, H-26, CH₃**), 1.33-1.37 (m, 2H, **cyclopropane, CH₂**), 1.14-1.17 (m, 2H, **cyclopropane, CH₂**);

¹³C NMR (100 MHz, CDCl₃) δ (ppm): 173.3 (d, ⁴J_{C-F} = 2.3 Hz, **C-6**), 167.5 (s, **C-22**), 166.5 (s, **C-17**), 156.2 (s, **C-19**), 155.5 (d, ¹J_{C-F} = 248.5 Hz, **C-9**), 148.8 (s, **C-4**), 144.1 (d, ²J_{C-F} = 10.8 Hz, **C-10**), 138.1 (s, **C-12**), 123.7 (d, ³J_{C-F} = 7.1 Hz, **C-7**), 113.5 (d, ²J_{C-F} = 23.8 Hz, **C-8**), 110.10 (s, **C-5**), 105.4 (d, ³J_{C-F} = 2.3 Hz, **C-11**), 79.8 (s, **C-23**), 51.8 (s, **C-18**), 49.8 (s, **C-13/14/15/16**), 49.4 (s, **C-13/14/15/16**), 44.1 (s, **C-20**), 41.9 (s, **C-13/14/15/16**), 41.5 (s, **C-13/14/15/16**), 34.3 (s, **C-3**), 28.0 (s, **C-24, C-25, C-26**), 7.7 (s, **C-1, C-2**);

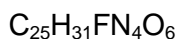
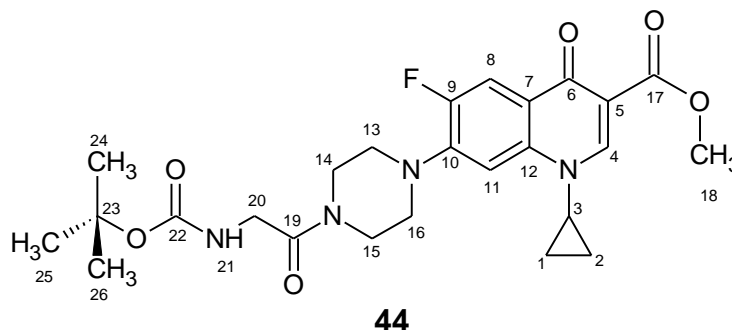
IR (KBr, cm⁻¹): 3297 (m, **NH**), 3068 (w, **CH**), 2974 (w, **CH**), 2844 (w, **CH**), 1715 (s, **C=O**), 1699 (s, **C=O**), 1654 (s, **C=O**), 1617 (s, **C=O**), 1544 (m, **NH**), 1491 (m, **CH₂**), 1474 (m, **CH₂**), 1454 (m, **CH₂**), 1433 (m, **CH₂**), 1352 (w, **CH₃**), 1323 (w, **CH₃**), 1237 (s, **C-F**), 1164 (m, **C-O**), 1082 (m, **C-O**), 1029 (m, **C-O**);

m.p. (°C): 193.4-193.5 °C;

m/z (ESI): 503 ([M+H]⁺, 100 %);

HRMS (ESI): Calc. for C₂₅H₃₂FN₄O₆ 503.2300 [M+H]⁺, found 503.2299 (0.2 ppm error).

4.6 Methyl 7-[4-(2{[(*tert*-butoxy) carbonyl] amino} acetyl) piperazin-1-yl]-1-cyclopropyl-6-fluoro-4-oxo-1,4-dihydroquinoline-3-carboxylate (**44**) – modified synthesis

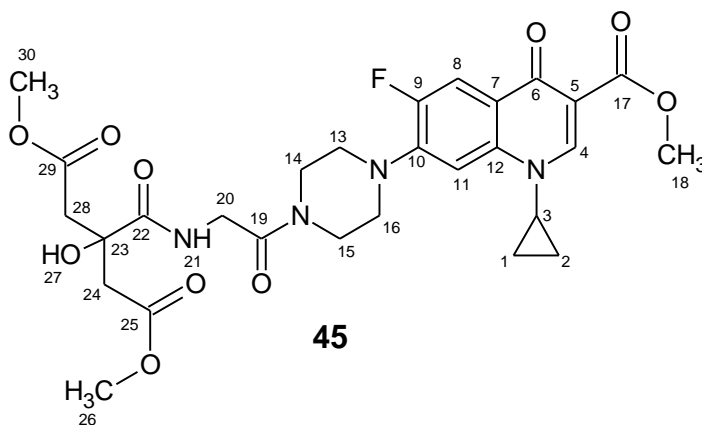


502.54 g/mol

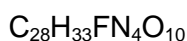
To a stirred suspension of methyl 1-cyclopropyl-6-fluoro-4-oxo-7-(piperazin-1-yl)-1,4-dihydroquinoline-3-carboxylate **42** (0.25 g, 0.724 mmol, 1 eq.), *N*-(*tert*-butoxycarbonyl)-Gly-OH **43** (0.13 g, 0.724 mmol, 1 eq.) and HOBt.H₂O (0.10 g, 0.724 mmol) in MeOH (3:2, 50 mL) were added - EDC.HCl (0.17 g, 0.87 mmol) and DIPEA (130 μ L, 0.75 mmol). The reaction was stirred at 40°C for 3 hours. Deionised water (30 mL) was added and the reaction was stirred at room temperature for an hour.

The solvent was removed *in vacuo* to give a white solid residue which was dissolved in deionised water (60 mL) and extracted with DCM (3x 80 mL). The organic extract was washed with deionised water (2x 50 mL), 0.05M aqueous HCl (2x 50 mL), 0.05M aqueous NaHCO₃ (2x 50 mL), brine (2x 50 mL) and deionised water (2x 50 mL). The organic extract was dried over anhydrous MgSO_{4(s)} and concentrated *in vacuo* to give **44** as a white solid (0.31 g, 0.61 mmol, 84 %).

4.7 1,5-Dimethyl-3-[(2-{4-(1-cyclopropyl-6-fluoro-3-(methoxycarbonyl)-4-oxo-1,4-dihydroquinoline-7-yl]piperazin-1-yl}-2-oxoethyl) carbamoyl]-3-hydroxypentanedioate (45)



45



604.58 g/mol

To methanolic HCl (4M, 20 mL) at 0-5 °C, methyl 7-[4-(2-[(*tert*-butoxy)carbonyl]amino)acetyl]piperazin-1-yl]-1-cyclopropyl-6-fluoro-4-oxo-1,4-dihydroquinoline-3-carboxylate **44** (0.20 g, 0.40 mmol, 1 eq.) was added. The reaction mixture was left to stir at room temperature for 16 hours. The reaction mixture was concentrated *in vacuo* and diluted with dry MeOH (~40 mL). The solution was basified using triethylamine (~0.5mL, pH~8-9) and stirring was continued for 1.5 hours. The solvent was removed *in vacuo* affording a cream solid.

The solid residue and 2-hydroxy-4-methoxy-2-(2-methoxy-2-oxoethyl)-4-oxobutanoic acid **40** (0.09 g, 0.40 mmol) were dissolved in dry DMF (20 mL). To this suspension, DIPEA (350 µL, 1.99 mmol), and HOBt.H₂O (0.06 g, 0.48 mmol) were added followed by EDC.HCl (0.09 g, 0.48 mmol). The reaction mixture was heated at 40 °C for 24 hours and cooled to room temperature. The solvent was removed *in vacuo* affording a brown oily residue.

The residue was dissolved in chloroform (60 mL) washed with saturated sodium hydrogen carbonate (5x 60 mL) and brine (5x 60 mL). The organic extract was dried over anhydrous MgSO₄ (s), and concentrated *in vacuo*. The

residue was triturated with diethyl ether to affording **45** as a cream solid (0.096 g, 0.16 mmol, 40 %).

Rf= 0.9 (CHCl₃: MeOH, 3:1);

¹H NMR (400 MHz, DMSO-d₆) δ (ppm): 8.45 (s, 1H, **H-4, CH**), 7.80 (t, ³J_{H-F} 4.4 Hz, 1H, **NH**), 7.78 (d, ³J_{H-F} 13.2 Hz, 1H, **H-8, CH**), 7.47 (d, ⁴J_{H-F} 7.5 Hz, 1H, **H-11, CH**), 4.04 (d, ³J₂₀₋₂₁ 4.4 Hz, 2H, **H-20, CH₂**), 3.93 (s, 3H, **H-18, CH₃**), 3.69-3.72 (m, 2H, **piperazine, CH₂**), 3.63-3.65 (m, 3H, **piperazine, CH₂, cyclopropane, CH**), 3.55 (s, 6H, **H-26, H-30, CH₃**), 3.22-3.32 (m, 4H, **piperazine, CH₂**), 2.85 (d, ²J_{H-F} 15.0 Hz, 2H, **H-24/ H-28, CH₂**), 2.69 (d, ²J_{H-F} 15.0 Hz, 2H, **H-24/ H-28, CH₂**), 1.23- 1.28 (m, 2H, **cyclopropane, CH₂**), 1.08-1.12 (m, 2H, **cyclopropane, CH₂**);

¹³C NMR (100 MHz, DMSO-d₆) δ (ppm): 173.7 (s, **C-22**), 172.5 (d, ⁴J_{C-F} 2.3 Hz, **C-6**), 170.6 (s, **C-25, C-29**), 167.4 (s, **C-17**), 166.8 (s, **C-19**), 153.3 (d, ¹J_{C-F} 247.0 Hz, **C-9**), 149.1 (s, **C-4**), 144.3 (d, ²J_{C-F} 10.8 Hz, **C-10**), 138.7 (s, **C-12**), 122.7 (d, J= 7.1 Hz, **C-7**), 112.2 (d, ²J_{C-F} 21.5 Hz, **C-8**), 109.5 (s, **C-12**), 107.1 (d, ³J_{C-F} 3.1 Hz, **C-11**), 73.9 (s, **C-23**), 55.1 (s, **C-18**), 51.5 (s, **C-30, C-26**), 50.2 (s, **C-13/ 14/ 15/ 16**), 49.4 (s, **C-13/ 14/ 15/ 16**), 43.1 (s, **C-20**), 41.3 (s, **C-13/ 14/ 15/ 16**), 40.9 (s, **C-13/ 14/ 15/ 16**), 38.4 (s, **C-24, C-28**), 34.9 (s, **C-3**), 7.5 (s, **C-1, C-2**);

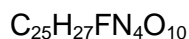
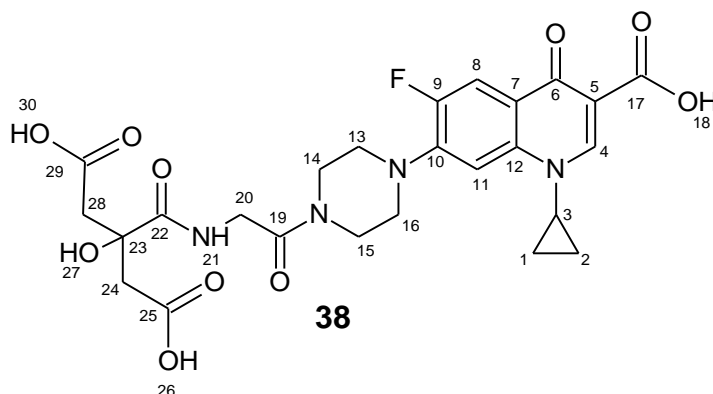
IR (KBr, cm⁻¹): 3407 (br, **OH**), 2998 (w, **CH**), 2949 (w, **CH**), 2847 (w, **CH**), 1719 (s, **C=O**), 1617 (s, **C=O**), 1486 (m, **CH₂**), 1474 (m, **CH₂**), 1437 (m, **CH₂**), 1380 (w, **CH₃**), 1348 (m, **CH₃**), 1311 (w, **CH₃**), 1241 (s, **C-F**), 1209 (m, **C-O**), 1164 (m, **C-O**), 1102 (m, **C-O**), 1082 (m, **C-O**), 1021 (s, **OH**);

m.p. (°C): 153.9-155.3 °C;

m/z (ESI): 605 ([M+H]⁺100 %);

HRMS (ESI): Calc. for C₂₈H₃₄FN₄O₁₀ 605.2253 [M+H]⁺, found 605.2257 (-0.7 ppm error).

4.8 3-({2-[4-(3-Carboxy-1-cyclopropyl-6-fluoro-4-oxo-1,4-dihydroquinoline-7-yl) piperazin-1-yl]-2-oxoethyl} carbamoyl)-3-hydroxypentanedioic acid (**38**)



562.5 g/mol

To a stirred solution of TBAH in MeOH (1M, 0.5 mL) and deionised water (4.5 mL), was added 1,5-dimethyl-3-[(2-{4-(1-cyclopropyl-6-fluoro-3-(methoxycarbonyl)-4-oxo-1,4-dihydroquinoline-7-yl]piperazin-1-yl)-2-oxoethyl}carbamoyl]-3-hydroxypentanedioate **45** (0.08 g, 0.132 mmol, 1 eq.). The reaction mixture was stirred at room temperature for 18 hours. The reaction was quenched with 0.2M pyruvic acid in deionised water (0.2M, 2.0 mL). The precipitate formed was isolated by filtration and washed with chloroform (2x 25 mL) to afford giving **38** (0.03 g, 0.053 mmol, 40 %).

R_f = 0.32 (CHCl₃: MeOH, 3:1);

¹H NMR (400 MHz, DMSO-d₆) δ (ppm): 8.68 (s, 1H, **H-4, CH**), 8.09 (t, ³J₂₁₋₂₀ = 5.3 Hz, ³J₂₁₋₂₀ = 5.3 Hz, 1H, **H-21, NH**), 7.95 (d, ³J_{H-F} = 13.2 Hz, 1H, **H-8, CH**), 7.60 (d, ⁴J_{H-F} = 7.6 Hz, 1H, **H-11, CH**), 4.03 (d, ³J₂₀₋₂₁ = 5.3 Hz, 2H, **H-20, CH₂**), 3.80-3.86 (m, 1H, **cyclopropane, CH**), 2.56-2.74 (m, 4H, **citric acid, CH₂**), 3.29-3.34 (m, 4H, **piperazine, CH₂**- hidden by water peak), 2.72 (d, ²J_{H-H} = 15.6 Hz, 1H, **H-24/H-28, CH**), 2.66 (d, ²J_{H-H} = 14.4 Hz, 1H, **H-24/H-28, CH**), 2.62 (d, ²J_{H-H} = 15.6 Hz, 1H, **H-24/H-28, CH**), 2.57 (d, ²J_{H-H} = 15.6 Hz, 1H, **H-**

24/H-28, CH, 1.30-1.35 (m, 2H, **cyclopropane, CH₂**), 1.12-1.23 (m, 2H, **cyclopropane, CH₂**);

¹³C NMR (100 MHz, DMSO-d₆) δ (ppm): 177.1 (s, **C-22**), 175.9 (d, ⁴J_{C-F} = 2.3 Hz, **C-6**), 172.0 (s, **C-25/ C-29**), 169.2 (s, **C-25/ C-29**), 167.7 (s, **C-17**), 166.6 (s, **C-19**), 154.8 (d, J_{C-F} = 201.0 Hz, **C-9**), 150.7 (s, **C-4**), 145.6 (d, ²J_{C-F} = 10.8 Hz, **C-10**), 139.7 (s, **C-12**), 119.3 (d, ³J_{C-F} = 7.2 Hz, **C-7**), 111.4 (d, ²J_{C-F} = 21.5 Hz, **C-8**), 107.2 (d, ³J_{C-F} = 3.2 Hz, **C-11**), 72.7 (s, **C-23**), 49.5 (s, **C-13/14/15/16**), 49.4 (s, **C-13/14/15/16**), 43.8 (s, **C-20**), 43.4 (s, **C-13/14/15/16**), 42.8 (s, **C-13/14/15/16**), 41.0 (s, **C-24/ C-28**), 40.6 (s, **C-24/ C-28**), 35.9 (s, **C-3**), 7.4 (s, **C-1, C-2**);

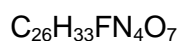
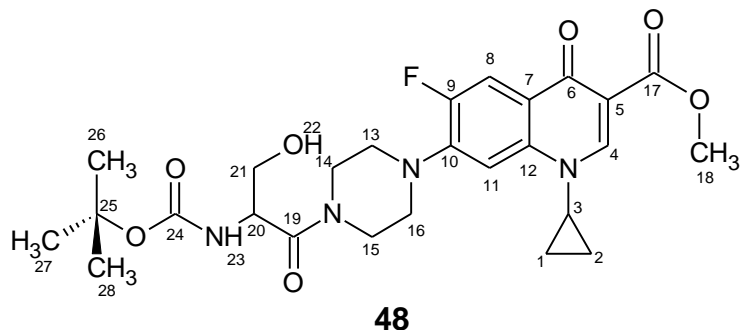
IR (KBr, cm⁻¹): 3384 (b, **OH**), 3058 (w, **CH**), 2919 (w, **CH**), 2844 (w, **CH**), 1720 (m, **C=O**), 1624 (s, **C=O**), 1465 (m, **CH₂**), 1386 (m, C-O), 1334 (m, C-O), 1243 (s, **C-F**), 1024 (s, **C-O**);

m.p. (°C): 179.4-181.2 °C;

HRMS (ESI): Calc. for C₂₅H₂₇FN₄O₁₁ 563.1802 [M+H]⁺, found 563.1784 (-3.2 ppm error);

CID: 563 [M+H]⁺, 545, 527, 509, 389 and 371

4.9 Methyl 7-[4-(2-[[*tert*-butoxy)carbonyl]amino]-3-hydroxypropanoyl) piperazin-1-yl]-1-cyclopropyl-6-fluoro-4-oxo-1,4-dihydroquinoline-3-carboxylate (**48**)



532.3 g/mol

To a stirred solution of methyl 1-cyclopropyl-6-fluoro-4-oxo-7-(piperazin-1-yl)-1,4-dihydroquinoline-3-carboxylate **42** (0.3 g, 0.869 mmol, 1eq.) and *N*-(*tert*-butoxycarbonyl)-L-Ser-OH **47** (0.18 g, 0.869 mmol, 1eq.) in anhydrous acetonitrile: DCM (3:2, 50 mL), was added DIPEA (162 μL , 0.90 mmol) and the mixture was stirred for 30 minutes at room temperature. After 30 minutes of stirring, HBTU (0.33 g, 0.90 mmol, 1 eq.) was added, and the reaction mixture was left to stir for 24 hours at room temperature.

The solvent was removed *in vacuo* and the residue was diluted with DCM (80 mL) and washed with deionised water (2x 50 mL), 0.05M aqueous HCl (2x 50 mL), 0.05M aqueous NaHCO_3 (2x 50 mL) and brine (2x 50 mL). The organic extract was dried over anhydrous MgSO_4 (s), and the solvent removed *in vacuo*. The residue was triturated with toluene giving **48** as a cream solid (0.33 g, 0.62 mmol, 72 %).

R_f = 0.86 (CHCl_3 : MeOH, 3:1);

^1H NMR (400 MHz, DMSO-d_6) δ (ppm): 8.44 (s, 1H, **H-4, CH**), 7.76 (d, $^3J_{\text{H-F}} = 13.4$ Hz, 1H, **H-8, CH**), 7.44 (d, $^4J_{\text{H-F}} = 7.3$ Hz, 1H, **H-11, CH**), 6.88 (d, $^3J_{\text{H-F}} = 8.2$ Hz, 1H, **NH**), 4.53 (sx, $^3J_{20-21} = 5.8$ Hz, $^3J_{20-21} = 5.8$ Hz, $^3J_{20-23} = 8.2$ Hz, 1H, **H-20, CH**), 4.44 (s (b), 1H, **OH**), 3.75-3.83 (m, 2H, **piperazine, CH₂**), 3.73 (s, 3H, **CH₃**), 3.68-3.72 (m, 2H, **piperazine, CH₂**), 3.63-3.67 (m, 1H,

cyclopropane, CH), 3.58 (dd, $^3J_{21-20} = 5.8$ Hz, $^2J_{21-21} = 11.0$ Hz, 1H, **H-21**), 3.48 (dd, $^3J_{21-20} = 5.8$ Hz, $^2J_{21-21} = 11.0$ Hz, 1H, **H-21, CH**), 3.18-3.31 (m, 4H, **piperazine, CH₂**), 1.38 (s, 9H, **H-26, H-27, H-28, CH₃**), 1.22-1.27 (m, 2H, **cyclopropane, CH₂**), 1.09-1.10 (m, 2H, **cyclopropane, CH₂**);

¹³C NMR (100 MHz, DMSO-*d*₆) δ (ppm): 172.2 (d, $^4J_{C-F} = 2.3$ Hz, **C-6**), 169.7 (s, **C-24**), 166.6 (s, **C-17**), 155.7 (s, **C-22**), 153.2 (d, $^1J_{C-F} = 247.0$ Hz, **C-9**), 148.9 (s, **C-4**), 144.1 (d, $^2J_{C-F} = 10.7$ Hz, **C-10**), 138.6 (s, **C-12**), 122.5 (d, $^3J_{C-F} = 7.6$ Hz, **C-7**), 112.0 (d, $^2J_{C-F} = 23$ Hz, **C-8**), 109.4 (s, **C-5**), 106.9 (d, $^3J_{C-F} = 3.1$ Hz, **C-11**), 78.4 (s, **C-25**), 61.8 (s, **C-21**), 52.3 (s, **C-18**), 51.4 (s, **C-20**), 49.9 (s, **C-13/14/15/16**), 49.6 (s, **C-13/14/15/16**), 44.8 (s, **C-13/14/15/16**), 41.3 (s, **C-13/14/15/16**), 34.8 (s, **C-3**), 28.1 (s, **C-24, C-25, C-26**), 7.4 (s, **C-1, C-2**);

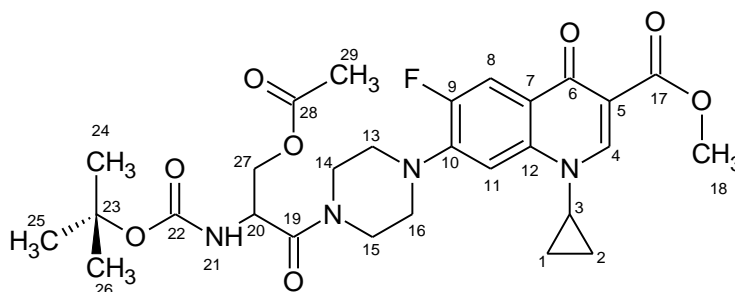
IR (KBr, cm⁻¹): 3423 (b, **OH**), 2970 (w, **CH**), 2945 (w, **CH**), 2925 (w, **CH**), 1695 (s, **C=O**), 1617 (s, **C=O**), 1495 (m, **CH₂**), 1474 (m, **CH₂**), 1446 (m, **CH₂**), 1388 (w, **CH₃**), 1364 (w, **CH₃**), 1343 (w, **CH₃**), 1311 (w, **CH₃**), 1241 (s, **C-F**), 1160 (m, **C-O**), 1082 (m, **C-O**), 1021 (m, **C-O**);

m.p (°C): 270.3-272.7 °C;

m/z (ESI): 533 ([M+H]⁺, 100 %);

HRMS (ESI): Calc. for C₂₆H₃₄FNO₇ 533.2406 [M+H]⁺, found 533.2407 (-0.1 ppm error).

4.10 Methyl 7-{4-[3-(acetyloxy)-2-[(*tert*-butoxy)carbonyl] amino} propanoyl]piperazin-1-yl}-1-cyclopropyl-6-fluoro-4-oxo-1,4-dihydroquinoline-3-carboxylate (50**)**



50

$C_{28}H_{35}FN_4O_8$

574.6 g/mol

Methyl 7-[4-(2-[(*tert*-butoxy)carbonyl]amino)-3-hydroxypropanoyl]piperazin-1-yl]-1-cyclopropyl-6-fluoro-4-oxo-1,4-dihydroquinoline-3-carboxylate **48** (0.30 g, 0.57 mmol, 1 eq.) was dissolved in acetic anhydride (0.16 mL, 1.70 mmol, 3 eq.). To this was added triethylamine (0.23 mL, 1.70 mmol, 3 eq.) and DMAP (1.4 mg, 0.01 mol, 0.02 eq.). The reaction mixture was allowed to stir at room temperature for 15 minutes.

The solvent was concentrated *in vacuo* affording a yellow oily residue which was diluted with chloroform (20 mL). The organic phase was washed with saturated sodium hydrogen carbonate ($NaHCO_3$, 3x 10 mL) and brine (2x 10 mL). The organic extract was dried over anhydrous $MgSO_4$ (s), and the solvent was removed *in vacuo*. Crude **50** was purified by column chromatography using a solvent system consisting of ethyl acetate: methanol: triethylamine (9:1:0.05), giving **50** as a cream solid (0.26 g, 0.45 mmol, 79 %).

Rf= 0.53 (EtOAc: MeOH: TEA, 9:1:0.05);

1H NMR (400 MHz, $DMSO-d_6$) δ (ppm): 8.46 (s, 1H, H-4, CH), 7.79 (d, $^3J_{H-F}$ = 13.4 Hz, 1H, H-8, CH), 7.46 (d, $^4J_{H-F}$ = 7.3 Hz, 1H, H-11, CH), 7.33 (d, $^3J_{21-20}$ = 8.8 Hz, 1H, NH), 4.74 (sx, $^3J_{20-27}$ = 5.4 Hz, $^3J_{20-27}$ = 5.4, $^3J_{20-21}$ = 8.8 Hz, 1H, H-

20, CH), 4.26 (dd, $^3J_{27-20}= 5.4$ Hz, $^2J_{27-27}= 11.2$ Hz, 1H, **H-27, CH**), 4.01 (dd, $^3J_{27-20}= 5.4$ Hz, $^2J_{27-27}= 11.2$ Hz, 1H, **H-27, CH**), 3.70-3.80 (m, 6H, **pipazine, CH₂, H-18 CH₃**), 3.63-3.68 (m, 2H, **cyclopropane, CH, pipazine, CH₂**), 3.17-3.32 (m, 4H, **pipazine, CH₂**), 1.99 (s, 3H, **acetyl, CH₃**), 1.39 (s, 9H, **H-24, H-25, H-26, CH₃**), 1.21-1.26 (m, 2H, **cyclopropane, CH₂**), 1.07-1.12 (m, 2H, **cyclopropane, CH₂**);

¹³C NMR (100 MHz, DMSO-d₆) δ (ppm): 172.2 (d, $^4J_{C-F}= 2.4$ Hz, **C-6**), 171.0 (s, **C-22**), 168.1 (s, **C-28**), 166.6 (s, **C-17**), 155.8 (s, **C-19**), 153.2 (d, $J_{C-F}= 244.8$ Hz, **C-9**), 148.9 (s, **C-4**), 144.0 (d, $^2J_{C-F}= 10.0$ Hz, **C-10**), 138.6 (s, **C-12**), 122.6 (d, $^3J_{C-F}= 7.5$ Hz, **C-7**), 112.0 (d, $^2J_{C-F}= 23.0$ Hz, **C-8**), 109.4 (s, **C-5**), 107.0 (d, $^3J_{C-F}= 3.3$ Hz, **C-11**), 78.8 (s, **C-23**), 63.5 (s, **C-27**), 51.4 (s, **C-18**), 49.6 (s, **C-13/14/15/16**), 49.5 (s, **C-13/14/15/16**), 49.0 (s, **C-20**), 44.6 (s, **C-13/14/15/16**), 41.4 (s, **C-13/14/15/16**), 34.8 (s, **C-3**), 28.1 (s, **C-24, C-25, C-26**), 20.5 (s, **C-29**), 7.4 (s, **C-1, C-2**);

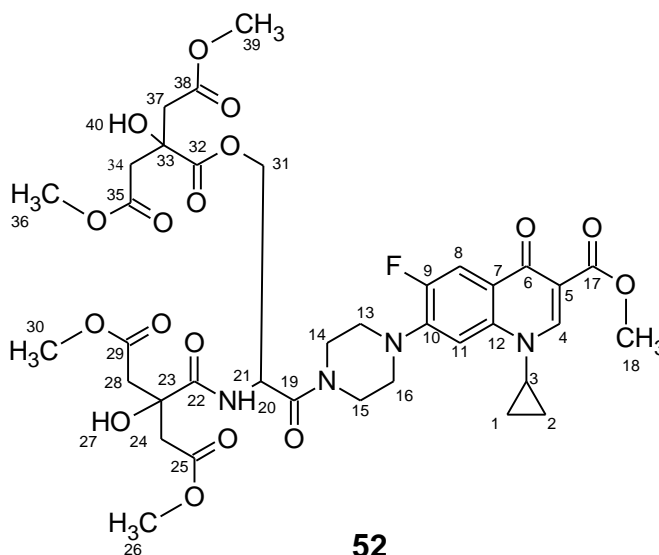
IR (KBr, cm⁻¹): 2974 (w, **CH**), 2945 (w, **CH**), 2925 (w, **CH**), 1728 (s, **C=O**), 1621 (s, **C=O**), 1491 (m, **CH₂**), 1474 (m, **CH₂**), 1442 (m, **CH₂**), 1388 (w, **CH₃**), 1360 (w, **CH₃**), 1343 (w, **CH₃**), 1311 (w, **C-O**), 1254 (s, **C-F**), 1160 (m, **C-O**), 1082 (m, **C-O**), 1021 (m, **C-O**);

m. p. (°C): 162.9-167.2 °C;

m/z (ESI): 575 ([M+H], 100 %);

HRMS (ESI): Calc. for C₂₈H₃₆FN₄O₈ 575.2512 [M+H]⁺, found 575.2527 (0.9 ppm error).

4.11 2-(3-{4-[1-Cyclopropyl-6-fluoro-3-(methoxycarbonyl)-4-oxo-1,4-dihydroquinoline-7-yl]piperazin-1-yl}-2-[2-hydroxy-4-methoxy-2-(2-methoxy-2-oxoethyl)-4-oxobutanamido]-3-oxopropyl) 1,3-dimethyl 2-hydroxypropane-1,2,3-tricarboxylate (52)



836.6 g/mol

To a methanolic HCl (4M, 20 mL) at 0-5 °C was added methyl 7-{4-[3-(acetyloxy)-2-{{*tert*-butoxy}carbonyl}amino]propanoyl]piperazin-1-yl}-1-cyclopropyl-6-fluoro-4-oxo-1,4-dihydroquinoline-3-carboxylate **50** (0.25 g, 0.4 mmol, 1 eq.). The reaction mixture was stirred at room temperature for 1 hour. The solvent was removed *in vacuo*, and anhydrous MeOH (40 mL) and triethylamine (0.5 mL) were added, stirring was continued at room temperature for 1.5 hours. The reaction was concentrated under reduced pressure affording a cream solid.

The solid residue and 2-hydroxy-4-methoxy-2-(2-methoxy-2-oxoethyl)-4-oxobutanoic acid **40** (0.02 g, 0.09 mmol, 2 eq.) were dissolved in anhydrous DMF (10 mL), DIPEA (54 µL, 0.31 mmol), HOBt. H₂O (0.01 g, 0.09 mmol) and EDC.HCl (0.02 g, 0.09 mmol) were added. The reaction mixture was stirred at 40 °C and small amounts of EDC.HCl (0.02 g, 0.087 mmol) were added every 3 hours. The reaction mixture was cooled to room temperature and

concentrated *in vacuo* to give an oily residue. The residue was dissolved in chloroform (100 mL), washed with saturated NaHCO₃ (5x 100 mL) and brine (5x 100 mL). The organic extract was dried over anhydrous MgSO₄ (s) and concentrated *in vacuo* to give crude **52** which was purified by column chromatography on silica gel using a solvent system consisting of chloroform: MeOH: TEA (9:1:0.05) to give **52** as a cream solid (0.20 g, 0.2 mmol, 56 %).

Rf = 0.71 (CHCl₃: MeOH: TEA, 3:1:0.05);

¹H NMR (400 MHz, CDCl₃) δ (ppm): 8.56 (s, 1H, **H-4, CH**), 8.06 (d, ³J_{H-F} = 12.8 Hz, 1H, **H-8, CH**), 7.94 (d, ³J₂₁₋₂₀ = 8.6 Hz, 1H, **H-21, NH**), 7.23 (d, ⁴J_{H-F} = 7.3 Hz, 1H, **H-11, CH**), 4.97- 5.02 (m, 1H, **H-20, CH**), 3.91 (s, 3H, **H-18, CH₃**), 3.83-3.85 (m, 1H, **H-31, CH**), 3.77-3.81 (m, 4H, **piperazine, CH₂**), 3.73-3.75 (m, 1H, **H-31, CH**), 3.71 (s, 3H, **H-26/ H-30/ H-36/ H-39, CH₃**), 3.70 (s, 3H, **H-26/ H-30/ H-36/ H-39, CH₃**), 3.67 (s, 3H, **H-26/ H-30/ H-36/ H-39, CH₃**), 3.64 (s, 3H, **H-26/ H-30/ H-36/ H-39, CH₃**), 3.40-3.45 (m, 1H, **cyclopropane, CH**), 3.24-3.29 (m, 4H, **piperazine, CH₂**), 2.77 (d, ²J_{H-H} = 15.9 Hz, 2H, **H-24/ H-28/ H-34/ H-37, CH₂**), 2.94 (d, ²J_{H-H} = 17.3 Hz, 2H, **H-24/ H-28/ H-34/ H-37, CH₂**), 2.98 (d, ²J_{H-H} = 15.9 Hz, 2H, **H-24/ H-28/ H-34/ H-37, CH₂**), 2.85 (d, ²J_{H-H} = 17.3 Hz, 2H, **H-24/ H-28/ H-34/ H-37, CH₂**), 1.36-1.31 (2H, **cyclopropane, CH₂**), 1.11-1.16 (2H, **cyclopropane, CH₂**);

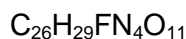
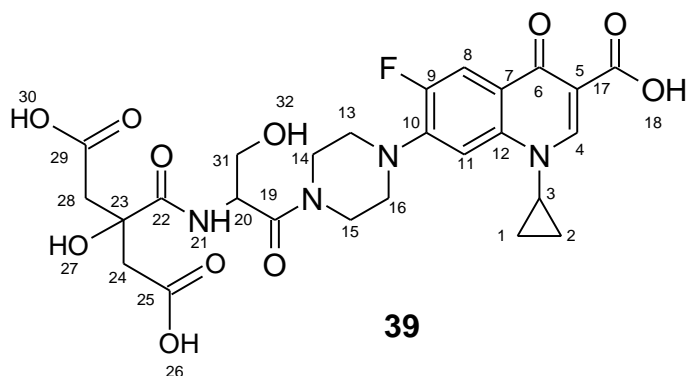
¹³C NMR (100 MHz, DMSO-d₆) δ (ppm): 173.1 (s, **C-22, C-32**), 172.7 (d, ⁴J_{C-F} = 2.3 Hz, **C-6**), 172.0 (s, **C-25, C-29, C-35, C-38**), 168.1 (s, **C-19**), 166.6 (s, **C-17**), 146.3 (d, ¹J_{C-F} = 247 Hz, **C-9**), 138.8 (s, **C-4**), 130.3 (d, ²J_{C-F} = 10.3 Hz, **C-10**), 129.7 (s, **C-12**), 124.6 (d, ³J_{C-F} = 7.6 Hz, **C-7**), 114.8 (d, ²J_{C-F} = 24.4 Hz, **C-8**), 110.1 (s, **C-5**), 104.9 (d, ³J_{C-F} = 3.8 Hz, **C-11**), 74.3 (s, **C-23**), 68.2 (s, **C-33**), 63.5 (s, **C-31**), 52.3 (s, **C-26/30/36/39**), 52.3 (s, **C-26/30/36/39**), 52.1 (s, **C-18**), 45.5 (s, **C-13/14/15/16**), 42.9 (s, **C-20**), 42.6 (s, **C-13/14/15/16**), 41.5 (s, **C-34, C-37**), 38.7 (s, **C-24, C-28**), 34.2 (s, **C-3**), 7.4 (s, **C-1, C-2**);

IR (KBr, cm⁻¹): 2958 (w, **CH**), 2929 (w, **CH**), 2872 (w, **CH**), 1732 (s, **C=O**), 1625 (s, **C=O**), 1491 (m, **CH₂**), 1437 (m, **CH₂**), 1442 (m, **CH₂**), 1372 (s, **C-F**), 1262 (w, **CH₃**), 1233 (w, **CH₃**), 1213 (w, **CH₃**);

m.p. (°C): 211.8-213.3 °C;

HRMS (ESI): Calc. for C₃₇H₄₆FN₄O₁₇ was 837.2837 [M+H]⁺, found 837.2849 (-1.5 ppm error).

4.12 3-({1-[4-(3-Carboxy-1-cyclopropyl-6-fluoro-4-oxo-1,4-dihydroquinoline-7-yl)piperazin-1-yl]-3-hydroxy-1-oxopropan-2-yl}carbamoyl)-3-hydroxypentanedioic acid (39)



592.5 g/mol

To a stirred suspension of TBAH in methanol (1M, 0.5 mL) and deionised water (4.5 mL) was added small portions of 2-(3-{4-[1-cyclopropyl-6-fluoro-3-(methoxycarbonyl)-4-oxo-1,4-dihydroquinoline-7-yl]piperazin-1-yl}-2-[2-hydroxy-4-methoxy-2-(2-methoxy-2-oxoethyl)-4-oxobutanamido]-3-oxopropyl) 1,3-dimethyl 2-hydroxypropane-1,2,3-tricarboxylate **52** (0.15 g, 0.18 mmol, 1 eq.). The reaction mixture was allowed to stir at room temperature for 18 hours. The reaction mixture was neutralised by addition of pyruvic acid in deionised water (0.2M, 3 mL). The precipitate formed was filtered to give **39** (0.03 g, 0.054 mmol, 30 %).

Rf= 0.11 (Chloroform: MeOH: Formic acid, 9:1:0.05);

¹H NMR (400 MHz, DMSO-*d*₆) δ (ppm): 8.67 (s, 1H, **H-4, CH**), 8.15 (dd, ³*J*_{H-H} = 4.6 Hz, ³*J*_{H-F} = 4.2 Hz, 1H, **H-21, NH**), 7.93 (d, ³*J*_{H-F} = 7.5 Hz, 1H, **H-8, CH**), 7.58 (d, ⁴*J*_{H-F} = 4.2 Hz, 1H, **H-11, CH**), 4.89 (s b, 1H, **OH**), 4.84 (m, 1H, **H-20, CH**), 3.63-3.84 (m, 4H, **piperazine, CH₂, CH, cyclopropane**), 3.60 (dd, ³*J*₃₁₋₂₀ = 3.3 Hz, ²*J*₃₁₋₃₁ = 5.7 Hz, 1H, **H-31, CH**), 3.46 (dd, ³*J*₃₁₋₂₀ = 3.3 Hz, ²*J*₃₁₋₃₁ = 5.7 Hz, **H-31, CH**), 3.22-3.35 (hidden by water peak, **CH₂, piperazine**), 2.70 (dd,

$^2J_{H-HF}$ = 8.8 Hz, 1H, **H-24/ H-28, CH**), 2.62 (dd, $^2J_{H-HF}$ = 8.1 Hz, 1H, **H-24/ H-28, CH**), 2.59 (dd, 1H, $^2J_{H-HF}$ = 8.8 Hz, 1H, **H-24/ H-28, CH**), 2.55 (dd, $^2J_{H-HF}$ = 8.1, 1H, **H-24/ H-28, CH**), 1.29-1.35 (m, 2H, **cyclopropane, CH₂**), 1.14-1.22 (m, 2H, **cyclopropane, CH₂**);

^{13}C NMR (100 MHz, DMSO- d_6) δ (ppm): 175.9 (s, **C-22**), 172.1 (d, $^4J_{C-F}$ = 3.1 Hz, **C-6**), 168.9 (s, **C-25, C-29**), 168.6 (s, **C-25, C-29**), 166.62(s, **C-17**), 154.5 (s, **C-19**), 152.4 (d, J_{C-F} = 248.0 Hz, **C-9**), 148.7 (s, **C-4**), 145.5 (d, $^2J_{C-F}$ = 10.2 Hz, **C-10**), 139.7 (s, **C-12**), 119.3 (d, $^3J_{C-F}$ = 7.1 Hz, **C-7**), 110.8 (d, $^2J_{C-F}$ = 22.2 Hz, **C-8**), 107.1 (d, $^3J_{C-F}$ = 3.8 Hz, **C-11**), 72.9 (s, **C-23**), 61.8 (s, **C-31**), 50.4 (s, **C-20**), 50.4 (**C-13/14/15/16**), 49.7 (**C-13/14/15/16**), 43.3 (**C-13/14/15/16**), 43.1 (**C-13/14/15/16**), 41.8 (s, **C-24, C-28**), 35.9 (s, **C-3**), 7.4 (s, **C-1, C-2**);

IR (KBr, cm^{-1}): 3412 (b, **OH**), 3052 (w, **CH**), 2848 (w, **CH**), 1732 (s, **C=O**), 1650 (s, **C=O**), 1626 (s, **C=O**), 1471 (m, **CH₂**), 1454 (m, **CH₂**), 1381 (m, **C-O**), 1340 (m, **C-O**), 1270 (s, **C-F**), 1021 (m, **C-O**);

m.p. ($^{\circ}\text{C}$): 230.3- 234.7 $^{\circ}\text{C}$;

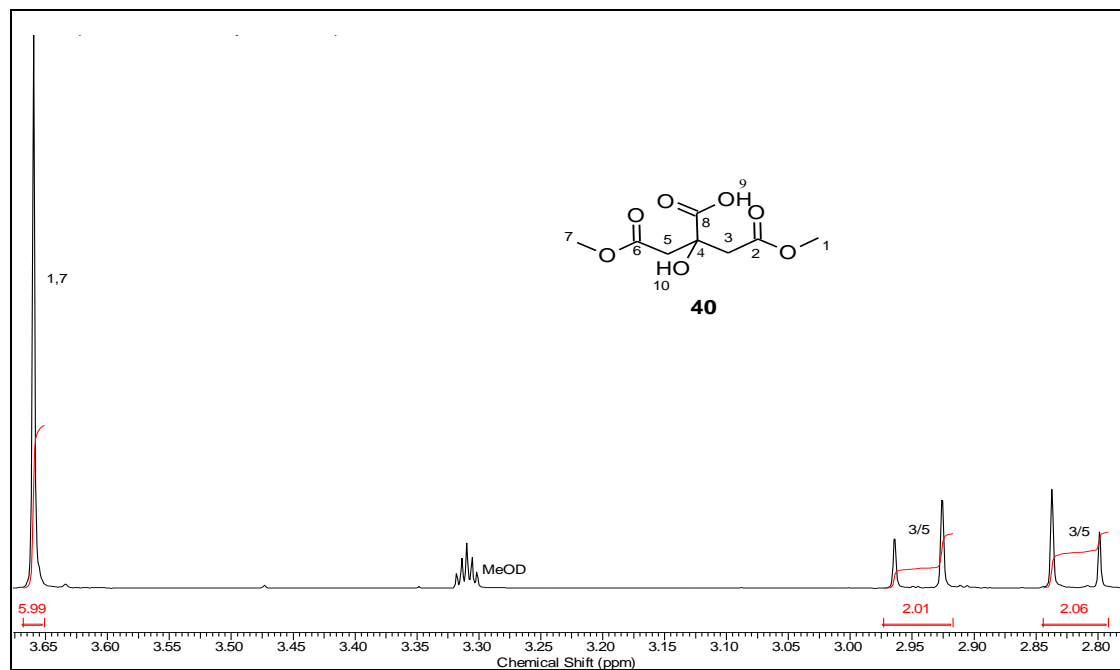
HRMS (ESI +ve): Calc. for $\text{C}_{26}\text{H}_{30}\text{FN}_4\text{O}_{11}$ was 593.1890 $[\text{M}+\text{H}]^+$, found 593.1912 (-3.8 ppm error);

HRMS (ESI -ve): Calc. for $\text{C}_{26}\text{H}_{28}\text{FN}_4\text{O}_{11}$ was 591.1744 $[\text{M}-\text{H}]^-$, found 591.1763 (-3.2 ppm error);

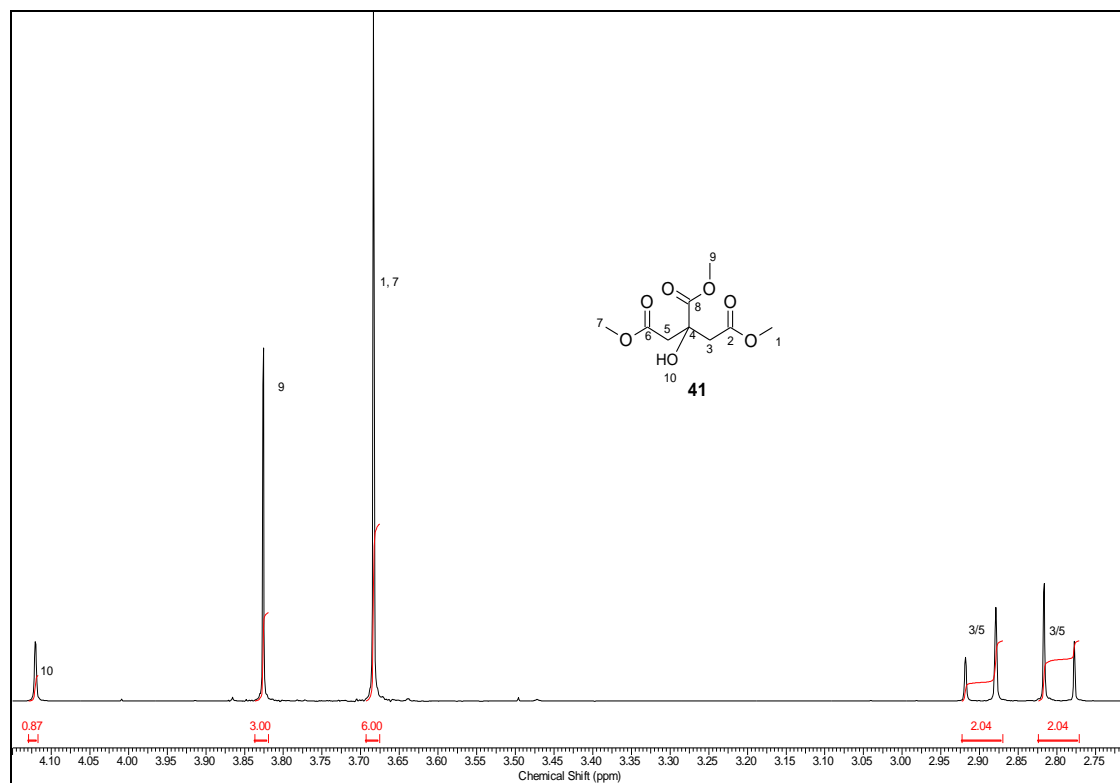
m/z (CID): 593 $[\text{M}+\text{H}]^+$, 575.2, 557.2, 539.2, 503.2, 419.2

5 Appendices

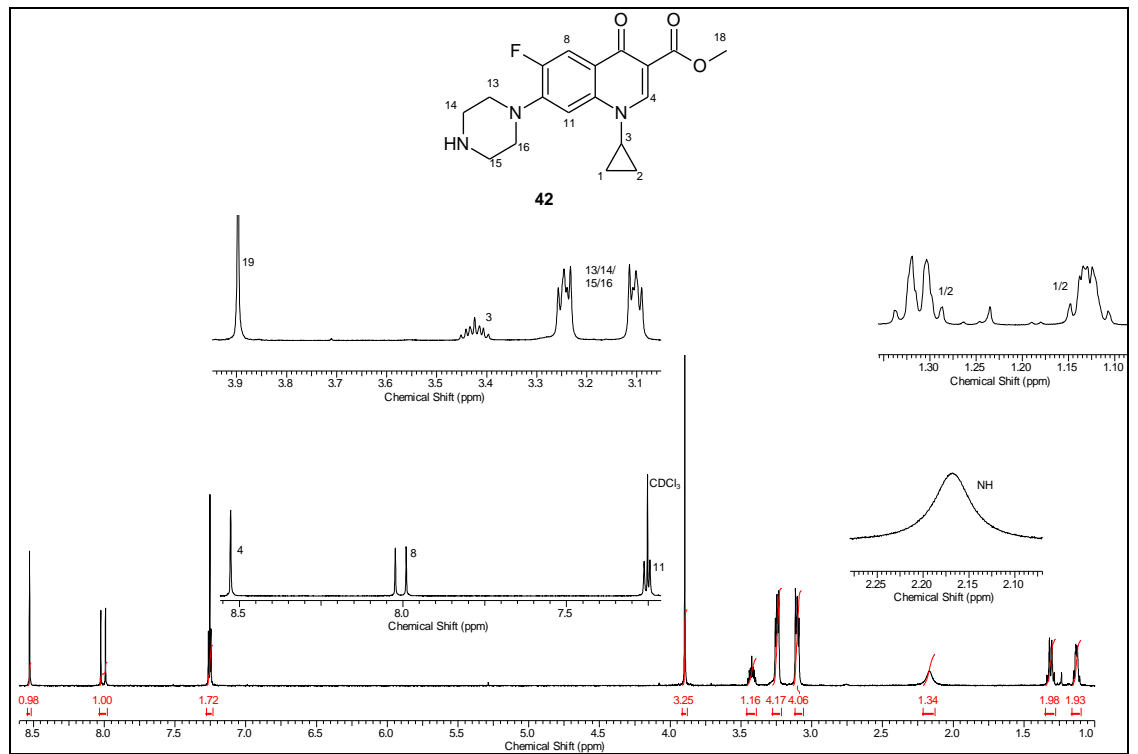
Appendix 1. ^1H NMR of 1, 5-dimethyl citrate **40**



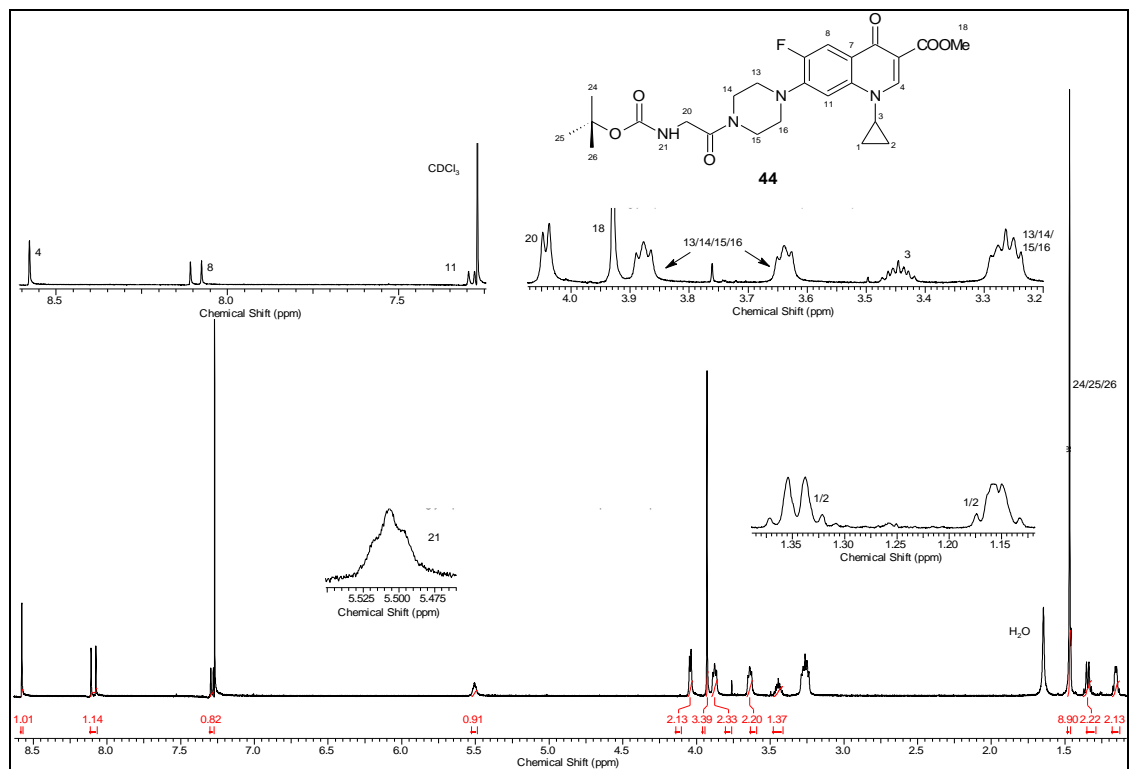
Appendix 2. ^1H NMR of 1, 3, 5-trimethyl citrate **41**



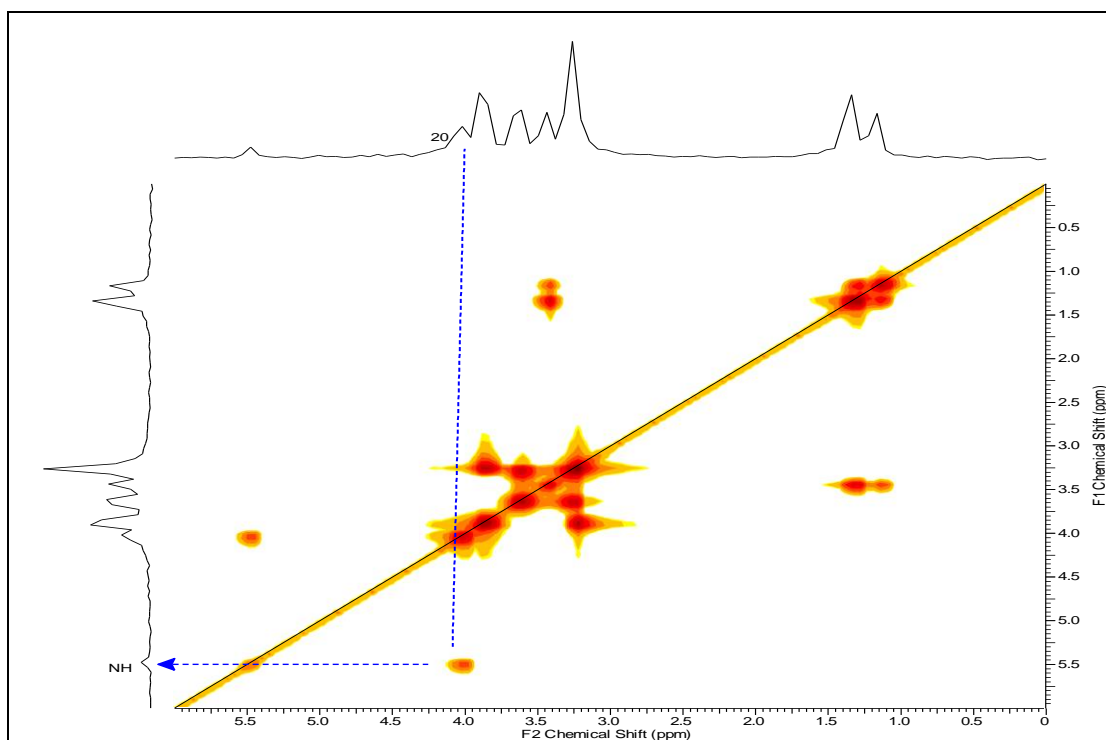
Appendix 3. ^1H NMR of ciprofloxacin methanoate **42**



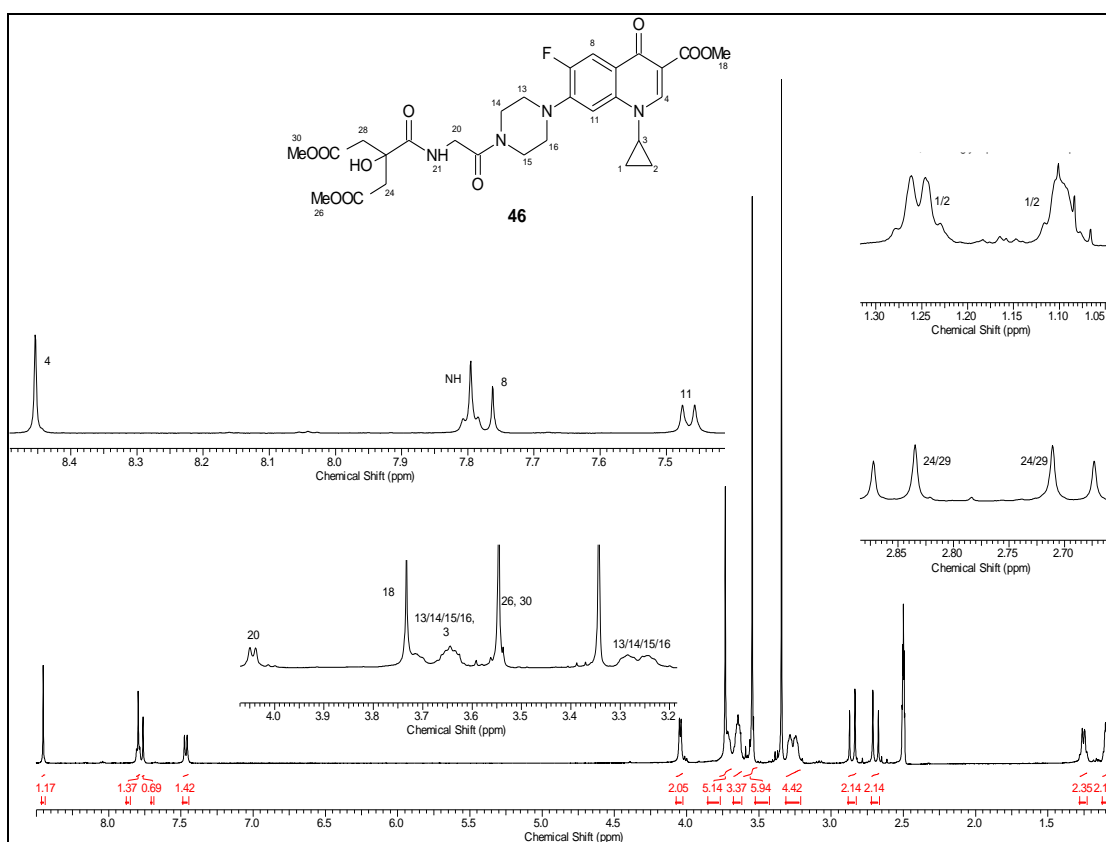
Appendix 4. ^1H NMR of linker-drug conjugate **44**



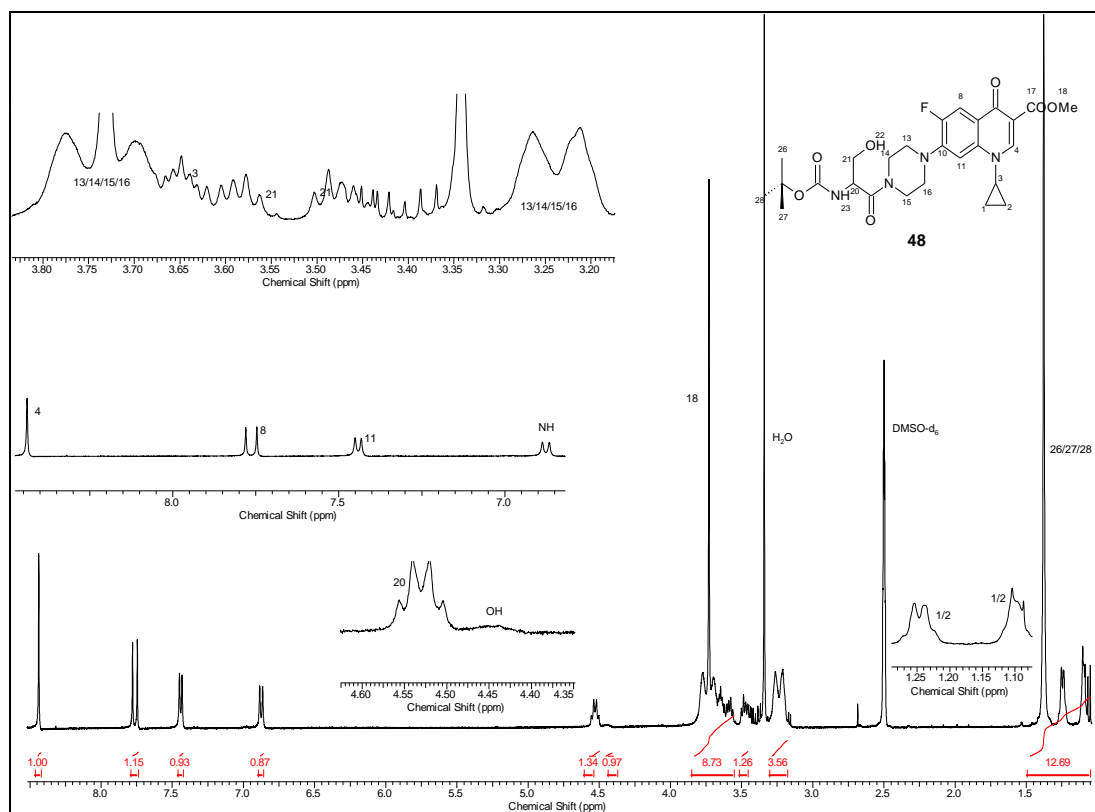
Appendix 5. COSY of linker-drug conjugate **44**



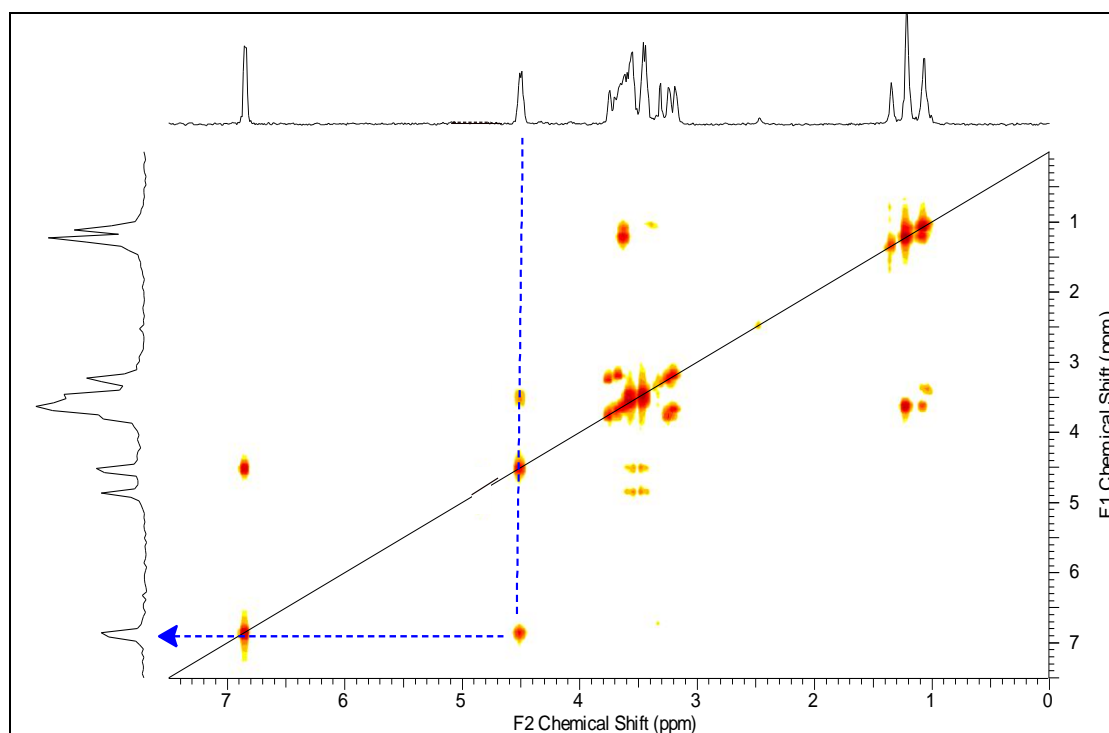
Appendix 6. ^1H NMR of protected siderophore-drug conjugate **46**



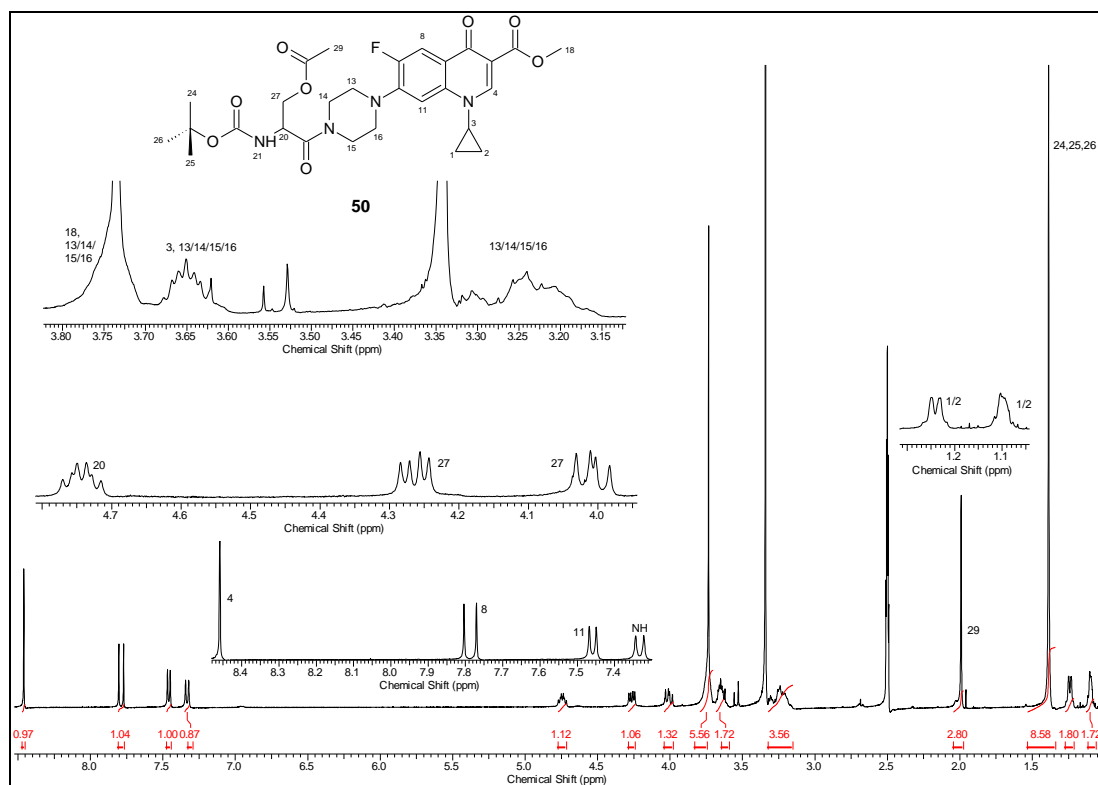
Appendix 7. ¹H NMR of linker-drug conjugate **48**



Appendix 8. COSY of linker-drug conjugate **48**



Appendix 9. ^1H NMR of linker-drug conjugate **50**



6 References

- [1] K. B. Raper, D. F. Alexander and R. D. Coghill, *J. Bacteriol.* **1944**, *48*, 639-659; L. A. Carpino, H. Imazumi, A. El-Faham, F. J. Ferrer, C. W. Zhang, Y. S. Lee, B. M. Foxman, P. Henklein, C. Hanay, C. Mugge, H. Wenschuh, K. Klose, M. Beyermann and M. Bienert, *Angew. Chem. Int. Edition* **2002**, *41*, 441-445.
- [2] P. Hawkey and R. Finch, *Clin. Microbiol. Infec.* **2007**, *13*, 354-362.
- [3] Salem, II and N. Duzgunes, *Int. J. Pharm.* **2003**, *250*, 403-414.
- [4] P. JR in *Some reactions of 1-methyl-4-quinolone-3-carboxylic acid, a degradation product of the alkaloids*, *Aust. J. Sci. Res.* **1949**, *217*, 272-281.
- [5] A. Bryskier, *Int. J. Antimicrob. Ag.* **1993**, *2*, 151-183.
- [6] P. Stapleton, P. J. Wu, A. King, K. Shannon, G. French and I. Phillips, *Antimicrob. Ag. Ch.* **1995**, *39*, 2478-2483.
- [7] T. Brun, J. Peduzzi, M. M. Canica, G. Paul, P. Nevot, M. Barthelemy and R. Labia, *Fems Microbiol. Lett.* **1994**, *120*, 111-117.
- [8] S. T. Chen and R. C. Clowes, *J. Bacteriol.* **1987**, *169*, 913-916; C. Mabilat, S. Goussard, W. Sougakoff, R. C. Spencer and P. Courvalin, *Plasmid* **1990**, *23*, 27-34.
- [9] N. Honore, M. H. Nicolas and S. T. Cole, *Embo. J.* **1986**, *5*, 3709-3714.
- [10] C. C. Sanders, *J. Antimicrob. Chemoth.* **1984**, *13*, 1-3.
- [11] J. D. Hayes and C. R. Wolf, *Biochem. J.* **1990**, *272*, 281-295.
- [12] J. Davies, *Science* **1994**, *264*, 375-382.
- [13] B. G. Spratt, *Science* **1994**, *264*, 388-393.
- [14] W. Wehrli, *Rev. Infect. Dis.* **1983**, *5*, S407-S411.
- [15] D. J. Jin and C. A. Gross, *J. Mol. Biol.* **1988**, *202*, 45-58.
- [16] H. Nikaido, *Science* **1994**, *264*, 382-388.
- [17] B. Robert A, *Clin. Microbiol. Newsletter* **1998**, *20*, 197-201.
- [18] G. Y. Leshner, E. J. Froelich, M. D. Gruett, J. H. Bailey and R. P. Brundage, *J. Med. Pharmaceut. Ch.* **1962**, *91*, 1063-1065.
- [19] P. C. Appelbaum and P. A. Hunter, *Int. J. Antimicrob. Ag.* **2000**, *16*, 5-15.
- [20] K. Drlica and M. Malik, *Curr. Top. Med. Chem.* **2003**, *3*, 249-282.
- [21] J. M. Domagala, *J. Antimicrob. Chemoth.* **1994**, *33*, 685-706.
- [22] R. E. W. Hancock, *J. Bacteriol.* **1987**, *169*, 929-933.
- [23] C. A. Caulcott, M. R. W. Brown and I. Gonda, *Fems Microbiol. Lett.* **1984**, *21*, 119-123.
- [24] K. E. Brighty and T. D. Gootz, *J. Antimicrob. Chemoth.* **1997**, *39*, 1-14.
- [25] L. L. Shen and A. G. Pernet, *PNAS.* **1985**, *82*, 307-311.
- [26] L. M. Fisher, K. Mizuuchi, M. H. Odea, H. Ohmori and M. Gellert, *PNAS-Biological Sciences* **1981**, *78*, 4165-4169; S. C. Kampranis and A. Maxwell, *PNAS.* **1996**, *93*, 14416-14421.
- [27] L. L. Shen, L. A. Mitscher, P. N. Sharma, T. J. Odonnell, D. W. T. Chu, C. S. Cooper, T. Rosen and A. G. Pernet, *Biochem.* **1989**, *28*, 3886-3894.
- [28] J. Ruiz, *J. Antimicrob. Chemoth.* **2003**, *51*, 1109-1117.
- [29] M. E. Cullen, A. W. Wyke, R. Kuroda and L. M. Fisher, *Antimicrob. Ag. Ch.* **1989**, *33*, 886-894; M. Oram and L. M. Fisher, *Antimicrob. Ag. Ch.* **1991**, *35*, 387-389; H. Yoshida, M. Bogaki, M. Nakamura and S. Nakamura, *Antimicrob. Ag. Ch.* **1990**, *34*, 1271-1272; S. M. Friedman, T. Lu and K. Drlica, *Antimicrob. Ag. Ch.* **2001**, *45*, 2378-2380.
- [30] D. C. Hooper, J. S. Wolfson, K. S. Souza, E. Y. Ng, G. L. McHugh and M. N. Swartz, *Antimicrob. Ag. Ch.* **1989**, *33*, 283-290.
- [31] J. I. Mitsuyama, Y. Itoh, M. Takahata, S. Okamoto and T. Yasuda, *Antimicrob. Ag. Ch.* **1992**, *36*, 2030-2036; Hooper DC, Wolf son JS, Souza KS, Tung C, Mc Hugh GL and S. MN. in

Genetic and biochemical characterization of norfloxacin resistance in E. coll., Antimicrob. Ag. Ch. **1986**, 29, 639-644.

[32] M. Micheahamzhepour, Y. X. Furet and J. C. Pechere, *Antimicrob. Ag. Ch.* **1991**, 35, 2091-2097.

[33] A. Cloeckaert and E. Chaslus-Dancla, *Vet. Res.* **2001**, 32, 291-300.

[34] T. Baba and O. Schneewind, *Trends Microbiol* **1998**, 6, 66-71.

[35] J. H. Tran and G. A. Jacoby, *PNAS.* **2002**, 99, 5638-5642.

[36] J. M. Roosenberg, Y. M. Lin, Y. Lu and M. J. Miller, *Curr. Med. Chem.* **2000**, 7, 159-197.

[37] B. F. Matzanke in *Iron Transport: Siderophores, Enc. Inorg. Chem.* **1994**, pp. 1915-1933.

[38] M. Sandy and A. Butler, *Chem. Rev.* **2009**, 109, 4580-4595.

[39] C. J. Carrano, H. Drechsel, D. Kaiser, G. Jung, B. Matzanke, G. Winkelmann, N. Rochel and A. M. AlbrechtGary, *Inorg. Chem.* **1996**, 35, 6429-6436.

[40] M. Miethke and M. A. Marahiel, *Microbiol. Mol. Biol. Rev.* **2007**, 71, 413-451.

[41] H. Drechsel and G. Jung, *J. Pept. Sci.* **1998**, 4, 147-181.

[42] G. Winkelmann, *Biochem. Soc. T.* **2002**, 30, 691-696.

[43] M. L. Guerinot, E. J. Meidl and O. Plessner, *J. Bacteriol.* **1990**, 172, 3298-3303.

[44] J. Meiwes, H. P. Fiedler, H. Haag, H. Zahner, S. Konetschnyrapp and G. Jung, *Fems Microbiol. Lett.* **1990**, 67, 201-205.

[45] A. Thieken and G. Winkelmann, *Fems Microbiol. Lett.* **1992**, 94, 37-42.

[46] J. R. Pollack and J. B. Neilands, *Biochem. Biophys. Res. Commun.* **1970**, 38, 989-992.

[47] E. A. Dertz, J. D. Xu, A. Stintzi and K. N. Raymond, *J. Am. Chem. Soc.* **2006**, 128, 22-23.

[48] J. Reichert, M. Sakaitani and C. T. Walsh, *Protein Sci.* **1992**, 1, 549-556.

[49] B. Bister, D. Bischoff, G. J. Nicholson, M. Valdebenito, K. Schneider, G. Winkelmann, K. Hantke and R. D. Sussmuth, *Biometals* **2004**, 17, 471-481.

[50] T. Emery, *Adv. Enzymol. Relat. Areas Mol. Biol.* **1971**, 35, 135-185.

[51] M. J. Miller and F. Malouin, *Accounts. Chem. Res.* **1993**, 26, 241-249.

[52] H. Bickel, G. E. Hall, W. Kellerschierlein, V. Prelog, E. Vischer and A. Wettstein, *Helv. Chim. Acta.* **1960**, 43, 2129-2138.

[53] S. Dhungana, P. S. White and A. L. Crumbliss, *J. Biol. Inorg. Chem.* **2001**, 6, 810-818.

[54] M. K. Wilson, R. J. Abergel, K. N. Raymond, J. E. L. Arceneaux and B. R. Byers, *Biochem. Biophys. Res. Commun.* **2006**, 348, 320-325.

[55] H. Stephan, S. Freund, W. Beck, G. Jung, J. M. Meyer and G. Winkelmann, *Biometals* **1993**, 6, 93-100.

[56] J. H. Crosa, Mey, A. R., Payne, S. M., Eds. in *Iron Transport in Bacteria*, ASM Press, Washington DC, **2004**; D. M. Templeton in *Molecular and Cellular Iron Transport*, Marcel Dekker, Inc, New York, **2002**.

[57] J. S. Brown and D. W. Holden, *Microbes. Infect.* **2002**, 4, 1149-1156.

[58] D. J. Ecker, B. F. Matzanke and K. N. Raymond, *J. Bacteriol.* **1986**, 167, 666-673; D. J. Ecker, L. D. Loomis, M. E. Cass and K. N. Raymond, *J. Am. Chem. Soc.* **1988**, 110, 2457-2464; G. Muller, B. F. Matzanke and K. N. Raymond, *J. Bacteriol.* **1984**, 160, 313-318; H. Huschka, H. U. Naegeli, H. Leuenbergerryf, W. Kellerschierlein and G. Winkelmann, *J. Bacteriol.* **1985**, 162, 715-721; G. Muller, S. J. Barclay and K. N. Raymond, *J. Biol. Chem.* **1985**, 260, 3916-3920.

[59] A. D. Ferguson, E. Hofmann, J. W. Coulton, K. Diederichs and W. Welte, *Science* **1998**, 282, 2215-2220; K. P. Locher, B. Rees, R. Koebnik, A. Mitschler, L. Moulinier, J. P. Rosenbusch and D. Moras, *Cell* **1998**, 95, 771-778.

[60] S. K. Buchanan, B. S. Smith, L. Venkatramani, D. Xia, L. Esser, M. Palnitkar, R. Chakraborty, D. van der Helm and J. Deisenhofer, *Nat. Struct. Biol.* **1999**, 6, 56-63.

[61] A. D. Ferguson, R. Chakraborty, B. S. Smith, L. Esser, D. van der Helm and J. Deisenhofer, *Science* **2002**, 295, 1715-1719.

[62] V. Braun and M. Braun, *Febs Lett.* **2002**, 529, 78-85.

- [63] V. Braun and M. Braun, *Curr. Opin. Microbiol.* **2002**, *5*, 194-201.
- [64] J. W. Coulton, P. Mason, D. R. Cameron, G. Carmel, R. Jean and H. N. Rode, *J. Bacteriol.* **1986**, *165*, 181-192.
- [65] M. D. Lundrigan and R. J. Kadner, *J. Biol. Chem.* **1986**, *261*, 797-801.
- [66] U. Pressler, H. Staudenmaier, L. Zimmermann and V. Braun, *J. Bacteriol.* **1988**, *170*, 2716-2724.
- [67] K. D. Krewulak and H. J. Vogel, *Biochim. Biophys. Acta-Biomembranes.* **2008**, *1778*, 1781-1804.
- [68] A. Hartmann and V. Braun, *J. Bacteriol.* **1980**, *143*, 246-255; T. J. Brickman and M. A. McIntosh, *J. Biol. Chem.* **1992**, *267*, 12350-12355; B. F. Matzanke, S. Anemuller, V. Schunemann, A. X. Trautwein and K. Hantke, *Biochem.* **2004**, *43*, 1386-1392.
- [69] I. J. Schalk, M. Hannauer and A. Braud, *Environ. Microbiol.* **2011**, *13*, 2844-2854.
- [70] I. J. Schalk, M. A. Abdallah and F. Pattus, *Biochem.* **2002**, *41*, 1663-1671; J. Greenwald, F. Hoegy, M. Nader, L. Journet, G. L. A. Mislin, P. L. Graumann and I. J. Schalk, *J. Biol. Chem.* **2007**, *282*, 2987-2995; F. Imperi, F. Tiburzi and P. Visca, *PNAS.* **2009**, *106*, 20440-20445; E. Yeterian, L. W. Martin, I. L. Lamont and I. J. Schalk, *Environ. Microbiol. Rep.* **2010**, *2*, 412-418.
- [71] G. Benz, T. Schroder, J. Kurz, C. Wunsche, W. Karl, G. Steffens, J. Pfitzner and D. Schmidt in *Konstitution der Desferriform der Albomycine*, *Angewandte Chem-Ger Edit.* **1982**, *94*, 552-553.
- [72] H. Bickel, P. Mertens, V. Prelog, J. Seibl and A. Walser, *Tetrahedron* **1966**, *22*, 171-179.
- [73] L. Vertesy, W. Aretz, H.-W. Fehlhaber and H. Kogler in *Salimycin -D*, *Helv. Chim. Acta.* **1995**, *78*, 46-60.
- [74] H. Budzikiewicz, *Curr. Top. Med. Chem.* **2001**, *1*, 73-82.
- [75] M. J. Miller, F. Malouin, E. K. Dolence, C. M. Gasparski, M. Ghosh, P. R. Guzzo, B. T. Lotz, J. A. McKee, A. A. Minnick and M. Teng, *Recent advances in the chemistry of anti-infective agents* **1993**, 135-159.
- [76] S. S. Wong in *Vol. Chemistry of Protein Conjugation and Cross- Linking*, CRC: Boca Raton, FL, **1991**.
- [77] M. Ghosh and M. J. Miller, *J. Org. Chem.* **1994**, *59*, 1020-1026.
- [78] A. Ghosh, M. Ghosh, C. Niu, F. Malouin, U. Moellmann and M. J. Miller, *Chem. Biol.* **1996**, *3*, 1011-1019.
- [79] A. Ghosh and M. J. Miller, *J. Org. Chem.* **1993**, *58*, 7652-7659.
- [80] S. R. Md-Saleh, E. C. Chilvers, K. G. Kerr, S. J. Milner, A. M. Snelling, J. P. Weber, G. H. Thomas, A.-K. Duhme-Klair and A. Routledge, *Bioorg. Med. Chem. Lett.* **2009**, *19*, 1496-1498.
- [81] G. E. Frost and Rosenber.H, *Biochim. Biophys. Acta* **1973**, *330*, 90-101; W. Wagegg and V. Braun, *J. Bacteriol.* **1981**, *145*, 156-163.
- [82] C. D. Cox, *J. Bacteriol.* **1980**, *142*, 581-587.
- [83] S. Hussein, K. Hantke and V. Braun, *Eur. J. Biochem.* **1981**, *117*; I. Gautier-Luneau, C. Merle, D. Phanon, C. Lebrun, F. Biaso, G. Serratrice and J. L. Pierre, *Chem. Eur. J.* **2005**, *11*, 2207-2219.
- [84] S. J. Milner in *Doctorate of Philosophy* University of York, **2011**.
- [85] H. Y. Guo, S. A. Naser, G. Ghobrial and O. Phanstiel, *J. Med. Chem.* **2002**, *45*, 2056-2063.
- [86] W. H. Miller, M. A. Seefeld, K. A. Newlander, I. N. Uzinskas, W. J. Burgess, D. A. Heerding, C. C. K. Yuan, M. S. Head, D. J. Payne, S. F. Rittenhouse, T. D. Moore, S. C. Pearson, V. Berry, W. E. DeWolf, P. M. Keller, B. J. Polizzi, X. Y. Qiu, C. A. Janson and W. F. Huffman, *J. Med. Chem.* **2002**, *45*, 3246-3256.
- [87] N. Nakajima and Y. Ikada, *Bioconjugate Chem.* **1995**, *6*, 123-130.

- [88] Y. J. Pu, R. K. Vaid, S. K. Boini, R. W. Towsley, C. W. Doecke and D. Mitchell, *Org. Process Res. Dev.* **2009**, *13*, 310-314.
- [89] G. Han, M. Tamaki and V. Hruby, *J. Pept. Res.* **2001**, *58*, 338-341.
- [90] J. T. Su, P. Vachal and E. N. Jacobsen, *Adv. Synth. Catal.* **2001**, *343*, 197-200.
- [91] P. D. A. Lüttringhaus and D. H. W. Dirksen in *Tetramethylurea as a Solvent and Reagent*, *Angew. Chem. Int. Edit.*, Germany **2003**, *3*, 260–269.
- [92] M. D. Bruch, *NMR Spectro. Tech.* Marcel Dekker, Inc., United States of America, **1996**.
- [93] F. S. Daft and R. D. Coghill, *J. Biol. Chem.* **1931**, *90*, 341-350.
- [94] J. C. Crawhall and D. F. Elliott, *Biochem. J.* **1951**, *48*, 237-238.